Check for updates

The cyclic 48-tungsto-8-phosphate [$H_7P_8W_{48}O_{184}$]$^{33-}$ Contant–Tézé polyanion and its derivatives [$H_6P_4W_{24}O_{94}$]$^{18-}$ and [$H_2P_2W_{12}O_{48}$]$^{12-}$: structural aspects and reactivity

Sib Sankar Mal, [iD] *ᵃ Abhishek Banerjee [iD] ᵇ and Ulrich Kortz [iD] *ᶜ

Polyoxometalates (POMs) are discrete, anionic metal-oxo clusters of early transition metals in high oxidation states (*e.g.*, W^{VI}, Mo^{VI}, V^{V}) usually comprised of edge- and corner-shared MO_6 octahedra. Lacunary POMs are defect heteropolyanions mainly of the Keggin or Dawson type, and they can be formed by the loss of one or more MO_6 octahedra by controlled base hydrolysis. The largest subclass of POMs are tungstophosphates, and several lacunary derivatives are known, such as the Keggin-based [$PW_{11}O_{39}$]$^{7-}$ and [PW_9O_{34}]$^{9-}$, and the Dawson-based [$P_2W_{17}O_{61}$]$^{10-}$ and [$P_2W_{15}O_{56}$]$^{12-}$. This review is based on the cyclic 48-tungsto-8-phosphate [$H_7P_8W_{48}O_{184}$]$^{33-}$ (**P₈W₄₈**) as well as its smaller derivatives [$H_6P_4W_{24}O_{94}$]$^{18-}$ (**P₄W₂₄**), and [$H_2P_2W_{12}O_{48}$]$^{12-}$ (**P₂W₁₂**), with a focus on structural aspects, solution stability and reactivity. All three polyanions can be considered as inorganic multidentate O-donor ligands that coordinate with d, f or p-block metal ions. Here we provide a comprehensive overview of guest metal-containing derivatives of the **P₈W₄₈** wheel, the **P₄W₂₄** half-wheel and the **P₂W₁₂** quarter wheel. The structures containing **P₂W₁₂** as a building unit are presented in a sequence of increasing number of POM units in the resulting assembly. Transition metal-containing POMs have been of interest for decades due to their remarkable capability of forming novel and unexpected structures associated with interesting and relevant physicochemical properties (*e.g.*, catalysis, magnetism, biomedicine, electrochemistry), and this also applies for derivatives containing **P₈W₄₈**, **P₄W₂₄** and **P₂W₁₂**.

1. Introduction

The field of polyoxometalate (POM) chemistry has seen increased interest in recent decades due to the extensive range of chemical and physical properties of such compounds. Berzelius reported the formation of a molydophosphate polyoxoanion in 1826, and more than a decade later, Keggin identified the crystal structure of $H_3[PW_{12}O_{40}]$ using powder X-ray diffraction.[1] As such, POMs were elucidated as discrete anionic metal-oxo clusters formed by condensation of simple oxoanions (*e.g.*, WO_4^{2-}) in aqueous media upon acidification. POMs consist of oxo-bridged early transition metal atoms of groups V and VI in high oxidation states, such as V^V, Nb^V, Ta^V, Mo^{VI}, or W^{VI}.[2] For the formation of stable polyanions, the metal addendum atom should possess vacant d orbitals,

which allows for d_π–p_π back bonding with terminal oxygen atoms. This phenomenon helps to terminate the condensation process at the level of discrete polyanions and disfavors the formation of extended metal oxide lattices.

Based on their chemical composition, POMs can be broadly subdivided into two main subclasses: (i) isopolyanions, which are composed exclusively of metal addenda M and oxo ligands, represented as [M_mO_y]$^{n-}$, and (ii) heteropolyanions, which contain one or more hetero atoms inside the polyanion, represented as [$X_xM_mO_y$]$^{q-}$ ($x \leq m$), where X is usually a main group element such as P, Si, Ge, or As. Due to their high thermal and redox stability as well as their radiation-resistant nature, isopolyanions have attracted increasing attention for applications involving the separation and sequestration of radioactive species.[3] It is important to note that the formation of polyoxotungstates is accompanied by very slow equilibration of the reaction system, compared to molybdates and vanadates. Prime examples of heteropolyanions are the Keggin ion (*e.g.* [$SiW_{12}O_{40}$]$^{4-}$) and the Wells–Dawson ion (*e.g.* [$P_2Mo_{18}O_{62}$]$^{6-}$), incorporating one or two tetrahedral XO_4 hetero groups, respectively. Pope and Müller reviewed the synthesis and characterization of POMs in 1991. Subsequently,

ᵃ*Materials and Catalysis Lab, Department of Chemistry, National Institute of Technology Karnataka, 575025 Surathkal, India. E-mail: malss@nitk.edu.in*
ᵇ*Department of Chemistry, Visvesvaraya National Institute of Technology, Nagpur, 440010, India. E-mail: abhishekbanerjee@chm.vnit.ac.in*
ᶜ*School of Science, Constructor University, Campus Ring 1, 28759 Bremen, Germany. E-mail: ukortz@constructor.university*

Hill, as guest editor, highlighted popular research themes within the field of POM chemistry in a thematic issue of *Chemical Reviews* in 1998.[4–9]

POMs have generated considerable interest across all areas of chemistry due to their versatile nature with regard to shape, size, composition, redox activity, solubility, photochemistry, and charge distribution.[7] Contemporary areas that have emerged in the multidisciplinary field of POM chemistry are mainly associated with various applications of POMs corresponding to developing new materials.[10] These have shown promise in the fields of nanotechnology,[11] biology,[12–15] surfaces,[14–17] catalysis,[18,19] supramolecular materials,[20,21] colloid science,[22] and electronic materials,[23] sensors,[24,25] molecular materials[26,27] and magnetism.[28] Crucial to the fast development of structural POM chemistry are advances in single-crystal X-ray diffraction (XRD), which allows for faster measurements on smaller crystals, allowing the characterization of large (with several hundred addenda atoms) polyanions.[29,30] Polyoxotungstates, in particular, have been observed to be effective homogeneous photocatalysts for the mineralization of organic pollutants.[31–35] As such, this review will focus on recent developments of the large, cyclic 48-tungsto-8-phosphate $[H_7P_8W_{48}O_{184}]^{40-}$ (abbreviated as **P8W48**) and its smaller fragments $[H_2P_2W_{12}O_{48}]^{12-}$ (abbreviated as **P2W12**) and $[H_6P_4W_{24}O_{94}]^{18-}$ (abbreviated as **P4W24**). Emphasis will be placed on the synthesis and structure of these polyanions.

In 1945, A. F. Wells suggested a detailed structure for the dimeric (18:2) tungstophosphate ion,[36] based on Pauling's principles and the structure Keggin had shown for the 12-tungstophosphate. In 1952, the formula $[P_2M_{18}O_{62}]^{6-}$ (M = Mo, W) proposed by Wells was experimentally established for the molybdo analogue by Tsigdinos. In 1953, Dawson investigated this polyanion using single-crystal X-ray diffraction,[37] and

demonstrated that the positions of the W atoms in $[P_2W_{18}O_{62}]^{6-}$ coincided with what was postulated by Wells. In 1975 Strandberg,[38] and in 1976 D'Amour,[39] reported complete and accurate X-ray crystal structures of $[\alpha-P_2Mo_{18}O_{62}]^{6-}$ and $[\alpha-P_2W_{18}O_{62}]^{6-}$, respectively.

2. The cyclic $[H_7P_8W_{48}O_{184}]^{33-}$ (P8W48) and its derivatives $[H_6P_4W_{24}W_{94}]^{18-}$ (P4W24) and $[\alpha-H_2P_2W_{12}O_{48}]^{12-}$ (P2W12)

The single-crystal X-ray structure for the $[P_2W_{18}O_{62}]^{6-}$ polyanion indicated that the eighteen metal centers are not equivalent. Thus, the distinction was made between the α_2 positions for the cap tungstens and the α_1 positions for the belt tungstens. The two caps in this Wells–Dawson structure are composed of three edge-shared MO_6 (M = W, Mo) octahedra, whereas the two equatorial belts are formed *via* alternating corner- and edge-shared MO_6 units. In 1979 Acerete showed by ^{183}W solution NMR that the β geometrical isomer of $[P_2W_{18}O_{62}]^{6-}$ differs from the α isomer by a 60° rotation of one W_3O_{13} cap.[40,41] The Wells–Dawson derivative can be seen as a derivative of the Keggin structure; the removal of a corner-shared W_3O_{13} triad from $[\alpha-PW_{12}O_{40}]^{3-}$ produces a lacunary structure formulated as $[A-\alpha-PW_9O_{34}]^{9-}$, which combines with another equivalent moiety to form the $[\alpha-P_2W_{18}O_{62}]^{6-}$ assembly.

Careful solution studies by Contant and Tézé on the chemistry of the complete (plenary) $[\alpha-P_2W_{18}O_{62}]^{6-}$ polyanion showed that upon basification a hydrolytic cleavage of W–O (W) bonds occurs, resulting in a mixture of the monovacant (lacunary) species $[\alpha_1-P_2W_{17}O_{61}]^{10-}$ and $[\alpha_2-P_2W_{17}O_{61}]^{10-}$,

Sib Sankar Mal

Dr Sib Sankar Mal received his Ph.D. degree in Chemistry from Jacobs University, Bremen, in 2008, under the supervision of Prof. Ulrich Kortz. Then he did postdoctoral work at the University of Ottawa, Canada, in 2011, and then moved to Hamburg University, Germany, as an Alexander von Humboldt postdoctoral fellow. After completing his postdoctoral work, he joined as an Assistant professor at the National Institute of Technology Karnataka, India, in 2013, where he is currently serving as an Associate professor in the Department of Chemistry. His primary research areas are energy storage, energy conversion, renewable energy, electrochemistry, catalysis, and polyoxometalates.

Abhishek Banerjee

Dr Abhishek Banerjee received his Ph.D. degree in Chemistry from Jacobs University, Bremen, Germany in 2012, under the supervision of Prof. Ulrich Kortz. After postdoctoral research work at Northwestern University, Evanston, USA, with Prof. Mercouri G. Kanatzidis, he joined Visvesvaraya National Institute of Technology, Nagpur, India in 2016, as an Assistant Professor. His primary research areas are in energy conversion, energy storage and oxidative catalysis using organic oxo-thiometalates. He is the recipient of several awards, including special Ph.D. distinction from Jacobs University, Bremen, Germany as well as Early Career Research Award from Science and Engineering Research Board (SERB), India.

respectively. Further, if the final pH is kept between 4 and 6, the $[\alpha_1\text{-}P_2W_{17}O_{61}]^{10-}$ anion is observed to transform to the $[\alpha_2\text{-}P_2W_{17}O_{61}]^{10-}$ anion readily.[42] At about pH 10, the trilacunary polyanion $[P_2W_{15}O_{56}]^{12-}$ is formed.[42] Alternatively, in the presence of tris(hydroxymethyl)aminomethane (tris base), the plenary $[\alpha\text{-}P_2W_{18}O_{62}]^{6-}$ transforms to the hexavacant polyanion $[\alpha\text{-}H_2P_2W_{12}O_{48}]^{12-}$ (P_2W_{12}).[42] This P_2W_{12} is labile and transforms quickly in aqueous, acidic medium to either the unstable, monolacunary polyanion $[\alpha_1\text{-}P_2W_{17}O_{61}]^{10-}$, which successively rearranges to either the more stable $[\alpha_2\text{-}P_2W_{17}O_{61}]^{10-}$,[42] or the large cyclic polyanion $[H_7P_8W_{48}O_{184}]^{40-}$ (P_8W_{48}).[43] Additionally, Contant and Tézé have revealed that two P_2W_{12} can be connected end-on to form the dimeric $[H_6P_4W_{24}O_{94}]^{18-}$ (P_4W_{24}) species in aqueous solution.[43] However, the exact linkage of the two P_2W_{12} units is still unknown.[44]

Lacunary derivatives of the plenary Wells–Dawson ion $[\alpha\text{-}P_2W_{18}O_{62}]^{6-}$ and their related terminology (α, α_1, α_2) have been thoroughly investigated by Contant.[42] More recently, Poblet and Cronin have studied the different rotational isomerisms of non-classical Wells–Dawson anions with different heteroatoms based on theoretical and mass spectrometry techniques.[45]

2.1 The metastable, hexalacunary $[\alpha\text{-}H_2P_2W_{12}O_{48}]^{12-}$ (P_2W_{12})

The hexalacunary 12-tungsto-2-phosphate P_2W_{12} is generated by the treatment of $[\alpha\text{-}P_2W_{18}O_{62}]^{6-}$ by tris(hydroxymethyl)aminomethane (tris base). The formation of P_2W_{12} can be visualized by removing six tungsten-oxo groups (W-O$_t$), one from each of the two caps and two from each of the two belts. The P_2W_{12} was first identified by Contant in 1985, who proved its existence by ^{31}P NMR (−8.6 ppm) in lithium chloride solution. The polyanion structure can be inferred from that of the cyclic

Prof. Ulrich Kortz performed Ph. D. studies at Georgetown University in Washington, DC under the supervision of Michael T. Pope (1990–1995). Then he did postdoctoral studies with Dante Gatteschi in Florence, Italy (1995–1996) as well as André Tézé and Gilbert Hervé in Versailles, France (1996–1997). In 1997 he started his independent academic career at the American University of Beirut (AUB) in Lebanon. In 2002 he joined Constructor University (formerly International University Bremen and Jacobs University Bremen) as Associate Professor and in 2007 became Full Professor. His research interests include synthetic inorganic and organometallic chemistry, structural chemistry, polyoxometalates, MOFs, catalysis, magnetism, and electrochemistry.

Ulrich Kortz

tetramer P_8W_{48}. This is due to the fact that P_2W_{12} is labile and readily undergoes rearrangement in aqueous, acidic medium to the more stable monolacunary $[\alpha_2\text{-}P_2W_{17}O_{61}]^{10-}$,[42] or cyclic P_8W_{48},[43] as stated earlier. As such, the ^{183}W NMR spectrum of this polyanion is not clean due to the presence of one or more transformation products in solution simultaneously, as Baker reported.[46] Very recently, the polyanion P_2W_{12} was characterized by single-crystal X-ray diffraction studies, as well as a W-bridged dimer and trimer.[47,48] Due to the presence of six lacunary sites in P_2W_{12}, the reactivity of this polyanion with guest metal ions has been explored in some detail, as will be discussed subsequently (*vide infra*, section 3).

2.2 The dimeric, multilacunary $[H_6P_4W_{24}O_{94}]^{18-}$ (P_4W_{24})

The P_4W_{24} polyanion has been known since 1985,[43] and very likely it comprises of two P_2W_{12} units, which are linked in a C- or S-shaped fashion, resulting in structures with C_{2v} or C_{2h} symmetry in solution (Fig. 1).[43] The ^{31}P and ^{183}W NMR spectra have proven the coexistence of both such forms in solution.[40,41,46,49] Only a few polyanions have been reported based on the dimeric P_4W_{24} unit till date. In 1998, Roussel *et al.* investigated the structure of P_4W_{24} by single-crystal X-ray diffraction studies and electron microscopy, which suggested P_4W_{24} to be a phosphate-containing derivative of a polyoxotungstate with the chemical formula $(PO_4)_4(WO_3)_{2m}$ ($m = 12$).[50]

2.3 The crown-shaped, superlacunary $[H_7P_8W_{48}O_{184}]^{33-}$ (P_8W_{48})

The crown-shaped polyanion $[H_7P_8W_{48}O_{184}]^{33-}$ (P_8W_{48}) comprises of four P_2W_{12} subunits, which are linked *via* the caps in a cyclic fashion, resulting in a structure with idealized D_{4h} symmetry (Fig. 2). The structural elucidation of the polyanion by single-crystal XRD showed the presence of eight potassium ions within the central cavity. This suggests a templating effect of the alkali ions, which may play an important role in the formation process of this cyclic polyanion. The P_8W_{48} is stable over a broad pH range (*ca.* 1–8), which represents a remarkable stability in POM chemistry. The presence of potassium ions inside the polyanion crown decreases the solubility of the salt and increases the tendency towards aggregation in solution, causing precipitation. Cronin reported two K-free salts of P_8W_{48}.[51]
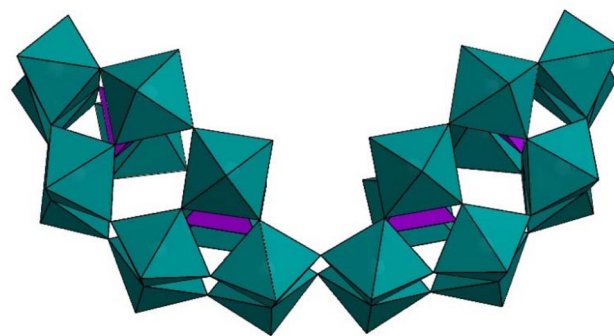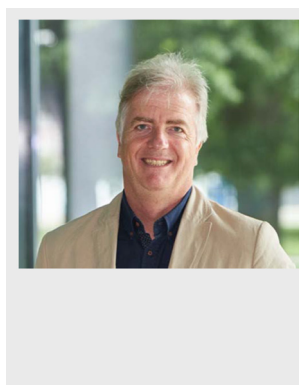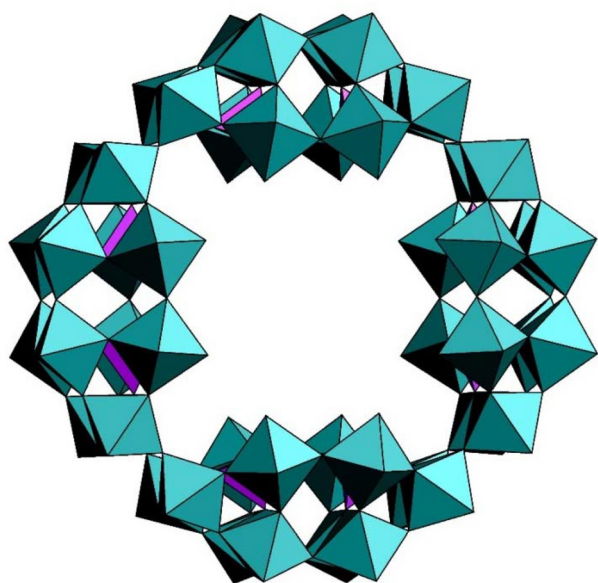

Fig. 1 Polyhedral representation of the C-shaped isomer of P_4W_{24}. Color code: WO$_6$ octahedra (green), PO$_4$ tetrahedra (pink).

Fig. 2 Polyhedral representation of P_8W_{48}. Color code: WO_6 octahedra (green), PO_4 tetrahedra (pink).[51]
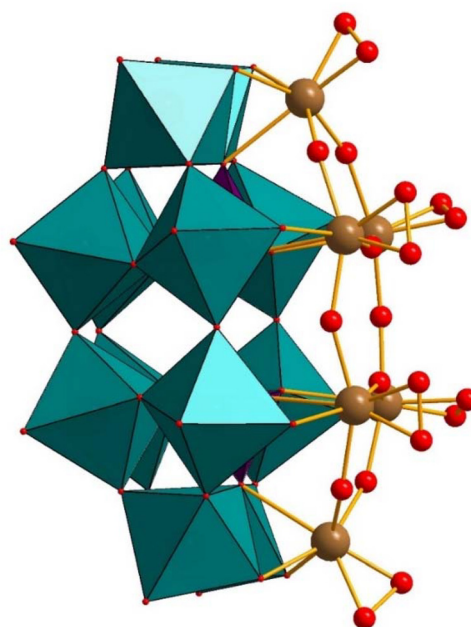

Fig. 3 Combined polyhedral/ball-and-stick representation of the peroxo-Nb polyanion $[P_2W_{12}(NbO_2)_6O_{56}]^{12-}$ ($P_2W_{12}(NbO_2)_6$). Color code: WO_6 octahedra (green), PO_4 tetrahedra (pink), O (red), Nb (brown).[53]

3. Metal complexes of $[\alpha\text{-}H_2P_2W_{12}O_{48}]^{12-}$

3.1 Monomeric structures

To date, only a limited number of transition metal-containing derivatives of P_2W_{12} have been reported.[52] Hill reported the peroxo-niobium-containing derivative $[P_2W_{12}(NbO_2)_6O_{56}]^{12-}$ ($P_2W_{12}(NbO_2)_6$), see Fig. 3.[53] This peroxo-polyanion was reported to be unstable both in solution and in the solid-state in the absence of hydrogen peroxide. However, the formation of $P_2W_{12}(NbO_2)_6$ in the presence of H_2O_2 has been demonstrated using several spectroscopic methods, such as infrared spectroscopy (IR), fast atom bombardment-mass spectroscopy (FAB-MS), and ^{31}P and ^{183}W NMR spectroscopy. The $P_2W_{12}(NbO_2)_6$ polyanion was prepared by the reaction of P_2W_{12} with the Lindqvist-type isopolyanion $[Nb_6O_{19}]^{8-}$ in the presence of aqueous H_2O_2 as an oxidant. The six Nb atoms in $P_2W_{12}(NbO_2)_6$ are connected by η^2-O ligands, and each has a terminal, side-on peroxo ligand.

In 2002, Nadjo reported the synthesis and characterization of five mixed 3d (Fe, Cu)-4d (Mo) metal-containing P_2W_{12}-based polyanions: $\alpha_2\text{-}[P_2W_{12}Fe(OH_2)Mo_5O_{61}]^{7-}$ ($P_2W_{12}FeMo_5$) and $\alpha_2\text{-}[P_2W_{13}Fe(OH_2)Mo_4O_{61}]^{7-}$ ($P_2W_{13}FeMo_4$), α_1- and α_2-$[P_2W_{12}Cu(OH_2)Mo_5O_{61}]^{8-}$ ($P_2W_{12}CuMo_5$) and $\alpha_2\text{-}[P_2W_{13}Cu(OH_2)Mo_4O_{61}]^{8-}$ ($P_2W_{13}CuMo_4$).[54] These compounds were characterized by IR, UV-vis, and ^{31}P NMR spectroscopy. No XRD structures could be obtained, but in particular, IR and ^{31}P NMR spectroscopy were useful tools for purifying the Fe^{3+} and Cu^{2+}-substituted derivatives. The authors have also studied the electrocatalytic properties of these polyanions, and the Cu and Fe-substituted derivatives showed good activity for the electrocatalytic reduction of nitrate.[55–57]

Gouzerh reported dimeric 3d transition metal (Fe^{3+}, Co^{2+}, Mn^{2+}, Ni^{2+}) containing derivatives of P_2W_{12}. The iron(III)-containing polyanion $[H_4P_2W_{12}Fe_9O_{56}(CH_3COO)_7]^{6-}$ ($Fe_9P_2W_{12}$), see Fig. 4a, was prepared by a simple one-pot reaction of P_2W_{12} with an excess of iron(III) chloride in aqueous solution containing lithium chloride and lithium acetate, at room temperature.[58] The monomeric $Fe_9P_2W_{12}$ structure is derived from P_2W_{12} by filling the six vacant sites with iron atoms, with the now-formed plenary Wells–Dawson type species $\{P_2W_{12}Fe_6\}$ having three additional iron(III) atoms grafted onto the hexa-iron-oxo face of the polyanion, resulting in $Fe_9P_2W_{12}$, which has idealized C_2 symmetry. Magnetic susceptibility measurements on $Fe_9P_2W_{12}$ showed intramolecular antiferromagnetic coupling between the two high-spin Fe^{3+} centers.

3.2 Dimeric structures

Upon further investigation of the Fe^{3+} and P_2W_{12} system by Gouzerh, it was observed that lowering the $Fe^{3+}:P_2W_{12}$ ratio and the solution pH, as well as prolonged heating, led to the formation of dimeric polyanions with the general formula $[H_yP_4W_{28+x}Fe_{8-x}O_{120}]^{(28-y-3x)-}$.[59] These species have extra tungsten atoms in the new polyanions (with slight variations in the value of x), which have been isolated as different salts. The polyanion $[H_{12}P_4W_{28}Fe_8O_{120}]^{16-}$ ($Fe_8P_4W_{28}$) comprises two $\{P_2W_{14}Fe_4\}$ units linked via Fe–O–Fe′ bonds, resulting in a cubic Fe_8 topology. The $Fe_8P_4W_{28}$ is formed by reaction of P_2W_{12} with hydrous iron(III) oxide or iron(III) acetate $[Fe_3O(OAc)_6(H_2O)_3]Cl\cdot5H_2O$.[58]

An extra tungsten atom arising from the decomposition of P_2W_{12} in situ or upon deliberate addition of tungstate to the

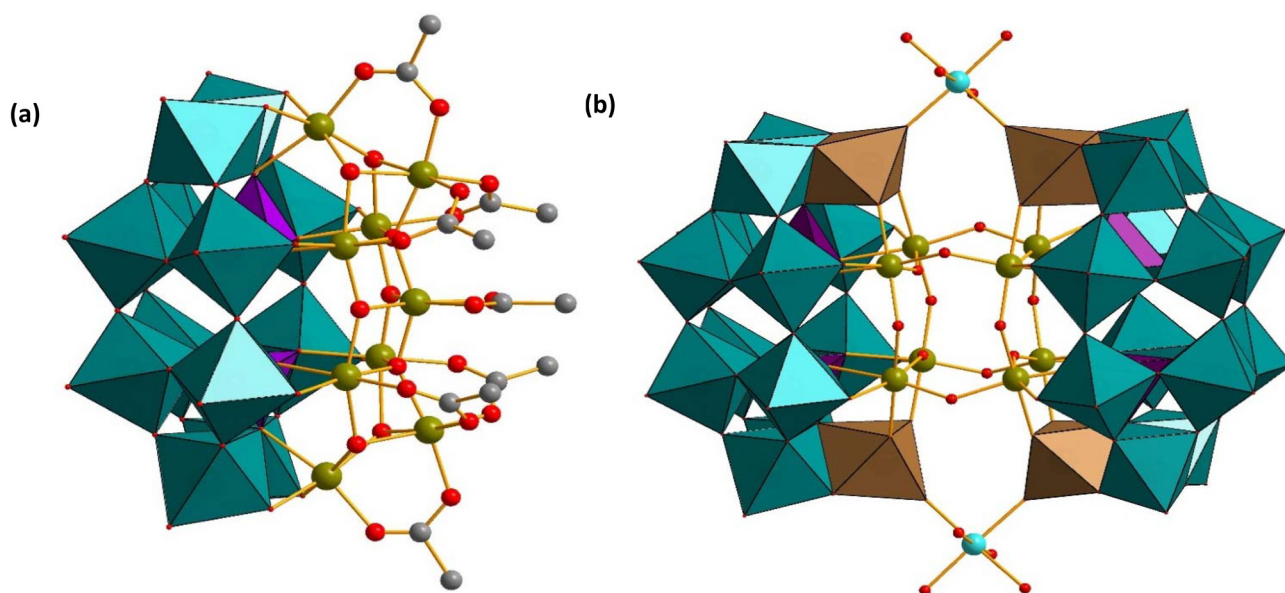**Fig. 4** Combined polyhedral/ball-and-stick representations of (a) $[H_4P_2W_{12}Fe_9O_{56}(CH_3COO)_7]_6^-$ (**Fe$_9$P$_2$W$_{12}$**), and (b) [{M (H$_2$O)$_4$}$_2${H$_{12}$P$_4$W$_{28}$Fe$_8$O$_{120}$}]$^{12-}$ (M = Co^{2+}, Mn^{2+}, Ni^{2+}). Color code: WO$_6$ octahedra (green and brown), PO$_4$ tetrahedra (pink), Fe (green), M (turquoise), O (red), C (grey). H atoms on carbon have been omitted for clarity.[58,59]

reaction mixture competes with the added metal ions, as has been observed in the reactions with lanthanide ions.[60,61] Frequently, adding of extra tungstate to the reaction mixture is not essential for the formation of such structures.[61] The cyclic voltammogram (CV) of the polyanion **Fe$_8$P$_4$W$_{28}$** displays four reduction waves. The first one at −0.32 V *vs.* SCE is attributed to the reduction of Fe^{3+} to Fe^{2+}.

A polyanion with the composition $[H_yP_4W_{28+x}Fe_{8-x}O_{120}]^{(28-y-3x)-}$ ($x \approx 2$) was characterized among the products obtained from a 1 : 4 : 2 aqueous mixture of **P$_2$W$_{12}$**, sodium tungstate, and iron(III) chloride at pH 4.2.[59] When **P$_2$W$_{12}$** is reacted with the mixed-metal complexes $[Fe_2^{III}M^{II}O(OAc)_6(H_2O)_3]$ (M = Co^{2+}, Mn^{2+}, Ni^{2+}), the polyanions $[\{M(H_2O)_4\}_2\{H_{12}P_4W_{28}Fe_8O_{120}\}]^{12-}$ (**M$_2$Fe$_8$P$_4$W$_{28}$**) (Fig. 4b) (M = Co^{2+}, Mn^{2+}, Ni^{2+}) are obtained, together with **Fe$_8$P$_4$W$_{28}$**.[59] These compounds were isolated as potassium salts. Magnetic susceptibility measurements on **Co$_2$Fe$_8$P$_4$W$_{28}$** are consistent with two non-interacting Co^{2+} centers, suggesting that the ground state of the Fe$_8$P$_4$W$_{28}$ unit is diamagnetic, along with the intramolecular antiferromagnetic coupling of the eight Fe^{3+} centers. In contrast, the parent polyanion **Fe$_8$P$_4$W$_{28}$** showed weak magnetization, arising either from paramagnetic impurities or a partial substitution of Fe for W.[59] The cyclic voltammogram indicated that the Co^{2+} centers are not electrochemically active in the potential range investigated.

Wang and coworkers investigated the reactivity of **P$_2$W$_{12}$** with Co^{2+} ions in an aqueous acidic medium. A new heart-shaped dimeric Co^{2+}-containing polyanion $[\{W_2Co_2O_8(H_2O)_2\}(P_2W_{12}O_{46})_2]^{20-}$ (**W$_2$Co$_2$(P$_2$W$_{12}$)$_2$**) was synthesized and structurally characterized by IR spectroscopy, thermogravimetry, electrochemistry, and single-crystal X-ray diffraction.[62] The

polyanion **W$_2$Co$_2$(P$_2$W$_{12}$)$_2$** comprises two subunits of **P$_2$W$_{12}$**, which are fused *via* four W–O–W bonds and grafting of two W and two Co atoms in the vacant positions. This type of W–O–W connectivity was observed for the first time by Kortz and coworkers in the dimethyletin-containing tungstophosphate [{Sn (CH$_3$)$_2$}$_4$(H$_2$P$_4$W$_{24}$O$_{92}$)$_2$]$^{28-}$ (*vide infra*, section 4). Notably, all the addenda positions in **W$_2$Co$_2$(P$_2$W$_{12}$)$_2$** are disordered in the cluster.

Very recently, a dimeric mixed-addenda Nb/W polyanion, $[H_6P_2W_{12}Nb_4O_{59}(NbO_2)_2]_2^{8-}$ (**P$_2$W$_{12}$Nb$_4$(NbO$_2$)$_2$)$_2$**), has been isolated under acidic condition by Yue, He, and coworkers.[63] This Nb-peroxo-containing polyanion was synthesized by the reaction of K$_7$H[Nb$_6$O$_{19}$]·13H$_2$O and **P$_2$W$_{12}$** in sodium formate buffer in the presence of H$_2$O$_2$. The polyanion was characterized by single-crystal X-ray diffraction and elemental analysis. The structure revealed that six Nb atoms occupy the vacant sites of the hexalacunary **P$_2$W$_{12}$** precursor to form a {P$_2$W$_{12}$Nb$_6$(O$_2$)$_2$} mixed-addenda subunit. Two such {P$_2$W$_{12}$Nb$_6$(O$_2$)$_2$} subunits are joined by two Nb–O–Nb bridges at the belt positions to form a dimeric unit. This polyanion, **(P$_2$W$_{12}$Nb$_4$(NbO$_2$)$_2$)$_2$**, is structurally different from the Nb-peroxo polyanions reported by Hill and coworkers, for example, **P$_2$W$_{12}$(NbO$_2$)$_6$**, as discussed in section 3.1 (*vide supra*).[53] In **P$_2$W$_{12}$(NbO$_2$)$_6$** structure, all niobium atoms have terminal peroxo ligands and exist as a six-membered Nb-peroxo monomer; whereas in **(P$_2$W$_{12}$Nb$_4$(NbO$_2$)$_2$)$_2$**, only two niobium ions have peroxo ligands, and the polyanion is a dimer. A common feature for both polyanions was that the polyanions aggregated to larger species when the peroxo groups in either P$_2$W$_{12}$Nb$_4$(NbO$_2$)$_2$ or P$_2$W$_{12}$(NbO$_2$)$_6$ were removed by heating or chemical reduction.[64-66]
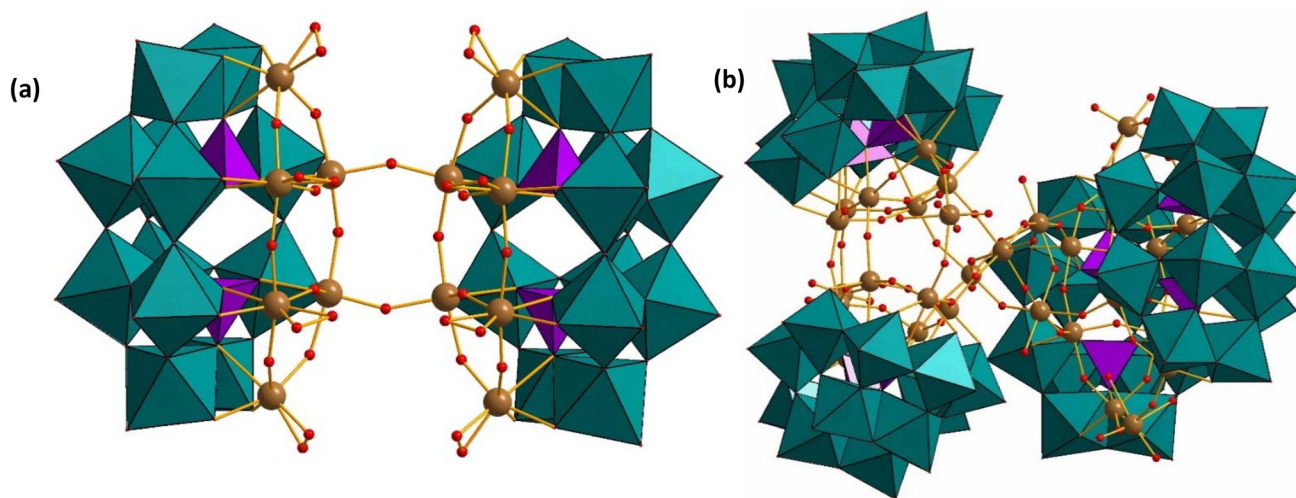
Fig. 5 Combined polyhedral, ball-and-stick representations of (a) $[H_{13}\{Nb_6(O_2)_4P_2W_{12}O_{57}\}_2]^{7-}$ and (b) $[H_{14}\{P_2W_{12}Nb_7O_{63}(H_2O)_2\}_4\{Nb_4O_4(OH)_6\}]^{16-}$, respectively. Color code: WO_6 octahedra (green), PO_4 tetrahedra (pink), Nb (brown), O (red).[67]

In 2015, Niu, Wang, and coworkers reported two new multi-Nb-containing POM structures, $[H_{13}\{Nb_6(O_2)_4P_2W_{12}O_{57}\}_2]^{7-}$ **($P_2W_{12}Nb_6(O_2)_4)_2$** (Fig. 5a) and $[H_{14}\{P_2W_{12}Nb_7O_{63}(H_2O)_2\}_4\{Nb_4O_4(OH)_6\}]^{16-}$ **($P_2W_{12}Nb_7)_4Nb_4$** (Fig. 5b).[67] Interestingly, **($P_2W_{12}Nb_7)_4Nb_4$** has the highest nuclearity of all niobium-containing heteropolyanions to date. The polyanion **$\{P_2W_{12}Nb_6(O_2)_4\}_2$** is a di-Nb–O–Nb-linked dimer of two **P_2W_{12}** units with the six vacant sites of each **P_2W_{12}** unit occupied by four niobium-peroxo groups (NbO$_2$) and two niobium-oxo groups (Nb–O). Further, **($P_2W_{12}Nb_7)_4Nb_4$** comprises dimeric $[P_4W_{24}Nb_{14}O_{126}(H_2O)_4]^{18-}$ subunits and an adamantane-like Nb$_4$O$_6$ core. The $[P_4W_{24}Nb_{14}O_{126}(H_2O)_4]^{18-}$ subunit in **($P_2W_{12}Nb_7)_4Nb_4$** comprises two $[Nb_6P_2W_{12}O_{61}]^{10-}$ units without any niobium-peroxo groups. The $[Nb_6P_2W_{12}O_{61}]^{10-}$ units are connected through Nb–O–Nb bridges. The adamantane-like $\{Nb_4O_6\}$ core is composed of four niobium metal atoms connected by oxo ligands. The authors have demonstrated that careful synthetic control can stabilize the $(Nb_6P_2W_{12})$ fragment in both polyanions as a dimer or a tetramer. Moreover, ^{31}P and ^{183}W NMR spectra indicated that **($P_2W_{12}Nb_7)_4Nb_4$** is stable in solution. The photocatalytic activity for H$_2$ evolution has been studied for both polyanions, and **($P_2W_{12}Nb_7)_4Nb_4$** exhibited good activity.

In 2018, Kögerler and coworkers reported an open dimeric structure based on the **P_4W_{24}** unit with $\{P_4W_{24}O_{29}\}$ being capped by two phenyl phosphonate or -arsonate ligands, $[(PhXO)_2P_4W_{24}O_{92}]^{16-}$ (X = P, As) (**PhXOP$_4$W$_{24}$**).[68] In 2006, Kortz and coworkers have also reported P$_4$W$_{24}$ units in the dimethyltin-grafted polyanion $[\{Sn(CH_3)_2\}_4(H_2P_4W_{24}O_{92})_2]^{28-}$ (**Sn (CH$_3$)$_2$P$_4$W$_{24}$**) (*vide infra*).[44] For **PhXOP$_4$W$_{24}$**, the ^{31}P NMR spectra confirm a stabilizing effect on the **P$_4$W$_{24}$** unit due to the presence of the two phoshonate/arsonate ligands. Further studies on the incorporation of Co^{2+} ions into the central cavity of **PhXOP$_4$W$_{24}$** resulted in the formation of $[\{(H_2O)_4Co\}$

$(PhXO)_2P_4W_{24}O_{92}]^{14-}$ units linked into an infinite 1D chain in the solid state *via* additional "outer" Co^{2+} centers.

Very recently, the same group reported an unprecedented discrete dimeric polyanion $[\{(o\text{-}H_2N\text{-}C_6H_4\text{-}AsO_3)_4P_4W_{24}O_{85}]^{14-}$ (**(o-NH$_2$-C$_6$H$_6$-AsO)$_4$P$_4$W$_{24}$O$_{92}$**), by the condensation reaction of o-aminophenylarsonic and **P$_2$W$_{12}$** in acidic media. The polyanion **(o-NH$_2$-C$_6$H$_6$-AsO)$_4$P$_4$W$_{24}$O$_{92}$** was further reacted with divalent transition metal ions Mn^{2+}, Co^{2+}, Ni^{2+}. The introduction of the divalent transition metal ions in the reaction mixture resulted in V-shaped one-dimensional (1D) coordination polymeric polyanions $[\{M(H_2O)_4\}P_4W_{24}O_{92}(C_6H_6AsNO)_2]^{14-}$ (M = Mn^{2+}, Co^{2+}, Ni^{2+}) (**M(o-NH$_2$-C$_6$H$_6$-AsO)$_2$P$_4$W$_{24}$**),[69,70] where a similar type of structure was first observed by Kortz group (*vide infra*). Each monomeric unit of **(o-NH$_2$-C$_6$H$_6$-AsO)$_4$P$_4$W$_{24}$O$_{92}$** consists of **P$_2$W$_{12}$**, comprising two **PW$_4$O$_{21}$** belts capped with two W$_2$O$_{10}$ units linked through oxygen atoms. The transition metal complex **M(o-NH$_2$-C$_6$H$_6$-AsO)$_2$P$_4$W$_{24}$** exhibits dimeric anionic assembly and coordinates one oxygen atom from the upper PW$_4$O$_{21}$ belt of each P$_2$W$_{12}$L subunits.

3.3 Trimeric structures

In 2008, Wang and coworkers were able to isolate three trimeric polyoxotungstates upon the reaction of 3d metal ions with **P$_2$W$_{12}$** at different pH, $[K_3\subset\{Mn(H_2O)_4\}_2\{WO_2(H_2O)_2\}_2\{WO(H_2O)\}_3(P_2W_{12}O_{48})_3]^{19-}$ (**Mn$_2$(P$_2$W$_{12}$)$_3$W$_5$**) (Fig. 6), K$_3$Na$_7$Li$_{5.5}$Ni$_{0.25}$ $[Na_3\subset\{Ni_{3.5}(H_2O)_{13}\}\{WO_2(H_2O)_2\}_2\{WO(H_2O)\}_3(P_2W_{12}O_{48})_3]$·64H$_2$O (**Ni$_{3.5}$(P$_2W_{12}$)$_3W_5$**), and $[Na_3\subset\{Cu_3(H_2O)_9\}\{WO_2(H_2O)_2\}_2\{WO(H_2O)\}_3(P_2W_{12}O_{48})_3]^{17-}$ (**Cu$_3$(P$_2$W$_{12}$)$_3$W$_5$**).[71] These polyanions were prepared by reaction of the corresponding transition metal salts (Mn^{2+}, Ni^{2+}, and Cu^{2+}) with **P$_2$W$_{12}$** and Na$_2$WO$_4$ in aqueous acidic solutions. The polyanion **Mn$_2$(P$_2$W$_{12}$)$_3$W$_5$** was obtained in a pH 4.0 solution, whereas the other two polyanions **Ni$_{3.5}$(P$_2$W$_{12}$)$_3$W$_5$** and **Cu$_3$(P$_2$W$_{12}$)$_3$W$_5$** were obtained in the pH
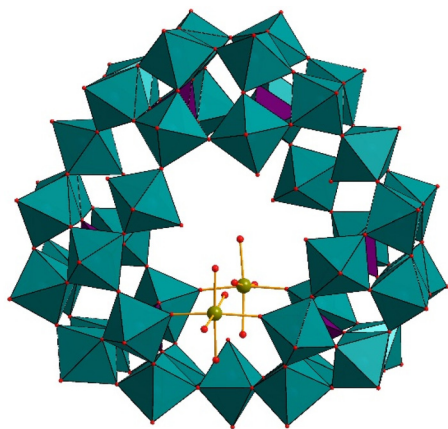
Fig. 6 Combined polyhedral/ball-and-stick representation of $[K_3 \subset \{Mn(H_2O)_4\}_2\{WO_2(H_2O)_2\}_2\{WO(H_2O)\}_3(P_2W_{12}O_{48})_3]^{19-}$. Color code: WO_6 octahedra (green), PO_4 tetrahedra (pink), Mn (teal), O (red).[71]

range 1.5–2.5.[71] As based on the formula, the Ni-containing polyanion appears to be a mixture of at least two species.

Yao *et al.* suggested that the pH plays an important role in forming these P_2W_{12}-based heteropolytungstates.[72] Upon further decreasing the pH to 1.0, they were able to isolate two new compounds, $[Na_3 \subset \{Co(H_2O)_4\}_6\{WO(H_2O)\}_3(P_2W_{12}O_{48})_3]^{15-}$ (**Co₆(P₂W₁₂)₃W₃**), and $[Na_3 \subset \{Ni(H_2O)_4\}_6\{WO(H_2O)\}_3(P_2W_{12}O_{48})_3]^{15-}$ (**Ni₆(P₂W₁₂)₃W₃**).[72] It is worth mentioning that all the vacant sites in **Co₆(P₂W₁₂)₃W₃** and **Ni₆(P₂W₁₂)₃W₃** are occupied by the 3d metal ions. Therefore, it is observed that a lower pH facilitates the combination of more transition metal atoms encapsulated within the $\{(P_2W_{12})_3W_3\}$ shell. All these polyanions have crown-type structures, comprising three P_2W_{12} subunits linked by three $\{WO(H_2O)\}$ fragments in a corner-sharing arrangement, resulting in the trimeric cluster $[P_6W_{39}O_{147}(H_2O)_3]^{30-}$ (abbreviated as **P₆W₃₉**). In such crown-shaped polyanions, the three W atoms in the hinges are all in a hexa-coordinated environment, with all transition metal atoms also fully coordinated. The six vacant sites on the polyanion **Mn₂(P₂W₁₂)₃{WO₂(H₂O)₂}{WO(H₂O)}₃** are occupied by two W^{VI} atoms, two Mn^{2+} ions, and two potassium counter cations, respectively. For the polyanion **Ni₃.₅(P₂W₁₂)₃{WO₂(H₂O)₂}₂{WO(H₂O)}₃**, two W^{VI} and four Ni^{2+} atoms fill up the six vacant sites of the **P₆W₃₉** shell, with all the Ni^{2+} centers fully occupied, except the Ni5 position which exhibits a crystallographic site-occupancy disorder with a Na atom, resulting in a total of two W^{VI} and 3.5 Ni^{2+} ions being incorporated in the structure. In a similar sense, for the polyanion **Cu₃(P₂W₁₂)₃{WO₂(H₂O)₂}₂{WO(H₂O)}₃**, two W^{VI} and four Cu^{2+} guest atoms occupy the six vacant sites of the **P₆W₃₉** unit. However, all these metal sites, except W40, also have site-occupancy disorder, resulting in two W^{VI} and 2.75 Cu^{2+} atoms as guests in the host structure.

More recently, Wang and coworkers have reported mixed 3d/4f metal ion-based **P₆W₃₉** structures, $[K_3 \subset \{GdMn(H_2O)_{10}\}\{HMnGd_2(tart)O_2(H_2O)_{15}\}\{P_6W_{42}O_{151}(H_2O)_7\}]^{11-}$ (**{MnGd}(HMn-**

$Gd_2P_6W_{42}\}_\infty$) and $[K_3 \subset \{GdCo(H_2O)_{11}\}_2\{P_6W_{41}O_{148}(H_2O)_7\}]^{13-}$ (**CoGdP₆W₄₁**)$_\infty$, with organic guests (tartrate and $(CH_3)_2NH \cdot HCl$ respectively).[73] According to the authors, the introduction of such secondary organic ligands stabilizes the lanthanide atoms and/or reduces the reactivity of the lanthanide atoms with the polyanions. The crown-shaped **P₆W₃₉** is formed by the encapsulation of transition metal and lanthanide atoms inside the cavity of the polyanion. The polyanion (**MnGd**)(**HMnGd₂P₆W₄₂**)$_\infty$ forms two-dimensional porous frameworks through the Gd and Mn linkers, whereas the polyanion (**CoGdP₆W₄₁**)$_\infty$ forms a one-dimensional chain linked through Gd ions, which exhibit a square-antiprismatic geometrical environment. These are the first POM structures comprising mixed lanthanide and transition metal atoms. Wang, Niu, and coworkers have isolated a trimeric assembly of **P₂W₁₂** units joined by Cr-atoms, $[H_{23}(Cr(H_2O)_2)_3(H_2P_2W_{12}O_{48})_3]^{4-}$ (**Cr₃(P₂W₁₂)₃**).[74] The structure bears similarity with a trimeric $\{P_6W_{39}\}$ unit, except that Cr has replaced the W-atoms.

3.4 Tetrameric structures

Following Gouzerh's report of the metastable polyanion **Fe₉(OAc)₇P₂W₁₂** (section 3.1, *vide supra*), which was isolated as a lithium–potassium salt,[58] subsequent heating of this polyanion in aqueous sodium acetate solution transformed it into different compounds, which were successively isolated as sodium–potassium salts, such as $Na_{16}K_{12}[H_{56}P_8W_{48}Fe_{28}O_{248}]$ (**Fe₂₈P₈W₄₈**) and $Na_{16}K_{10}[H_{55}P_8W_{49}Fe_{27}O_{248}]$ (**Fe₂₇P₈W₄₉**).[58] The polyanion **Fe₂₈P₈W₄₈** was characterized by electrochemistry and magnetic measurements and by determination of the unit cell parameters. Subsequently, the formula of the polyanion **Fe₂₇P₈W₄₉** was proposed on the basis of an X-ray diffraction study. Godin *et al.* hinted at other novel compounds' formation by lowering either the pH or the $Fe^{3+}:P_2W_{12}$ ratio. However, IR spectroscopy and chemical analysis were insufficient to determine the composition and purity of these species. The polyanion **Fe₂₇P₈W₄₉** comprises four $\{P_2W_{12}Fe_6\}$ units, each bridged through Fe–O–Fe linkages to an $\{Fe_4O_6\}$ cluster core. The linkage is through pairs of three Fe–O–Fe bridges involving the three outer iron atoms. According to crystallographic refinement, the polyanion **Fe₂₇P₈W₄₉** seems to have 25% W and 75% Fe occupancy, suggesting a mixture of polyanions. The polyanion exhibits antiferromagnetic coupling between the Fe^{3+} centers (Fig. 7).

Wang and coworkers have reported the 3d transition metal (Co^{2+}, Ni^{2+}) modified $\{P_8W_{49}\}$ polyanions $\{[Co(H_2O)_2Cl][Co(H_2O)_3]_2[Co(H_2O)_5]_{1.5}[Co(H_2O)_3H_4P_8W_{49}O_{187}(H_2O)]\}^{26-}$ (**[Co(H₂O)₂][Co(H₂O)₃]₂[Co(H₂O)₅]₁.₅P₈W₄₉**) and $\{[Ni(H_2O)_3]_2\{[Ni(H_2O)_3]_{1.5}H_3P_8W_{49}O_{187}(H_2O)]\}^{30-}$ (**[Ni(H₂O)₃]₂[Ni(H₂O)₃]₁.₅P₈W₄₉**), respectively, by the reaction of **P₂W₁₂** with the respective transition metal salt.[75] The transformation from **P₂W₁₂** to **P₈W₄₉** happens during the reaction performed in an aqueous acidic medium. The structural arrangements of Co^{2+} and Ni^{2+} in **[Co(H₂O)₂][Co(H₂O)₃]₂[Co(H₂O)₅]₁.₅P₈W₄₉** and **[Ni(H₂O)₃]₂[Ni(H₂O)₃]₁.₅P₈W₄₉** are different from that of several other Mn^{2+} complexes reported by Cronin's and Proust's groups (see section 5).[21,76,77]

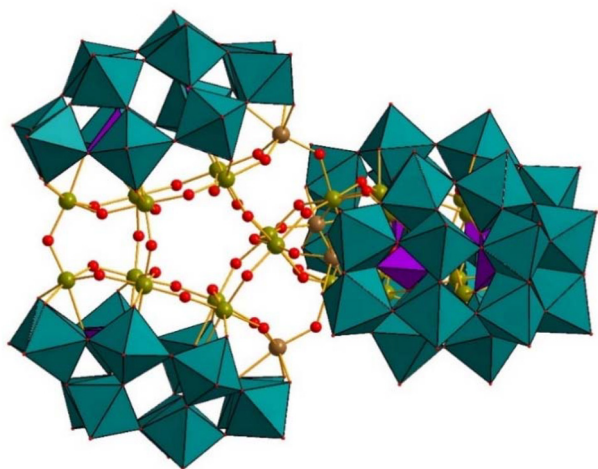**Fig. 7** Combined polyhedral/ball-and-stick representation of $[H_{55}P_8W_{49}Fe_{27}O_{248}]^{27-}$. Color code: WO_6 octahedra (green), PO_4 tetrahedra (pink), O (red), Fe (green-yellow), Fe/W (brown).[58]

Fig. 8 Combined polyhedral/ball-and-stick representation of $[H_{123}Nb_{36}P_{12}W_{72}Mn^{III}_{12}Mn^{II}_3NaO_{424}]^{10-}$. Color code: WO_6 octahedra (green), W (black), Nb (yellow), MnO_6 octahedra (light pink), PO_4 tetrahedra (pink), O (red), Na (turquoise).[80]

In 2014, Niu and coworkers reported the gigantic Nb_{28} cluster encapsulated in a hexa-lacunary $\{P_2W_{12}\}$ precursor, $[\{Nb_4O_6(OH)_4\}\{Nb_6P_2W_{12}O_{61}\}_4]^{36-}$ **$((Nb_4O_6)(Nb_6P_2W_{12})_4)$**.[78] This polyanion was formed directly by controlling the reaction parameters (*e.g.*, pH, concentration, temperature) and isolated as a sodium salt. The salt was characterized by single-crystal X-ray diffraction, IR spectroscopy, and elemental analysis. The structure of **$(Nb_4O_6)(Nb_6P_2W_{12})_4$** reveals that the polyanion comprises two $[P_4W_{24}Nb_{12}O_{122}]^{20-}$ dimeric units, rotated 180° with respect to each other and connected by four Nb–O–Nb bridges, resulting in an adamantane-type $\{Nb_4O_6\}$ core.

Very recently, Zhang and coworkers have reported the formation of $Na_{24}[Mn_8(H_2O)_{32}P_8W_{48}O_{184}]\cdot58H_2O$, $K_4Na_{16}H_4[Co_8(H_2O)_{32}P_8W_{48}O_{184}]\cdot76H_2O$, and $Na_{20}H_4[Ni_8(H_2O)_{32}P_8W_{48}O_{184}]\cdot72H_2O$ **$(M_8P_8W_{48}, M = Mn^{2+}, Co^{2+}, Ni^{2+})$** by reaction of the respective divalent metal ion with the hexavalent P_2W_{12} at room temperature in aqueous solution.[79] The direct reaction of the metal ions with P_8W_{48} was not successful.

3.5 Hexameric structures

In 2015, Niu, Wang, and coworkers reported a hexameric $\{Nb_6P_2W_{12}\}$-based Mn_{15}-oxo cluster, $[H_{123}Nb_{36}P_{12}W_{72}Mn^{III}_{12}Mn^{II}_3NaO_{424}]^{10-}$ **$(Mn_{15}(Nb_6P_2W_{12})_6)$**, with single-molecule magnet (SMM) properties.[80] The polyanion structure consists of three main parts: six peroxo-free $\{Nb_6P_2W_{12}\}$ units, four $\{Mn^{III}_3\}$ trinuclear cores, and four $\{Mn^{II}\}$ hinges. The $\{Mn^{III}_3\}$ unit is made of three mutually corner-bridged $\{Mn^{III}O_6\}$ octahedra (Fig. 8). Two of the Mn···Mn distances in the trinuclear $\{Mn^{III}_3\}$ unit are observed to be identical and slightly longer or shorter than the third Mn···Mn distance, having an overall shape of an equivalent isosceles triangle. Each $\{Mn^{III}_3\}$ unit is surrounded by three Wells–Dawson $\{Nb_6P_2W_{12}\}$ units and six Mn–O–Nb bridges. Further, each $\{Mn^{II}\}$ hinge shows crystallographic positional disorder of Mn^{2+} and Na^+ (0.75 : 0.25), being coordinated by three μ_2-oxo

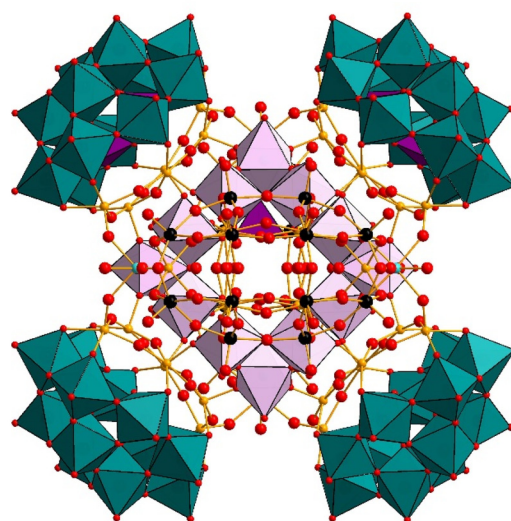groups and four-terminal oxygen atoms (water molecules), thus leading to a distorted octahedral geometry. Therefore, the authors suggest that the disordered metal centre should be formulated as $[Mn^{II}_{0.75}Na_{0.25}(H_2O)_4]^{1.75+}$.

In 2016, Mizuno and coworkers isolated a giant hexameric ring-shaped manganese-substituted polyanion, $[\{\gamma-P_2W_{12}O_{48}Mn_4(acac)_2(OAc)\}_6]^{42-}$ (acac = acetylacetonate, OAc = acetate) **$\{P_2W_{12}O_{48}Mn_4\}_6$** by reaction of the hexavacant lacunary P_2W_{12} precursor with $Mn(acac)_3$ in organic medium.[81] The polyanion **$\{P_2W_{12}O_{48}Mn_4\}_6$** is composed of six manganese-substituted monomeric $\{P_2W_{12}O_{48}Mn_4\}$ units, overall resulting in a cyclic, hexameric structure. Each $\{P_2W_{12}Mn_4\}$ monomeric unit consists of two types of Mn-coordinated ligands acetyl acetonate (acac) and acetate, respectively, so the polyanion has two different active sites. Interestingly, the hexameric polyanion transforms to the tetrameric polyanion, $[\{\gamma-P_2W_{12}O_{48}Mn_4(H_2O)_6\}_4(H_2O)_4]^{24-}$ **$\{P_2W_{12}O_{48}Mn_4\}_4$** in the absence of the organic ligands capping the manganese ions.

Following the report of Mizuno's 2016 work, Yamaguchi and coworkers in 2019 have reported the synthesis of the tetra-*n*-butylammonium (TBA) salts of a series of new isostructural divalent transition metal substituted polyanion family, $(TBA_5[\gamma-P_2W_{12}O_{44}M_2(OAc)(CH_3CONH_2)_2]\cdot nH_2O\cdot mCH_3CN$; M = Mn^{2+}, Co^{2+}, Ni^{2+}, Cu^{2+}, or Zn^{2+}; OAc = acetate) **$(\gamma-P_2W_{12}O_{44}M_2(OAc))$** including unique edge-shared bis (square-pyramidal) $\{O_2M(\mu_3-O)_2(\mu-OAc)MO_2\}$ core. The metal ions occupy the vacant belt positions of the $\gamma-P_2W_{12}$ precursor, whereas the two acetamide (CH_3CONH_2) groups stabilize the $\gamma-P_2W_{12}$ unit.[82]

3.6 Rearrangement of $[H_2P_2W_{12}O_{48}]^{12-}$ in acidic medium

Lanthanide-containing POMs are interesting due to potentially attractive photoluminescence, Lewis acid catalysis, electro-

chemistry, and magnetic properties. Due to the larger size and resulting higher coordination number of lanthanide ions as compared to d-block metal ions, they cannot be fully incorporated into the vacant sites of lacunary POMs and hence tend to link two or more polyanions, as observed in one of the largest polyanions, $[As_{12}^{III}Ce_{16}^{III}(H_2O)_{36}W_{148}O_{524}]^{76-}$ (W_{148}), reported by Pope and coworkers.[83]

In 2000, Pope's group reported the polyanion $[Ce_4(OH_2)_9(OH)_2(\alpha_1,\alpha_1-P_2W_{16}O_{59})_2]^{14-}$ ($Ce_4(\alpha_1\alpha_1-P_2W_{16})_2$) in which the P_2W_{12} precursor picks up extra tungsten atoms and then incorporates four cerium(III) ions.[60] The polyanion $Ce_4(\alpha_1\alpha_1-P_2W_{16})_2$ exhibits a dimeric structure with C_{2v} symmetry, comprising two $\{\alpha_1,\alpha_1-P_2W_{16}O_{59}\}$ (abbreviated as P_2W_{16}) units connected via a central core of four cerium atoms. There are two structural types of cerium in this polyanion, the first one has 10-coordination and the other has 9-coordination. The ^{31}P and ^{183}W NMR studies in aqueous solution suggested that the polyanion is stable in solution.

In 2003, Kortz reported the lanthanum-substituted polyanion $[\{La(CH_3COO)(H_2O)_2(\alpha_2-P_2W_{17}O_{61})\}_2]^{16-}$ ($La(OAc)-(\alpha_2-P_2W_{17})_2$), which was synthesized by reaction of La^{3+} ions with the hexalacunary polyanion P_2W_{12}.[84] It was observed that P_2W_{12} rearranges quickly in an aqueous, acidic medium to the monolacunary $[\alpha_1-P_2W_{17}O_{61}]^{10-}$ which in turn rearranges to $[\alpha_2-P_2W_{17}O_{61}]^{10-}$. The polyanion $La(OAc)-(\alpha_2-P_2W_{17})_2$ is composed of two $[\alpha_2-P_2W_{17}O_{61}]^{10-}$ fragments connected by two lanthanum acetato dimers $(La_2(CH_3COO)_2(H_2O)_4)^{4+}$, resulting in a head-on, transoid dimer with C_{2h} symmetry. Each La^{3+} atom exhibits a nine-coordinatied geometry.[61] The monolacunary Wells–Dawson ion $[\alpha_2-P_2W_{17}O_{61}]^{10-}$ is known to react with lanthanide ions to form Pope's "head-on dimers" or Francesconi's "side-on dimers".[61,85]

The Enbo Wang group has shown considerable interest in synthesizing metal–organic frameworks containing the Wells–Dawson ion. In 2008, they reported three transition metal-containing Wells–Dawson-based assemblies, using the P_2W_{12} anion as a reagent, $K_4Na_{10}[\alpha_1-CuP_2W_{17}O_{60}(OH)]_2\cdot58H_2O$ ($Cu_2P_4W_{34}$), $Na_2[H_2en][H_2hn]_{0.5}[Cu(en)_2]_{4.5}[\alpha_1-CuP_2W_{17}O_{60}(OH)]_2\cdot43H_2O$ $\{Cu(en)_2\alpha_1-CuP_2W_{17}\}_\infty$, and $Na_3[H_2hn]_{2.5}[P_2W_{17}O_{60}Cu(OH)_2]\cdot14H_2O$ $((H_2hn(CuP_2W_{17})_2)_\infty)$, where en = 1,2-ethylenediamine; hn = 1,6-hexamethylene diamine).[86] The $Cu_2P_4W_{34}$ polyanion consists of two $\alpha_1-P_2W_{17}$ units with the vacant α_1 (belt) position being occupied by a Cu^{2+} atom and the two Wells–Dawson units are connected by two W-OH-Cu groups resulting in a dimeric $[\alpha_1-CuP_2W_{17}O_{60}(OH)]_2^{14-}$ ($Cu_2P_4W_{34}$) assembly.

The $(Cu(en)_2\alpha_1-CuP_2W_{17})_\infty$ constitutes the first 2-D organic–inorganic hybrid network based on such double-Dawson-type polyanion (DDTP) building blocks and (Cu(en)$_2$)$^{2+}$ bridging units, representing a large polyoxotungstate building block for the construction of extended organic–inorganic hybrid materials. Subsequently, $\{(H_2hn)(CuP_2W_{17})_2\}_\infty$ possesses a 3-D hybrid supramolecular framework with 1-D channels that are constructed from the half-unit of the 'DDTP' and 'hn' cations. A magnetic study of $(Cu(en)_2\alpha_1-CuP_2W_{17})_\infty$ indicated weak antiferromagnetic interactions and that the two types of Cu^{2+} centers are well separated.

All the above examples consist of mono-Cu^{2+} substituted Wells–Dawson-type polyanions. Further exploration by the Wang group focused on feasible synthetic routes by adjusting the composition of Wells–Dawson polyanions to capture more transition metal ions. Subsequently, they reported a 1-D inorganic polymer formed by the reaction of P_2W_{12} with Mn^{2+} ions, $Na_8H_2L(H_2enMe)_4[Mn(H_2O)_2$ ($W_4Mn_4O_{12}$) $(P_2W_{14}O_{54})_2]\cdot17H_2O$, $\{W_4Mn_4(MnP_2W_{14})_2\}_\infty$ (L = pyromellitic dianhydride PMDA).[87] The structure of this compound consists of two tetravacant Dawson moieties $[P_2W_{14}O_{54}]^{14-}$ (P_2W_{14}) sandwiching an eight-metal cluster with W–O–$W_{(Mn)}$ and P–O–$W_{(Mn)}$ connecting modes. The metal centers in this eight-metal cluster form an almost regular cubane-like (W_4Mn_4) cluster. The solid-state network is completed by multi-Mn^{2+}-substituted DDTP and Mn^{2+} linkers with idealized C_2 symmetry, which is further connected into a 3-D supramolecular network via extensive hydrogen-bonding interactions.
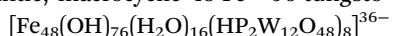
Fang, Kögerler, and coworkers have isolated potassium and lithium salts of a 40-manganese(III)-containing polyanion, $[(P_8W_{48}O_{184})\{(P_2W_{14}Mn_4O_{60})(P_2W_{15}Mn_3O_{58})_2\}_4]^{144-}$ ($(P_8W_{48})(Mn_4P_2W_{14})_4(Mn_3P_2W_{15})_8$), using hexavacant P_2W_{12} as a reagent.[88] Single-crystal XRD revealed that the polyanion ($(P_8W_{48})(Mn_4P_2W_{14})_4(Mn_3P_2W_{15})_8$) consists of P_2W_{14}, P_2W_{15}, and P_8W_{48} units. The polyanion was synthesized by reacting P_2W_{12} with $[Mn_{12}O_{12}(OAc)_{16}(H_2O)_4]\cdot4H_2O\cdot2HOAc$ in lithium acetate/acetic acid medium. Interestingly, although the cyclic P_8W_{48} is present in the pocket of the polyanion, no Mn^{3+} ions are found inside the cavity of the P_8W_{48} unit. It appears that P_8W_{48} acts as a template, reducing the steric repulsion between the tri-Dawson ($\{P_2W_{14}Mn_4\}\{P_2W_{15}Mn_3\}_2$) units. Magnetic measurements revealed intramolecular antiferromagnetic coupling between the Mn^{3+} ions.

In 2013, Yang and coworkers reported three lanthanide derivatives of P_8W_{48}, $\{[Ln_2(\mu-OH)_4(H_2O)x]_2(H_{24}P_8W_{48}O_{184})\}^{12-}$ (Ln = Nd, Sm, Tb) ($Ln_4P_8W_{48}$), and a manganese derivative, $[K(H_2O)_2]_4[K_4(\mu-H_2O)_8]_2[K(H_2O)]_8[Mn_8(H_2O)_{16}](H_4P_8W_{48}O_{184})\}$ ($K_8Mn_8P_8W_{48}$), starting from P_2W_{12} as precursor and working under hydrothermal conditions.[89] The cavities of P_8W_{48} in $Ln_4P_8W_{48}$ are occupied by lanthanide ions bridged by hydroxyl groups, and the 8 lanthanide ions have a 50% occupancy each. The $K_8Mn_8P_8W_{48}$ polyanion is formed by incorporating eight Mn^{2+} atoms inside the eight vacant sites within the cavity of the cyclic P_8W_{48}. These Mn^{2+} atoms are observed to be disordered over eight positions with K^+ atoms. The compounds were characterized by single-crystal XRD, FTIR, elemental analysis, thermogravimetry, and powder XRD.

In 2020, Abramov and coworkers reported the dimeric triniobium-substituted P_2W_{15} polyanion, $[cis-(P_2W_{15}Nb_3O_{61})_2]^{14-}$ ($P_2W_{15}Nb_3$), and two phases of the disordered derivative $[trans-(P_2W_{14.7}Nb_{3.3}O_{61})_2]^{14.6-}$ using P_2W_{12} as a precursor.[90] The main structural unit consists of the dimeric $[(P_2W_{16}Nb_4O_{60})_2(\mu-O)_2]^{n-}$ archetype anion based on two Wells–Dawson-type subunits, connected by two Nb–O–Nb bridges. Interestingly, out of the 12 niobium positions, only four are fully occupied. The addition of Me_2NH_2Cl to the reaction media yields a mixture of triclinic and orthorhombic crystal-

line phases. The dimeric units are comprised of two Dawson anions connected *via* Nb–O–Nb bridges. In 2020, Kortz and co-workers reported the gigantic, macrocyclic 48-Fe[III]-96-tungsto-16-phosphate, $[Fe_{48}(OH)_{76}(H_2O)_{16}(HP_2W_{12}O_{48})_8]^{36-}$ (**Fe₄₈(P₂W₁₂)₈**), which was prepared by reaction of **P₂W₁₂** and the 22-iron(III)-containing coordination complex $[Fe_{22}O_{14}(OH)_3(O_2CMe)_{21}(mda)_6]\cdot(ClO_4)_2$ (mdaH₂ = *N*-methyldiethanolamine) and isolated as a potassium salt, $K_{36}[Fe_{48}(OH)_{76}(H_2O)_{16}(HP_2W_{12}O_{48})_8]$.[91] The crystal structure of **Fe₄₈(P₂W₁₂)₈** revealed that there are eight equivalent {Fe₆P₂W₁₂} Dawson-type subunits linked to each other *via* Fe–O–Fe/W bonds, resulting in a cyclic assembly with idealized D_2 point group symmetry and a cavity of *ca.* 24 Å × 13 Å. Magnetic studies indicated that the 48 Fe³⁺ centers in **Fe₄₈(P₂W₁₂)₈** share several exchange pathways. The averaged exchange coupling constant was estimated to be $J_{av} = -7.07$ K. The electrochemical study of **Fe₄₈(P₂W₁₂)₈** exhibited redox transitions, suggesting the electroactivity of the Fe³⁺ and W^VI ionic states.

4. Metal complexes of $[H_6P_4W_{24}O_{94}]^{18-}$

Kortz and co-workers first showed that the super-lacunary Preyssler–Jeannin–Pope ion $[H_2P_4W_{24}O_{94}]^{22-}$ (**P₄W₂₄**) can react with electrophiles. The dimethyltin-containing hybrid organic–inorganic polyanion $[\{Sn(CH_3)_2\}_4(H_2P_4W_{24}O_{92})_2]^{28-}$ (**{Sn(CH₃)₂}₄(P₄W₂₄)₂**) (Fig. 9) was prepared by reaction of $(CH_3)_2SnCl_2$ with **P₄W₂₄** in an aqueous, acidic medium at ambient temperature and isolated as a potassium salt.[44] The polyanion comprises two **P₄W₂₄** units linked through four dimethyltin groups, leading to a structure with D_{2d} point group symmetry. The two **P₄W₂₄** units of the polyanion **{Sn(CH₃)₂}₄(P₄W₂₄)₂** are oriented orthogonally to each other and held together by four dimethyltin groups. Room temperature ¹¹⁹Sn [δ (ppm) = −243.2 ppm], ³¹P [δ (ppm) = −7.1, −8.7 ppm], ¹³C [δ (ppm) = 8.6 ppm], and ¹H [δ (ppm) = 0.7 ppm] NMR studies in aqueous medium proved the integrity of the solid-state structure in solution.

The continued study of Kortz and coworkers of the lacunary precursor **P₄W₂₄** has produced interesting new compounds with interesting physical and chemical properties. Kortz and coworkers studied the interaction of phosphotungstates with actinide ions, especially uranyl, as these complexes can potentially have rich structural, magnetic, and electrochemical properties. In 2008, the uranyl-peroxo-containing 36-tungsto-8-phosphate $[Li(H_2O)K_4(H_2O)_3\{(UO_2)_4(O_2)_4(H_2O)_2\}_2(PO_3OH)_2P_6W_{36}O_{136}]^{25-}$ (**Li(UO₂)₄(O₂)₄(PO₃OH)₂P₆W₃₆**) (Fig. 10) was synthesized and structurally characterized using **P₄W₂₄** as precursor.[92] The structure comprises three **P₂W₁₂** units encapsulating two independent, neutral $[(UO_2)(O_2)]_4$ units in the central cavity, resulting in a U-shaped **(P₂W₁₂)₃** assembly. Notably, the resulting polyanion could not be isolated using **P₂W₁₂** as a reagent instead of **P₄W₂₄**. Notably, from the single-crystal X-ray diffraction data, a lithium atom embedded in the structure was observed, which is rare in polyoxotungstate chemistry,
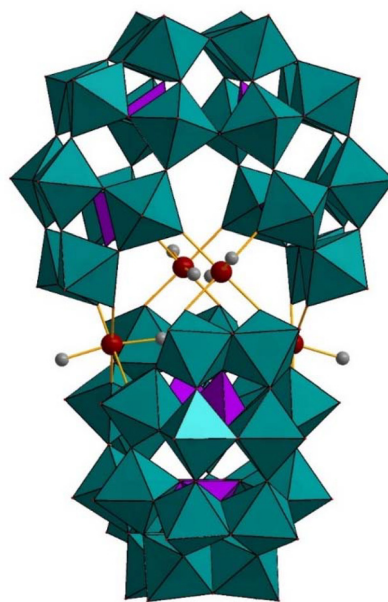

Fig. 9 Combined polyhedral/ball-and-stick representation of $[\{Sn(CH_3)_2\}_4(H_2P_4W_{24}O_{92})_2]^{28-}$. Color code: WO₆ octahedra (green), PO₄ tetrahedra (pink), C (grey), Sn (red). No hydrogen atoms are shown for clarity.[44]
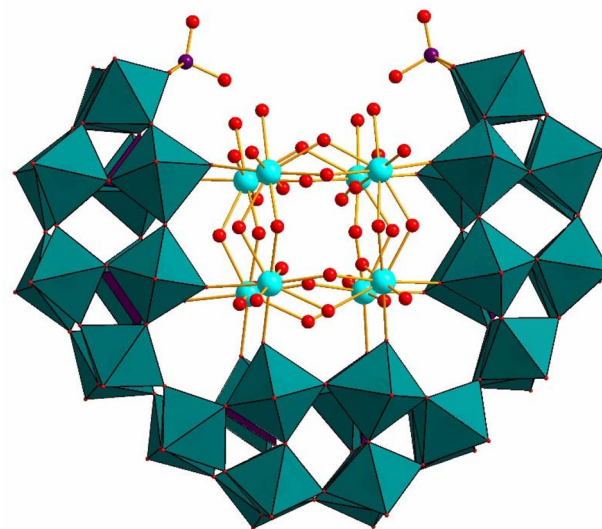

Fig. 10 Combined polyhedral/ball-and-stick representation of $[Li(H_2O)K_4(H_2O)_3\{(UO_2)_4(O_2)_4(H_2O)_2\}_2(PO_3OH)_2P_6W_{36}O_{136}]^{25-}$. Color code: WO₆ octahedra (green), PO₄ tetrahedra (pink), U (turquoise), P (pink), O (red).[92]

given that the high electron density of the W atoms generally tends to obscure such a low electron-dense atom. The coordination of the central uranium-peroxo unit $\{(UO_2)_4(O_2)_4(H_2O)_2\}_2$ comprises eight uranyl-peroxo units subdivided in two $[(UO_2)(O_2)]_4$ squares, the η²-peroxo ions being bound side-on to each

pair of uranium atoms. The room temperature ^{31}P NMR spectrum of the polyanion in water was fully consistent with its solid-state structure.

A mixed-valent vanadium derivative $[Rb_3 \subset \{V^VV_3^{IV}O_7(H_2O)_6\}_2\{H_6P_6W_{39}O_{147}(H_2O)_3\}]^{15-}$ ($(V^VV_3^{IV}O_7)_2(P_6W_{39})$) (Fig. 11) was also reported by Kortz and coworkers.[93] This polyanion was synthesized by the reaction of vanadium(IV) and vanadium(V) with P_4W_{24} in an acidic aqueous medium (pH 3.2–3.7). A mixed rubidium/potassium salt was isolated and characterized by single-crystal XRD, elemental analysis, TGA, IR, and ^{31}P NMR spectroscopy. The polyanion is composed of three P_2W_{12} subunits, which form a macrocyclic template of P_6W_{39}, capped by two mixed-valent $\{(V^V=O)(V^{IV}=O)_3(\mu_2-O)_3(H_2O)_6\}^{3+}$ ($\{V^VV_3^{IV}\}$) groups. Each $\{V^VV_3^{IV}\}$ cap comprises three octahedrally-coordinated V^{IV} atoms and one tetrahedrally-coordinated V^V atom. Each of the P_2W_{12} units is linked through $\{WO(H_2O)\}$ groups to form a cyclic P_6W_{39} assembly in this polyanion. The connectivity mode of the P_2W_{12} units in this polyanion resembles what Wang and coworkers had seen previously.[58] In the polyanion $(V^VV_3^{IV}O_7)_2P_6W_{39}$, the tetrahedral $V^V=O$ oxo group of each $\{V^VV_3^{IV}\}$ cap is bridged by three $V^{IV}O_6$ octahedra, which occupy the hexavacant positions in the P_6W_{39} unit. Notably, the terminal oxo-ligands of both the V^{IV} and V^V metal centers are directed towards the interior of the polyanion. The solid-state structure of the polyanion $(V^VV_3^{IV}O_7)_2P_6W_{39}$ was maintained in solution, as confirmed by ^{31}P NMR. The same type of connectivity and geometry of vanadium(IV/V) has been observed before for Müller's/Pope's mixed-valent vanadium-containing polyanion $[K_8 \subset \{V_4^VV_2^{IV}O_{12}(H_2O)_2\}_2\{P_8W_{48}O_{184}\}]^{24-}$ ($(V_4^VV_2^{IV}O_{12})_2P_8W_{48}$) (vide infra, section 6).[94]
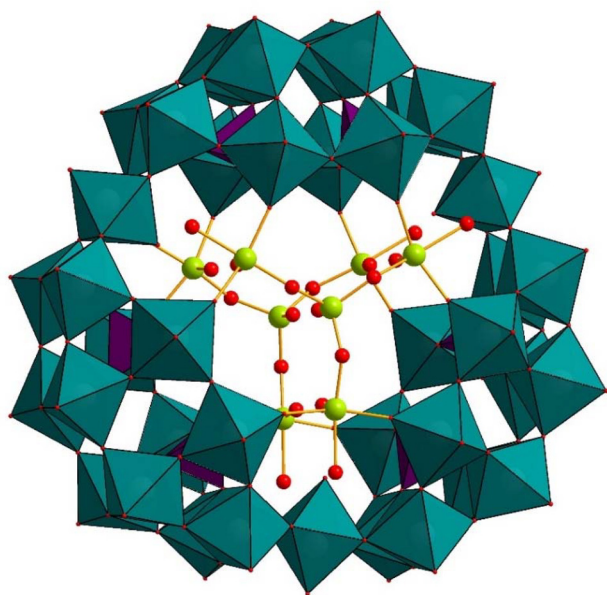
5. Metal complexes of $[H_7P_8W_{48}O_{184}]^{33-}$

Since the pioneering discovery of the Cu^{2+}-containing polyanion $[Cu_{20}Cl(OH)_{24}(H_2O)_{12}(P_8W_{48}O_{184})]^{25-}$ ($Cu_{20}ClP_8W_{48}$) (Fig. 12) in 2005, the chemistry of P_8W_{48} has continued to inspire chemists to study this unique cyclic, multilacunary polyanion. Since then, numerous compounds have been reported using the wheel-shaped P_8W_{48} polyanion as a precursor, which includes distinct anionic species as well as zeolitic frameworks.[95]

The first transition metal-containing P_8W_{48} polyanion, $Cu_{20}ClP_8W_{48}$, was synthesized by Kortz and coworkers by reacting Cu^{2+} ions with P_8W_{48} in an aqueous medium, and the product was fully characterized by IR, ^{31}P NMR, single-crystal X-ray diffraction and magnetic studies.[96] The 20-copper-oxo cluster in $Cu_{20}ClP_8W_{48}$ comprises three structurally unique types of copper(II) atoms with respect to their coordination geometry, namely octahedral, square-pyramidal, and square-planar, with a central chloride ion acting as a template. The copper ions are connected by μ_3-hydroxo-ligands, resulting in a highly symmetrical, cage-like copper-hydroxo cluster assembly, $\{Cu_{20}(OH)_{24}\}^{16+}$. In order to study the variation of the magnetic properties of the cluster in the presence of different halide ions, Mal et al. prepared derivatives of $Cu_{20}ClP_8W_{48}$, with the central chloride guest being replaced by a bromide and an iodide ion, $[Cu_{20}Br(OH)_{24}(H_2O)_{12}(P_8W_{48}O_{184})]^{25-}$ ($Cu_{20}BrP_8W_{48}$) and $[Cu_{20}I(OH)_{24}(H_2O)_{12}(P_8W_{48}O_{184})]^{25-}$ ($Cu_{20}IP_8W_{48}$).[97]

DFT calculations were performed on the $Cu_{20}ClP_8W_{48}$ polyanion in order to obtain additional information on the pro-

Fig. 11 Combined polyhedral/ball-and-stick representation of $[Rb_3 \subset \{V^VV_3^{IV}O_7(H_2O)_6\}_2\{H_6P_6W_{39}O_{147}(H_2O)_3\}]^{15-}$. Color code: WO$_6$ octahedra (green), PO$_4$ tetrahedra (pink), O (red), V (yellow).[93]
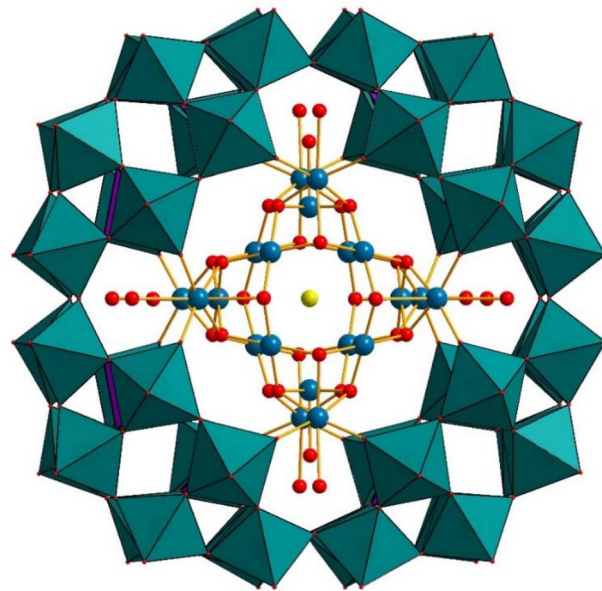
Fig. 12 Combined polyhedral/ball-and-stick representation of $[Cu_{20}X(OH)_{24}(H_2O)_{12}(P_8W_{48}O_{184})]^{25-}$ (X = Cl, Br, I). Color code: WO$_6$ octahedra (green), PO$_4$ tetrahedra (pink), O (red), Cu (blue), X (yellow).[96]

perties of the anionic guest inside the cavity created by the 20-copper-hydroxo cage, related to its electronic structure and energies of encapsulation.[98] The DFT calculations indicated the central halide ion to be extremely stable inside the polyanion cavity and cannot be released even at higher temperatures, without the destruction of the POM framework. Magnetic measurements showed that the Cu^{2+} atoms in all halide-derivatives are antiferromagnetically coupled, leading to an overall diamagnetic ground state.[97]

The solution stability of the polyanion $Cu_{20}ClP_8W_{48}$ was investigated by electrochemical studies at varying pH.[98] It was observed that the resolution of the reduction wave for Cu^{2+} to Cu^0 through Cu^+ was much better at pH 5.0, than compared with measurements performed at lower or higher pH values. It was also observed that all 20 Cu^{2+} centers within the polyanionic complex remain electroactive, as observed using controlled potential coulometry measurements and strong electrocatalytic reduction behavior towards NO_x.[98,99]

Scanning tunneling microscopic (STM) and scanning tunneling spectroscopic (STS) studies were performed on a highly oriented pyrolytic graphite (HOPG) surface at room temperature to visualize the 20-copper cluster.[100] STS measurements were done especially to better understand the STM results of $Cu_{20}ClP_8W_{48}$, such as the Cu⋯Cu distances and the orientation of the polyanion after deposition. The STM and STS images show a regular assembly of the polyanions and the regularly separated single copper atoms in the organic matrix. Several types of polyanion arrangements were observed by STM measurements on the HOPG surface, ostensibly due to the different concentration levels of $Cu_{20}ClP_8W_{48}$.

Most POMs exhibit hydrophilicity accompanied by high solubility of the corresponding salt in polar solvents, mainly due to a substantial negative charge and oxo/hydroxo/aqua ligands on the surface. Based on such a notion, Kortz and coworkers investigated several solution properties of the $Cu_{20}ClP_8W_{48}$ polyanion, for example, the investigation of supramolecular interaction resulting in "blackberry-type" structures, where the highly soluble homogeneous electrolytes tend to self-assemble into single layer, spherical, vesical-like structures in dilute solution.[101,102] Earlier reports of such studies were limited to polyoxomolybdate structures,[103–106] until Liu, Kortz, and coworkers showed that polyoxotungstates could also form "blackberry-type" arrangements. Such phenomena were mainly studied by dynamic light scattering (DLS), static light scattering (SLS), and zeta potential measurements.[103–106] The DLS studies showed that a slow supramolecular assembly formation in an aqueous $Cu_{20}ClP_8W_{48}$ solution starts spontaneously on the 11th day of the experiment, accompanied by continuous growth until 40 days before finally becoming stable.[101,102] Further studies using SLS indicated that the "blackberry-type" structure solution is relatively stable over prolonged periods, as evidenced by no change in scattering intensity for a month-old solution. It should be noted that the "blackberry-type" structure for $Cu_{20}ClP_8W_{48}$ only forms at 50 °C. DLS and SLS also provide important information regarding the mechanism of formation

of such "blackberry-type" structures. The individual $Cu_{20}ClP_8W_{48}$ polyanions first overcome the high kinetic energy barrier,[107–110] and then slowly nucleate together, quickly forming a "blackberry-type" structure with an average radius of 38 nm. It was also observed that the counter cations play a major role in forming the blackberry solution.[111]

The $Cu_{20}ClP_8W_{48}$ polyanion was also investigated for the fabrication of organized thin films by the Langmuir–Blodgett (LB) technique. The polyanions can be introduced into organic–inorganic hybrid films using different LB techniques, resulting in well-defined layered structures. Dimethyldioctadecylammonium bromide (DODA) was observed to react with $Cu_{20}ClP_8W_{48}$ to form a surfactant-encapsulated $Cu_{20}ClP_8W_{48}$, which was characterized by different analytical techniques, such as NMR, FT-IR, TGA, powder X-ray diffraction (XRD), and elemental analysis. XRD studies indicated that two different types of DODA-$Cu_{20}ClP_8W_{48}$ structures are present (DODA/$Cu_{20}ClP_8W_{48}$ and DODA-$Cu_{20}ClP_8W_{48}$) based on the diameter and thickness of the layer spacing. The two types of LB films were successfully fabricated onto the substrate by using different deposition methods. It was also observed that $Cu_{20}ClP_8W_{48}$ exhibits different packing modes in the two LB films, depending on the deposition strategy used.[112,113] Further studies on $Cu_{20}ClP_8W_{48}$ include electrocatalytic reduction of NO_x.[98] The polyanion $Cu_{20}ClP_8W_{48}$ has also been shown to be a very efficient heterogeneous catalyst for the solvent-free aerobic oxidation of n-hexadecane.[114] In such a study, $Cu_{20}ClP_8W_{48}$ was first supported on 3-aminopropyltriethoxysilane (apts)-modified SBA-15 and then subsequently used for the aerobic oxidation of n-hexadecane, showing an exceptionally high turnover frequency (TOF) of 20 000 h^{-1} and resistance to CS_2 poisoning. The efficiency of the polyanion catalyst was observed to increase dramatically upon immobilization on mesoporous support due to a large increase in the surface area, which enhanced the oxidation of n-hexadecane into ketones and alcohols. Moreover, it was found that the supported catalyst can be reused at least five times, retaining almost the same catalytic activity as the fresh catalyst.

Mialane and coworkers have been exploring POMs containing azido ligands since 2003.[115] The azido ligands can act as connectors between the 3d metal centers embedded in a POM unit and also act as intermolecular linkers between different POM subunits, leading to high-nuclearity POM complexes. Pichon et al. have shown that azido groups can also function as ligands in P_8W_{48} by preparing the large azido-POM $[P_8W_{48}O_{184}Cu_{20}(N_3)_6(OH)_{18}]^{24-}$ ($Cu_{20}(N_3)_6P_8W_{48}$).[116] The polyanion $Cu_{20}(N_3)_6P_8W_{48}$ has two $\{Cu_5(OH)_4\}^{6+}$ and two $\{Cu_5(OH)_2(\mu_{1,1,3,3}\text{-}N_3)\}^{7+}$ subunits encapsulated in the crown-shaped P_8W_{48}.

In each of the four subunits $\{Cu_5(OH)_4\}^{6+}$ and $\{Cu_5(OH)_2(\mu_{1,1,3,3}\text{-}N_3)\}^{7+}$, the five Cu^{2+} atoms form a square pyramid with two μ_3-hydroxo ligands connecting the apical Cu^{2+} center to the four basal copper atoms. Interestingly, in each $\{Cu_5(OH)_4\}^{6+}$ fragment, the apical copper atom has an axially distorted coordination geometry, and the four remain-

ing Cu centers exhibit a distorted trigonal–bipyramidal geometry. Moreover, the $\{Cu_5(OH)_4\}^{6+}$ fragments in $\mathbf{Cu_{20}(N_3)_6P_8W_{48}}$ are crystallographically disordered between the hydroxo and azido ligands connecting the Cu^{2+} atoms. Hence, the polyanion is a mixture of species containing two different $\{Cu_5(OH)_4\}^{6+}$ subunits.

Kortz, Müller, and coworkers have synthesized the 16-Fe^{3+} containing polyanion $[P_8W_{48}O_{184}Fe_{16}(OH)_{28}(H_2O)_4]^{20-}$ ($\mathbf{Fe_{16}P_8W_{48}}$) (Fig. 13a), which was prepared independently.[117] The polyanion contains a cationic 16-iron(III)-hydroxo nanocluster $\{Fe_{16}(OH)_{28}(H_2O)_4\}^{20+}$ in the cavity of the crown-shaped $\mathbf{P_8W_{48}}$. The $\{Fe_{16}(OH)_{28}(H_2O)_4\}^{20+}$ cluster comprises eight pairs of structurally equivalent, edge-shared $\{Fe_2O_{12}\}$ octahedra, which are connected to each other via corners. Notably, the binding mode of the 16 Fe^{3+} centers in $\mathbf{Fe_{16}P_8W_{48}}$ differs from the 20 Cu^{2+} centers in $\mathbf{Cu_{20}ClP_8W_{48}}$. In $\mathbf{Fe_{16}P_8W_{48}}$, each of the 16 equivalent Fe^{3+} centers is connected to $\mathbf{P_8W_{48}}$ by Fe–O(W) and a Fe–O(P) bonds, resulting in a tight anchoring of the 16-iron-hydroxo core, $\{Fe_{16}(OH)_{28}(H_2O)_4\}^{20+}$, to the wheel-shaped POM host. In $\mathbf{Cu_{20}ClP_8W_{48}}$, only eight of the 20 Cu^{2+} ions form two Cu–O(W) bonds each and hence are bound to the $\mathbf{P_8W_{48}}$ host. On the other hand, the eight phosphate hetero groups of $\mathbf{P_8W_{48}}$ are not directly bonded to the cationic $\{Cu_{20}(OH)_{24}\}^{16+}$ cluster. Nevertheless, $\mathbf{Cu_{20}ClP_8W_{48}}$ is quite stable in solution. In fact, $\mathbf{Fe_{16}P_8W_{48}}$ is structurally more closely related to Mialane's Cu_{20}-azide derivative, $\mathbf{Cu_{20}(N_3)_6P_8W_{48}}$.[116] In $\mathbf{Cu_{20}(N_3)_6P_8W_{48}}$, 16 of the 20 Cu^{2+} ions are connected to the inner cavity of $\mathbf{P_8W_{48}}$ in the same fashion as the Fe^{3+} centers in $\mathbf{Fe_{16}P_8W_{48}}$. The sites of the remaining four unique Jahn–Teller distorted Cu^{2+} atoms in $\mathbf{Cu_{20}(N_3)_6P_8W_{48}}$ are observed to remain empty in $\mathbf{Fe_{16}P_8W_{48}}$. Kortz and coworkers further investigated the $\mathbf{Fe_{16}P_8W_{48}}$ polyanion toward incorporating lanthanide ions in the remaining vacancies. They successfully prepared an unprecedented,

horseshoe-shaped 16-iron(III)-containing polyanion $[Fe_{16}O_2(OH)_{23}(H_2O)_9P_8W_{49}O_{189}Ln_4(H_2O)_{19}]^{11-}$ (Ln = Eu, Gd) ($\mathbf{Fe_{16}Ln_4P_8W_{49}}$) (Fig. 13b) with a central $[Fe_{16}(OH)_{28}(H_2O)_4]^{20+}$ guest.[118] These $\mathbf{Fe_{16}Ln_4P_8W_{49}}$ polyanions can be called open derivatives of $\mathbf{Fe_{16}P_8W_{48}}$, where the $\mathbf{P_8W_{48}}$ template wheel does not remain intact and is cut open. The $\{Fe_{16}\}$ ring in $\mathbf{Fe_{16}Ln_4P_8W_{49}}$ is cleaved between four Fe atoms (Fe1/Fe2 on one side and Fe15/Fe16 on the other). Interestingly, an extra tungsten atom is incorporated into the $\mathbf{P_8W_{48}}$ framework, resulting in an open $\{P_8W_{49}\}$ unit. The extra W atom occupies the cap of the P_2W_{12} Wells–Dawson fragment and is connected to the novel open $\mathbf{P_8W_{48}}$ fragment through one μ_4-oxo and two μ_2-oxo bridges.

Kortz and coworkers have also reported Co^{2+}, Mn^{2+}, Ni^{2+}, and V^V-containing derivatives based on the $\mathbf{P_8W_{48}}$ wheel. For the Mn and Ni derivatives, the tungsten-oxo wheel has accumulated two extra tungsten atoms, resulting in the unprecedented $\mathbf{P_8W_{50}}$ unit.[120] All four compounds, $K_{12}Li_{16}Co_2[Co_4(H_2O)_{16}P_8W_{48}O_{184}]$ ($\mathbf{Co_4P_8W_{48}}$),[121] (Fig. 14a) $K_{12}Li_{10}Mn_3[Mn_4(H_2O)_{16}(P_8W_{48}O_{184})(WO_2(H_2O)_2)_2]$ ($\mathbf{Mn_4P_8W_{50}}$),[121] $K_{14}Li_8Ni_3[Ni_4(H_2O)_{16}(P_8W_{48}O_{184})(WO_2(H_2O)_2)_2]$ ($\mathbf{Ni_4P_8W_{50}}$) (Fig. 14b),[121] and $K_{20}Li_{16}[(VO_2)_4(P_8W_{48}O_{184})]$ ($\mathbf{(VO_2)_4P_8W_{48}}$),[121] were synthesized and characterized by single-crystal XRD, FTIR, elemental analysis, electrochemistry, magnetic susceptibility, and EPR techniques.

The $\mathbf{Co_4P_8W_{48}}$ and $\mathbf{(VO_2)_4P_8W_{48}}$ were prepared by reacting Co^{2+} and VO^{2+} with $\mathbf{P_8W_{48}}$ in aqueous solution, respectively. Bassil et al. have isolated the manganese(II) derivative $\mathbf{Mn_4P_8W_{50}}$ and its nickel(II) analogue $\mathbf{Ni_4P_8W_{50}}$, using similar synthetic procedures but in the presence of small amounts of H_2O_2.[121]

The solid-state structure of $\mathbf{Co_4P_8W_{48}}$ consists of four Co^{2+} atoms coordinated to the hinge-oxygens at the inner rim of $\mathbf{P_8W_{48}}$. As perceived from the structures of similar transition
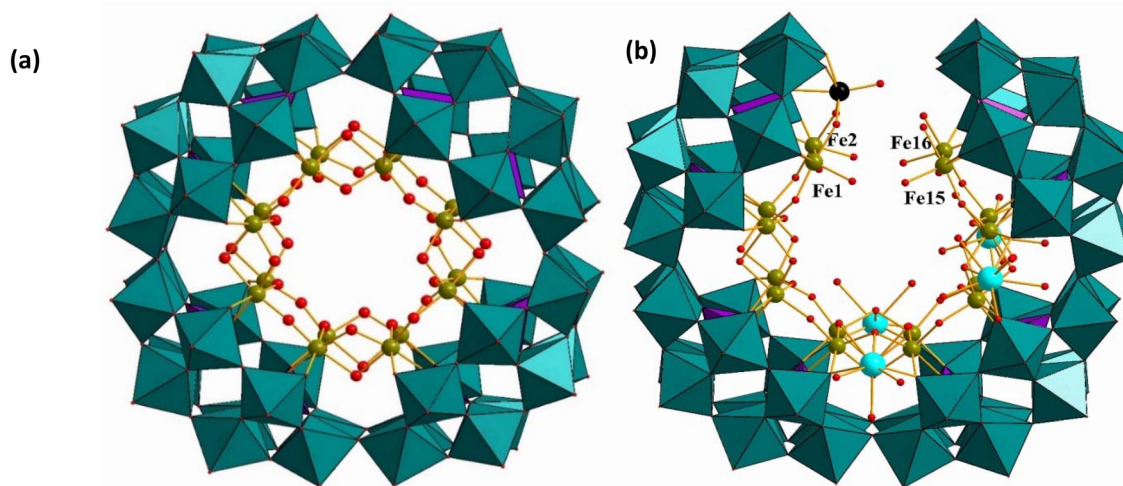
Fig. 13 Combined polyhedral/ball-and-stick representations of (a) $[P_8W_{48}O_{184}Fe_{16}(OH)_{28}(H_2O)_4]^{20-}$ and (b) $[Fe_{16}O_2(OH)_{23}(H_2O)_9P_8W_{49}O_{189}Ln_4(H_2O)_{19}]^{11-}$ (Ln = Eu, Gd). Color code: WO_6 octahedra (green), PO_4 tetrahedra (pink), O (red), Fe (green), Ln (turquoise), W (black).[118,119]
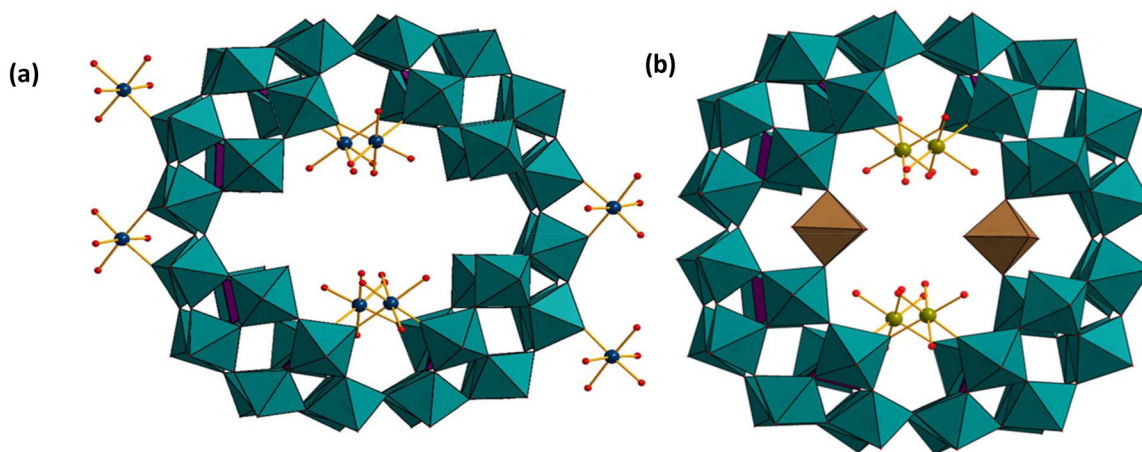
Fig. 14 (a) Combined polyhedral/ball-and-stick representations of (a) $[Co_4(H_2O)_{16}P_8W_{48}O_{184}]^{32-}$ and (b) $[Ni_4(H_2O)_{16}(P_8W_{48}O_{184})(WO_2(H_2O)_2)_2]^{28-}$. Color code: WO_6 octahedra (green and brown), PO_4 tetrahedra (pink), O (red), Co (deep blue), Ni (green). The brown WO_6 octahedra have an occupancy of 50% each.[121]

metal derivatives of P_8W_{48},[71,72] the terminal W–O oxygen atoms are observed to point towards the center of the polyanion. Interestingly, in $Co_4P_8W_{48}$ only half of the eight equivalent hinge sites are occupied by the four Co^{2+} atoms that are coordinated in a *cis* fashion to two oxo(W) ligands from two adjacent P_2W_{12} subunits. Aqua ligands occupy the remaining four terminal coordination sites. In addition to the four inner Co^{2+} ions, two outer Co^{2+} ions were found in $Co_4P_8W_{48}$, linking adjacent polyanions and forming a one-dimensional chain in the solid state. Magnetic studies indicated that the two types of Co^{2+} centers are non-interacting with each other.

Cronin and coworkers have reported a cobalt(II) salt of a cobalt(II)-containing P_8W_{48} assembly $\{Co_4[Co_6(P_8W_{48}O_{184})]\}_\infty^8$ ($Co_4(Co_6P_8W_{48})_\infty$) with six internal and four external Co^{2+} ions bridging neighboring polyanions, resulting in a 1D chain or 3D network, respectively.[122] Kortz's group reported the tetra-cobalt(II)-containing polyanion $Co_4P_8W_{48}$ (which crystallized with two extra cobalt(II) counter cations). The coordination of two pairs of Co^{2+} ions in diagonally related positions of $Co_4P_8W_{48}$ led to a subtle distortion of the P_8W_{48} assembly, as reflected by a difference of *ca.* 1.6 Å between the polyanion diameter of opposite W centers where the Co^{2+} ions are bound and the diameter of opposite W centers perpendicular to the previous one. Wang, Su, and coworkers have synthesized three Co^{2+} linked derivatives of P_8W_{48}, $Na_8Li_8Co_5[Co_{5.5}(H_2O)_{19}P_8W_{48}O_{184}]\cdot60H_2O$ ($Co_5(Co_{5.5}P_8W_{48})_\infty$), $K_2Na_4Li_{11}Co_5[Co_7(H_2O)_{28}P_8W_{48}O_{184}]Cl\cdot59H_2O$ ($Co_5(Co_7P_8W_{48})_\infty$), and $K_2Na_4LiCo_{11}[Co_8(H_2O)_{32}P_8W_{48}O_{184}](CH_3COO)_4Cl\cdot47H_2O$ ($Co_{11}(Co_8P_8W_{48})_\infty$), which were characterized by FTIR, thermogravimetric analysis, elemental analysis, and magnetic measurements.[123] In $Co_5\{Co_{5.5}P_8W_{48}\}_\infty$ and $Co_5\{Co_7P_8W_{48}\}_\infty$, four external cobalt(II) ions are observed to link adjacent polyanions, resulting in two-dimensional networks, while $Co_{11}\{Co_8P_8W_{48}\}_\infty$ is observed to form three-dimensional networks. $Co_{11}\{Co_8P_8W_{48}\}_\infty$ exhibits the largest cobalt(II) containing P_8W_{48} to date when counterions are also considered.

Kortz's group reported the polyanions $Mn_4P_8W_{50}$ and $Ni_4P_8W_{50}$ with four Mn^{2+}/Ni^{2+} ions bound in the cavity of P_8W_{48} as the Co^{2+} ions in $Co_4P_8W_{48}$, and two additional $\{WO_6\}$ octahedral units disordered over the four equivalent positions perpendicular to the plane of the Mn^{2+}/Ni^{2+} ions, resulting in a polyanion with C_{2h} point group symmetry. The "extra" tungsten centers in $Mn_4P_8W_{50}$ and $Ni_4P_8W_{50}$ are coordinated to oxygens of the P_8W_{48} wheel just like the Mn^{2+}/Ni^{2+} ions, but in a *trans*-related fashion. The average M–O(W) distance for the Mn^{2+} centers in $Mn_4P_8W_{50}$ and for the Ni^{2+} centers in $Ni_4P_8W_{50}$ is 2.13(2) Å and 2.02(2) Å, respectively. The average Mn^{2+}–O(aqua) bond in $Mn_4P_8W_{50}$ and the Ni^{2+}–O(aqua) bond in $Ni_4P_8W_{50}$ are 2.20(2) and 2.06(2) Å, respectively.

Cronin and coworkers, as well as Proust and coworkers, have reported Mn-based P_8W_{48} derivatives, which differ in the number and location of the Mn^{2+} ions and their network arrays. The Cronin group reported an open framework nanocube-based, $[Mn_8(H_2O)_{48}P_8W_{48}O_{184}]^{24-}$ ($\{Mn_8(H_2O)_{48}P_8W_{48}\}_\infty$) and a multidimensional framework $[Mn_{14}(H_2O)_{30}P_8W_{48}O_{184}]^{12-}$ ($\{Mn_{14}P_8W_{48}\}_\infty$) polyanion.[21,76] Each P_8W_{48} fragment is linked by Mn–O–W coordination bonds, which form a higher-order packing arrangement. Proust and coworkers have reported two new Mn^{II} derivatives of P_8W_{48}: $[Mn_8(H_2O)_{26}(P_8W_{48}O_{184})]^{24-}$ ($Mn_8(H_2O)_{26}P_8W_{48}$) and $[Mn_6(H_2O)_{22}(P_8W_{48}O_{184})\{WO_2(H_2O)_2\}_{1.5}]^{25-}$ ($Mn_6\{WO_2(H_2O)_2\}_{1.5}P_8W_{48}$).[77] In $Mn_8(H_2O)_{26}P_8W_{48}$, six Mn^{2+} centers are observed to be located inside the P_8W_{48} cavity, while two other Mn^{2+} centers are coordinated to the outer rim of P_8W_{48}. The internal six Mn^{2+} ions are distributed among the eight hinges between the $\{P_2W_{12}\}$ subunits. Four of the sites are fully occupied by the four Mn^{2+}, which is the orthogonal plain to the main $\{P_8W_{48}\}$, and the remaining two Mn^{2+} centers are disordered over the four other positions, which resembles the Co^{2+} complex reported by the Cronin group.[122] In $Mn_6\{WO_2(H_2O)_2\}_{1.5}P_8W_{48}$, four Mn^{2+} centers are located inside the P_8W_{48} cavity, while two other Mn^{2+} centers are coordinated to the outer rim of P_8W_{48}, as in the former structure.

Müller and coworkers have also studied the interaction of P_8W_{48} with VO^{2+} and Mo^{VI} in acetate buffer. They have successfully isolated the mixed-valent vanadium(IV/V) containing polyanion $[P_8W_{48}O_{184}\{V_4^VV_2^{IV}O_{12}(H_2O)_{12}\}_2]^{32-}$ ($(V_4^VV_2^{IV})_2P_8W_{48}$) (Fig. 15a),[94] and the mixed-valent molybdenum(V/VI) $[\{P_8W_{48}O_{184}\}\{Mo^{VI}O_2\}_4\{(H_2O)(O=)Mo^V(\mu_2\text{-}O)(O=)Mo^V(\mu_2\text{-}H_2O) (\mu_2\text{-}O)_2Mo^V(=O)(\mu_2\text{-}O)_2Mo^V(=O)(H_2O)\}_2]^{32-}$ ($Mo_4^{VI}Mo_4^VP_8W_{48}$), the first examples of mixed-valent complexes incorporated in P_8W_{48}.[124] In $(V_4^VV_2^{IV})_2P_8W_{48}$, two $\{V_4^VV_2^{IV}O_{12}(H_2O)_2\}^{4+}$ units are observed to be trapped inside the cavity of the polyanion. The $\{V_4^VV_2^{IV}O_{12}(H_2O)_2\}^{4+}$ unit consists of two octahedrally-coordinated V^{IV} and four tetrahedrally-coordinated V^V centers. The oxidation of V^{IV} to V^V occurs *in situ* due to air. Such type of oxidation has also been observed for $(VO_2)_4P_8W_{48}$, as reported by Kortz and coworkers.[121] Wu's and Bi's groups have reported the reduction of Au^{3+} in the presence of $(V_4^VV_2^{IV})_2P_8W_{48}$, acting as a stabilizing and reducing agent, forming the bamboo joint-like gold microstructure in aqueous medium at ambient temperature.[125]

$Mo_4^{VI}Mo_4^VP_8W_{48}$ was observed to consist of two neutral tetranuclear $\{Mo_4^VO_{10}(H_2O)_3\}$ and four $\{Mo^{VI}O_2\}^{2+}$ units connected to the P_8W_{48} ring *via* Mo–O–W bonds. Furthermore, the $\{Mo_4^VO_{10}(H_2O)_3\}$ unit contains two of the well-known diamagnetic $\{Mo_2^VO_4\}^{2+}$-type units. The four trapped $\{Mo^{VI}O_2\}^{2+}$ units bind to two oxygen atoms of adjacent P_2W_{12} units, resulting in tetrahedral coordination of the Mo atoms. The ^{31}P and ^{183}W NMR data fully support the solid-state structure.

Cadot and coworkers have reported molybdenum oxothiocation complexes with the cyclic P_8W_{48}.[126] The reaction of the $[Mo_2S_2O_2(H_2O)_6]^{2+}$ oxothiocation with P_8W_{48} in an aqueous acidic medium resulted in two new molybdenum oxothiocation based compounds: $[K_4\{Mo_4O_4S_4(H_2O)_3(OH)_2\}_2(WO_2)(P_8W_{48}O_{184})]^{30-}$ ($(Mo_4O_4S_4)_2(WO_2)P_8W_{48}$) and $[\{Mo_4O_4S_4(H_2O)_3(OH)_2\}_2(P_8W_{48}O_{184})]^{36-}$ ($(Mo_4O_4S_4)_2P_8W_{48}$) (Fig. 15b). In $(Mo_4O_4S_4)_2(WO_2)P_8W_{48}$, the two disordered $[Mo_4O_4S_4$

$(OH)_2(H_2O)_3]^{2+}$ oxothiomolybdenum clusters are observed to be grafted on both sides of the cyclic P_8W_{48} surface, resulting in two geometrical isomers where the two $\{Mo_4O_4S_4(H_2O)_3(OH)_2\}^{2+}$ groups are arranged either in a perpendicular or parallel mode. The structure also comprises of a $\{WO_2\}^{2+}$ group, which is disordered over four positions in P_8W_{48}. The polyanion $(Mo_4O_4S_4)_2(WO_2)P_8W_{48}$ is closely related to the compound $Mo_4^{VI}Mo_4^VP_8W_{48}$,[124] where the oxocation $\{Mo_2O_4\}^{2+}$ exhibits a similar mode of connectivity as is usually observed for oxothio $\{Mo_2O_2S_2\}$-based polyanions. In $Mo_4^{VI}Mo_4^VP_8W_{48}$, the neutral core $[Mo_4O_{10}(H_2O)_3]$ is observed to be formed by connections of two dinuclear units through a double oxo-bridge. In contrast, in the oxothio derivative $(Mo_4O_4S_4)_2WP_8W_{48}$, such connections are through a double hydroxo bridge. The polyanion $(Mo_4O_4S_4)_2P_8W_{48}$ is observed to be composed of the same two disordered $[Mo_4O_4S_4(OH)_2(H_2O)_3]^{2+}$ oxothiomolybdenum clusters but without the extra $\{WO_2\}^{2+}$ group. Both compounds were characterized in the solid-state by XRD and solution by NMR.

Kortz and coworkers have further investigated the reactivity of the cyclic P_8W_{48} with 4d transition metal ions in a buffer solution. Interaction of $[Ru(p\text{-cymene})Cl_2]_2$ with P_8W_{48} in lithium buffer solution at pH 6.0 resulted in the polyanion $[\{K(H_2O)\}_3\{Ru(p\text{-cymene})(H_2O)\}_4P_8W_{49}O_{186}(H_2O)_2]^{27-}$ ($Ru_4P_8W_{49}$) (Fig. 16).[127] The structure of the polyanion $Ru_4P_8W_{49}$ reveals that it has four $\{Ru(p\text{-cymene})(H_2O)\}^{2+}$ groups covalently attached to the inner rim of the cyclic P_8W_{48} unit, resulting in a structure with C_i symmetry. Each organoruthenium group is bound to P_8W_{48} *via* two Ru–O(W) bonds involving belt oxygens of each of two adjacent, hexalacunary P_2W_{12} building blocks and the extra tungsten atom, resulting in $Ru_4P_8W_{49}$, which has been observed previously for other related polyanions.[121]

Pope and coworkers have investigated the interaction of the P_8W_{48} ion with early lanthanide metal ions. They have synthesized and structurally characterized a family of four new
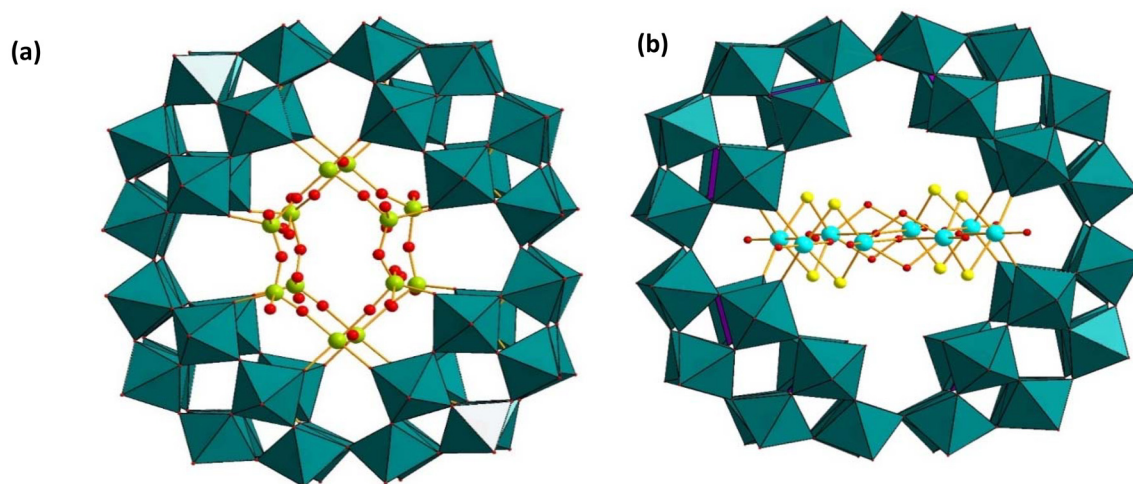
Fig. 15 Combined polyhedral/ball-and-stick representations of (a) $[P_8W_{48}O_{184}\{V_4^VV_2^{IV}O_{12}(H_2O)_{12}\}_2]^{32-}$, and (b) $[\{Mo_4O_4S_4(H_2O)_3(OH)_2\}_2(P_8W_{48}O_{184})]^{36-}$. Color code: WO_6 octahedra (green), PO_4 tetrahedra (pink), Mo (turquoise), V (green), S (yellow), O (red).[94,126]
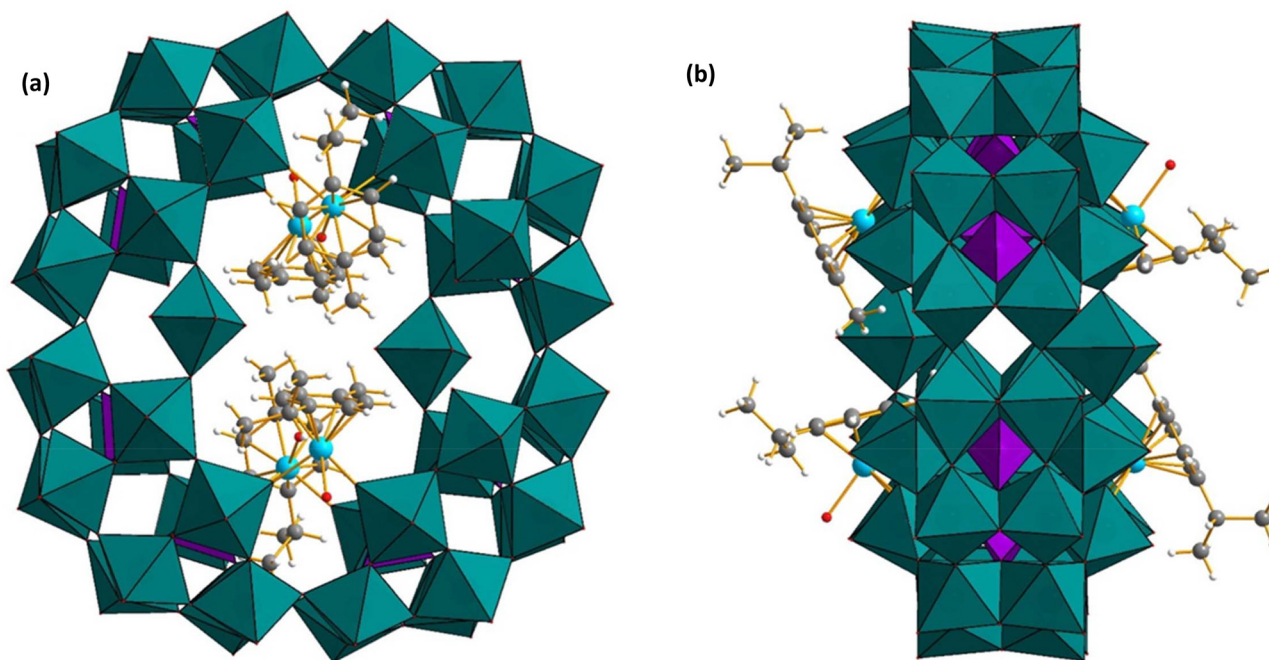
Fig. 16 Combined polyhedral/ball-and-stick representation of $[\{K(H_2O)\}_3\{Ru(p\text{-cymene})(H_2O)\}_4P_8W_{49}O_{186}(H_2O)_2]^{27-}$. (a) Front-view, (b) side-view. Color code: WO_6 octahedra (green), PO_4 tetrahedra (pink), Ru (sky blue), O (red), C (grey), H (white).[127]

lanthanide-substituted polyoxotungstates, $[K\subset P_8W_{48}O_{184}(H_4W_4O_{12})_2Ln_2(H_2O)_{10}]^{25-}$ (**Ln₂(W₄O₁₂)₂P₈W₄₈**) (Ln = La, Ce, Pr, Nd) (Fig. 17) and all polyanions were characterized by infrared spectroscopy, ^{31}P NMR, and X-ray crystallography.[128] The structural elucidation of the polyanions reveals that the

Fig. 17 Combined polyhedral/ball-and-stick representation of $[K\subset P_8W_{48}O_{184}(H_4W_4O_{12})_2Ln_2(H_2O)_{10}]^{25-}$. Color code: WO_6 octahedra (green and brown), PO_4 tetrahedra (pink), O (red), Ce (turquoise), K (grey).[128]

central cavity of **P₈W₄₈** is occupied by two additional $\{W_4O_{12}\}$ groups, along with four lanthanides and two potassium ions, each with an occupancy of 50%. Therefore, the polyoxotungstate shell comprises two **P₂W₁₆** and two **P₂W₁₂** subunits, with equivalent ones facing each other.

In 2015, Kögerler and coworkers reported the reactivity of the main group element Sn^{2+} with **P₈W₄₈** in aqueous solution and isolated the Sn^{2+}-containing $[K_{4.5}\subset(ClSn)_8P_8W_{48}O_{184}]^{17.5-}$ (**(ClSn)₈P₈W₄₈**) (Fig. 18).[129] Interestingly, a color change from bright-orange (reduction of W^{VI} to W^V) to brown and then to dark-green (air oxidation of W^V to W^{VI}) was observed during the reaction. In the polyanion **(ClSn)₈P₈W₄₈**, all eight Sn^{2+} atoms are incorporated in the central cavity of **P₈W₄₈**, occupying the eight equivalent vacant hinge-positions of the **P₈W₄₈** moiety. The rate of evaporation of the reaction solution, temperature, and concentration of Sn^{2+} play a crucial role in the formation of this polyanion. The structure of **(ClSn)₈P₈W₄₈** comprises eight $\{ClSn\}$ groups, with each Sn^{2+} atom in a trigonal-pyramidal coordination geometry and the chloride ligand of $\{ClSn\}$ pointing towards the center of the **P₈W₄₈** cavity. The bond distance of Sn–Cl in **(ClSn)₈P₈W₄₈** is 2.515(6) Å, which is comparable with $Cs[SnCl_3]$ (2.523 Å) and $[SnCl_2(H_2O)]\cdot H_2O$ (2.595 Å). Similarly, the Sn–O bond is in good agreement with the Sn–O bond lengths in $[SnCl_2(H_2O)]\cdot H_2O$ (2.169 Å) and other Sn^{2+}-containing polyoxotungstates.[130]

Recently, Kögerler and coworkers have reported aromatic organoarsenate-functionalized **P₈W₄₈**, $[(RAs^VO)_4P_8^VW_{48}^{VI}O_{184}]^{32-}$ [R = C_6H_5 or $p\text{-}(H_2N)C_6H_4$] (**(RAsO)₄P₈W₄₈**, R = C_6H_5 or $p\text{-}(H_2N)C_6H_4$).[131] Recrystallization of the K^+/Li^+/dimethylammonium salt of (**$p\text{-}(H_2N)C_6H_4AsO)_4P_8W_{48}$**) from 4 M LiCl solution was
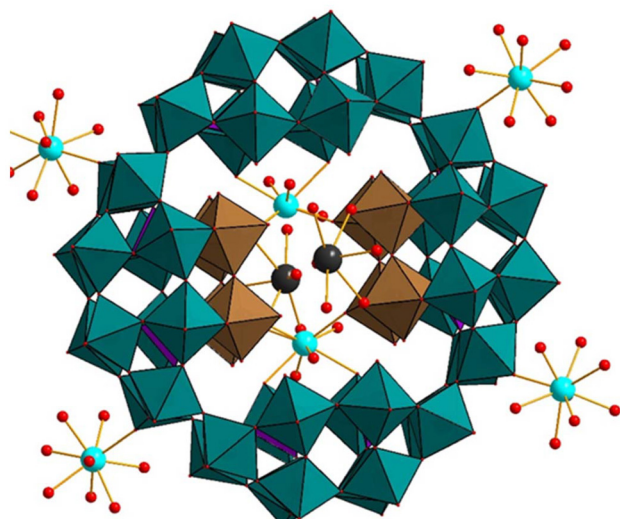
Fig. 18 Combined polyhedral/ball-and-stick representation of $[K_{4.5} \subset (ClSn)_8 P_8 W_{48} O_{184}]^{17.5-}$. Color code: WO_6 octahedra (green), PO_4 tetrahedra (pink), O (red), Sn (brown), K (grey), Cl (green).[129]

observed to yield a further functionalized product, $[(H_3NC_6H_4AsO)_3P_8W_{48}O_{184}H_x\{WO_2(H_2O)_2\}_{0.4}]^{(30.2-x)-}$, revealing dissociation of the organoarsonate groups in slightly acidic aqueous solution followed by their rearrangement within the inner polyanion cavity.[131]

In 2018, Khashab and coworkers isolated two main group 3 metal-substituted P_8W_{48} in aqueous acidic solution, $\{[Na(NO_3)(H_2O)]_4[Al_{16}(OH)_{24}(H_2O)_8(P_8W_{48}O_{184})]\}^{16-}$ (**$Al_{16}P_8W_{48}$**) and its Ga analogue $[Ga_{16}(OH)_{32}(P_8W_{48}O_{184})]^{24-}$ (**$Ga_{16}P_8W_{48}$**).[132] The connectivity of Al^{3+}/Ga^{3+} in $Al_{16}P_8W_{48}$ and **$Ga_{16}P_8W_{48}$** is similar to that of $Fe_{16}P_8W_{48}$ reported by Kortz and coworkers (Fig. 13a).[117] The incorporated "$\{Al_{16}\}$ ring" comprises eight pairs of structurally equivalent, edge-shared AlO_6 octahedra that are interconnected via corners. The degree of protonation is different in the cationic aluminum-hydroxo core $\{Al_{16}(OH)_{24}(H_2O)_8\}^{24+}$ compared to the isostructural Ga^{3+} analogue $\{Ga_{16}(OH)_{32}\}^{16+}$. This is due to different reaction pH (pH 4.0 for $Al_{16}P_8W_{48}$ vs. pH 5.0 for $Ga_{16}P_8W_{48}$). The bond distances of Al^{III}–O, Ga^{III}–O, and Fe^{III}–O fall in the range of 1.796(10)–2.044(9), 1.896(5)–2.068(5), and 1.895(12)–2.153(12) Å, respectively, and the corresponding Al–O–Al, Ga–O–Ga, and Fe–O–Fe angles are similar within the respective range of 92.7(4)°–148.0(5)°, 96.4(2)°–143.9(3)°, and 94.2(5)°–139.6(7)°, respectively.

In 2019, Wang and coworkers introduced selenium into the cavity of P_8W_{48} and isolated a mixed potassium–lithium salt, $K_{26}Li_6[(SeO)_4P_8W_{48}O_{184}]\cdot 98H_2O$ (**$Se_4P_8W_{48}$**).[133] Four $[SeO_3]^{2-}$ ions were grafted in the cavity of the crown-shaped P_8W_{48}, like for $Co_4P_8W_{48}$, resulting in a structure with D_{2h} point group symmetry.

Sokolov and coworkers reported the incorporation of $\{NbO\}^{3+}$ units into the cyclic **P_8W_{48}** ion via reaction with the Nb–O_x reagent in different ratios (4:1, 8:1, and 16:1) and different concentrations. They have isolated mixed salts of

different compounds with differing numbers of coordinated $\{NbO(H_2O)\}^{3+}$ groups, disordered over the eight equivalent binding sites. The formulas suggest that the compounds are likely mixtures of two or more polyanions: $K_{25.7}Li_5(NH_4)_5[(HP_8W_{48}O_{184})(NbO(C_2O_4)(H_2O))_{3.3}]\cdot 73H_2O$ (**$(NbO(C_2O_4)(H_2O))_{3.3}P_8W_{48}$**), $K_{30.8}Li_{3.5}(NH_4)_3[(P_8W_{48}O_{184})(NbO(C_2O_4)(H_2O))_{1.7}]\cdot 74.5H_2O$ (**$(NbO(C_2O_4)(H_2O))_{1.7}P_8W_{48}$**), $K_{21.6}Li_5(NH_4)_8H_{6.8}[(P_8W_{48}O_{184})(NbO(H_2O))_{4.4}(C_2O_4)_{1.5}]\cdot 66H_2O$ (**$(NbO(C_2O_4)_{1.5}(H_2O))_{4.4}P_8W_{48}$**), $K_{24.4}Li_5(NH_4)_{5.5}[(HP_8W_{48}O_{184})(NbO(C_2O_4)(H_2O))_{3.1}]\cdot 59H_2O$ (**$(NbO(C_2O_4)(H_2O))_{3.1}P_8W_{48}$**), $K_{26.7}Li_4(NH_4)_{5.5}H_{2.6}[(P_8W_{48}O_{184})(NbO(H_2O))_{3.8}(C_2O_4)_{2.5}]\cdot 55.5H_2O$ (**$(NbO(C_2O_4)_{2.5}(H_2O))_{3.8}P_8W_{48}$**).[134]

Duval and coworkers have introduced the uranyl cation into the cavity of the cyclic P_8W_{48} polyanion, resulting in the salt $K_{11.3}Li_{8.1}Na_{22}[(UO_2)_{7.2}(HCOO)_{7.8}(P_8W_{48}O_{184})Cl_8]\cdot 89H_2O$ (**$(UO_2)_{7.2}(HCOO)_{7.2}P_8W_{48}$**) (Fig. 17).[135] This is the first time that actinide elements were incorporated in the cavity of P_8W_{48}. The structure of **$(UO_2)_{7.2}(HCOO)_{7.2}P_8W_{48}$** revealed that the 7.2 uranyl cations are disordered over eight positions, suggesting the presence of mixtures of two or more polyanions in the material.[126] Interestingly, Kortz and coworkers first introduced the peroxouranium containing wheel-shaped P_8W_{48}, resulting in peroxouranium complex $K_{18}Li_{22}[(UO_2)_8(O_2)_8(P_8W_{48}O_{184})]\cdot 133H_2O$ (**$(UO_2)_4(O_2)_4P_8W_{48}$**).[136] The polyanion (**$(UO_2)_4(O_2)_4P_8W_{48}$**) consists of four peroxo groups, and each one is connected to two uranium cations. The $\{(UO_2)_4(O_2)_4\}$ unit comprises neutral four uranyl atoms and four peroxo groups, connecting to each other by side-on peroxo bridges, which is similar to previously reported (**$Li(UO_2)_4(O_2)_4(PO_3OH)_2P_6W_{36}$**) by the same group.[92]

In 2019, Ibrahim et al. reported an isopoly tetratungsten-oxo cluster incorporated inside the rim of P_8W_{48} along with six internal and four external Mn^{2+} ions, resulting in $[(P_8W_{48}O_{184})(W_4O_{16})K_{10}Li_4Mn_{10}Na(H_2O)_{50}Cl_2]^{15-}$ (**$Mn_{10}W_4P_8W_{48}$**).[137] The Mn–O bond lengths are in the range of 2.087–2.315 Å, while Mn–Cl is 2.365 Å. The oxidation states of the Mn ions were checked by bond valence sum analysis,[138–140] and all were shown to be Mn^{2+}. The outer Mn^{2+} ions assist the formation of a 3D network through intermolecular Mn–O(W) bonding together with potassium ions. Interestingly, the origin of the one Na^+ ion in the compound is ambiguous.

Kögerler and coworkers studied the isomerization of the four $\{\alpha-P_2W_{12}O_{48}\}$ units comprising the P_8W_{48} wheel in the presence of Cu^{2+} ions in 0.66 M acetate buffer at pH 5.2. They were able to isolate $K_7Li_2Na_{27}[\alpha\gamma\alpha\gamma-P_8W_{48}O_{184}\{Cu(H_2O)\}_2]\cdot 78H_2O$ (**$Cu_2-\alpha\gamma\alpha\gamma-P_8W_{48}$**), $K_{7.5}Na_{17}Cu_{2.425}(WO_2)_{1.325}[\gamma\gamma\gamma\gamma-P_8W_{48}O_{184}\{Cu(H_2O)_{0.5}\}_4]\cdot 102H_2O$ (**$Cu_4-\gamma\gamma\gamma\gamma-P_8W_{48}$**), and $K_7Li_2Na_{19.5}Cu_{1.75}(WO_2)[\alpha\gamma\gamma\gamma-P_8W_{48}O_{184}\{Cu(H_2O)\}_3]\cdot 72H_2O$ (**$Cu_3-\alpha\gamma\gamma\gamma-P_8W_{48}$**).[141] The molar ratio of Cu^{2+} to P_8W_{48}, temperature, and reaction time played a crucial role when trying to prepare the three compounds. The synthesis of Kortz's **$Cu_{20}P_8W_{48}$**,[78] and Mialane's **$Cu_{20}(N_3)_6P_8W_{48}$**[90] took 1 h and 15 min, respectively, at 80 °C, whereas **$Cu_2-\alpha\gamma\alpha\gamma-P_8W_{48}$** was isolated after 2 h reaction time at 95 °C, in order to transform two P_2W_{12} units from α to γ in the P_8W_{48} wheel. According to the authors, Li^+ ions also play a crucial role in such isomeric transformation.

In the same year, Suzuki, Yamaguchi, and coworkers synthesized a series of P_8W_{48} ions with eight incorporated 3d metal ions from mixed organic solvent. The products were isolated as tetra-n-butylammonium (TBA) salts, TBA$_{14}$H$_2$-[$\{M_2^{II}$ (OH$_2$)$_2\}_2\{M^{II}$(OH$_2$)$_2\}_4$P$_8$W$_{48}$O$_{176}$(OCH$_3$)$_8$]·nH$_2$O·mCH$_3$CN, where M^{II} = Mn, Co, Ni, Cu, Zn ($M_8P_8W_{48}O_{176}$).[142] Edge-shared bis (square pyramidal) metal-aqua sites $\{(\mu\text{-O})_2(M\text{-OH}_2)$ $(\mu_3\text{-O})_2(M\text{-OH}_2)(\mu\text{-O})_2\}$ were incorporated in the cavity of P_8W_{48}. Interestingly, a new type of α,γ,α,γ-type P_8W_{48} was observed after the reaction with the 3d metal ions, with two of the four α-P_2W_{12} units having been transformed to γ-P_2W_{12}. The Co^{2+} ions are disordered over two of the four P_2W_{12} units. However, with increased methanol concentration in the reaction, the Co^{2+} ions fully occupied each of the four P_2W_{12} units. The Mn^{2+} and Ni^{2+}-containing P_8W_{48} polyanions exhibit the first examples of edge-shared bis(square pyramidal)manganese-aqua and nickel-aqua complexes. The M–O axial bond length increased for the metal ion M from left to right in the periodic table. For example, in the Mn^{2+} derivative $Mn_8P_8W_{48}O_{176}$, the axial Mn–O bond lengths of 2.17–2.22 Å (Mn3–O13, Mn3–O60, Mn4–O14, Mn4–O59) were similar to the equatorial bond lengths of 2.10–2.24 Å (Mn3–O3, Mn3–O4, Mn3–O39, Mn3–O42; Mn4–O5, Mn4–O6, Mn4–O40, Mn4–O41). On the other hand, for the Co^{2+} and Ni^{2+} derivatives, the axial bonds (2.13–2.18 Å) are longer than the equatorial ones (1.99–2.07 Å). As expected, for the Cu^{2+} derivative, the Cu–O axial bonds (2.22–2.27 Å) are much longer than the equatorial bonds (1.98–2.08 Å). For the Mn^{2+} and Co^{2+} derivatives, a decrease in magnetic susceptibility was observed upon cooling, implying antiferromagnetic interactions between the 3d metal ions. However, ferromagnetic interactions were observed for the Ni^{2+} and Cu^{2+} derivatives. The same authors have also reported two high-nuclear manganese derivatives of P_8W_{48}, (C$_{24}$PH$_{20}$)$_{17}$ H$_{37}$[Mn$_{18}$P$_8$W$_{48}$O$_{214}$]·16H$_2$O·4CH$_3$CN ($Mn_{18}P_8W_{48}O_{214}$) and (C$_{16}$H$_{36}$N)$_{12}$H$_{16}$[Mn$_{20}$P$_8$W$_{48}$O$_{216}$]·4C$_2$H$_3$N·C$_2$Cl$_2$H$_4$ ($Mn_{20}P_8W_{48}$ O_{216}).[143] The $Mn_{18}P_8W_{48}O_{214}$ polyanion is a mixed-valent species with 18 $Mn^{2+/3+}$ ions in the cavity of P_8W_{48}. Bond valence sum calculations revealed the presence of 8 Mn^{2+} and 10 Mn^{3+} ions. The four P_2W_{12} units isomerized from α- to γ-type in $situ$ in the presence of the transition metal ions, which was observed previously.[98,138] The $Mn_{20}P_8W_{48}O_{216}$ polyanion was obtained by reacting P_8W_{48} with 20 equivalents of Mn(OAc)$_3$ in acetonitrile medium. This polyanion was also found to be mixed-valent as per bond valence sum calculations, showing the presence of 12 Mn^{3+} and 8 Mn^{4+} ions. All 20 Mn ions are bound in the cavity of P_8W_{48} and all four units of P_2W_{12} remained as α-type. The connectivity of the Mn ions in $Mn_{20}P_8W_{48}O_{216}$ is different from $Mn_{18}P_8W_{48}O_{214}$. In the former, four Mn^{3+} ions are bound to each α-P_2W_{12} unit, and four Mn ions are bound at the hinges of the four α-P_2W_{12} units. Eight Mn ions of oxidation state either +3 or +4 are bound to the vacant sites within the cavity of the cyclic P_8W_{48}, which are disordered over eight positions together with K^+ ions.[88] Two Mn ions occupy the middle part of opposing P_2W_{12} units, and four Mn ions are at the hinges of the four P_2W_{12} units. Very recently, Suzuki, Yamaguchi, and coworkers

have reported a series of multi-nuclear copper(II)-containing P_8W_{48} derivatives, which were synthesized in organic solvent. The four compounds thus reported were formulated as TBA$_{11}$H$_{13}$[Cu$_4$(H$_2$O)$_4$P$_8$W$_{48}$O$_{176}$(OCH$_3$)$_8$]·28H$_2$O·3CH$_3$NO$_2$ ($Cu_4P_8W_{48}$), TBA$_{14}$H$_2$[Cu$_8$(H$_2$O)$_{12}$P$_8$W$_{48}$O$_{176}$(OCH$_3$)$_8$]·24H$_2$O·CH$_3$CN ($Cu_8P_8W_{48}$), TBA$_{14}$H$_2$[Cu$_{12}$(H$_2$O)$_{16}$P$_8$W$_{48}$O$_{184}$]·4H$_2$O ($Cu_{12}P_8W_{48}$), and TBA$_{16}$H$_8$[Cu$_{16}$(OH)$_{16}$(H$_2$O)$_4$P$_8$W$_{48}$O$_{184}$]·12H$_2$O·C$_3$H$_6$O ($Cu_{16}P_8W_{48}$), respectively.[144] Interestingly, the authors were able to obtain the high nuclearity polyanions from the reaction of low nuclearity polyanions with copper(II) salt, for example, $Cu_8P_8W_{48}$ from $Cu_4P_8W_{48}$, $Cu_{12}P_8W_{48}$ from $Cu_8P_8W_{48}$, and $Cu_{16}P_8W_{48}$ from $Cu_{12}P_8W_{48}$, respectively. Moreover, in the case of $Cu_4P_8W_{48}$ and $Cu_8P_8W_{48}$, two P_2W_{12} units with copper ions connected transformed from α to γ-type isomers by 60° rotation of the central $\{PO_4\}$ hetero groups. The reactive sites of the remaining two $\{$α-$P_2W_{12}\}$ units are occupied by methoxy groups. This result was similar to the previously reported cobalt-containing P_8W_{48} work by the same group where eight cobalt(II) ions were introduced without affecting the presence of the methoxy groups,[145] suggesting that they act as a protecting organic ligands being essential for metal incorporation inside the cavity of P_8W_{48} without disorder. In $Cu_{12}P_8W_{48}$ and $Cu_{16}P_8W_{48}$ comprising the same γ,γ,γ,γ-type P_8W_{48} framework, the copper(II) coordination geometry differs from each other. The arrangements and connectivity of the copper(II) ions in these structures are also different from the $Cu_{20}P_8W_{48}$ polyanion.[94] Very recently, the same group has demonstrated the H_2-based reduction of copper(II) ions in the cavity of P_8W_{48}, resulting in a catalyst which is active for the catalytic hydrogenation of several organic substrates, such as alkenes, alkynes, as well as carbonyl- and nitro-containing compounds.[146]

In 2019, Cronin and coworkers reported that P_8W_{48} self-assembled into inorganic frameworks in the presence of silver ions, enabling interaction with the POM wheel and linking them together. It was observed that P_8W_{48} was highly reactive towards silver ions, resulting in the formation of fragments as seen in the compounds Li$_8$K$_{9.5}$Ag$_{21}$[H$_{16}$P$_{10}$W$_{66}$O$_{251}$]$_{0.5}$ [H$_{14}$P$_9$W$_{63}$O$_{235}$]·0.5Cl$_2$·50H$_2$O ($Ag_{21}P_9W_{63}O_{235}$), Li$_8$K$_{13}$Ag$_{13}$ [H$_{12}$P$_8$W$_{51}$O$_{196}$]·50H$_2$O ($Ag_{13}P_8W_{51}O_{196}$), and Li$_{10}$K$_{12}$Ag$_4$[H$_{14}$P$_8$W$_{48}$O$_{184}$]·170H$_2$O ($Ag_4P_8W_{48}O_{148}$), respectively.[147] The species $Ag_{21}P_9W_{63}O_{235}$ revealed two cocrystallized P_8W_{48} units connected by 10 Ag^+ ions, forming a "POMzite" framework. In $Ag_{13}P_8W_{51}O_{196}$, the P_8W_{48} units are linked forming a framework with 9 Ag^+ ions per formula unit. Further tuning of the reaction conditions yields $Ag_4P_8W_{48}O_{148}$, where 4 Ag^+ ions are linked to P_8W_{48}, resulting in a cubic array, and surprisingly, no Ag^+ ions were detected in the cavity of P_8W_{48}. Very recently, Suzuki, Yamaguchi, and coworkers have reported a (Ag_{30}) cluster within P_8W_{48}, TBA$_{17}$H [Ag$_{30}$(P$_8$W$_{48}$O$_{184}$)]·10DMF·30H$_2$O ($Ag_{30}P_8W_{48}$), which was synthesized from a $\{Ag_{16}\}$ cluster-containing P_8W_{48} derivative.[145] The $Ag_{30}P_8W_{48}$ nanocluster possesses an additional 14 silver atoms that were introduced into the Ag$_{16}$ cavity, resulting in an Ag_{30} nanocluster with distorted body-centered-cubic atom arrangements inside the P_8W_{48} polyanion, revealed by single crystal X-ray crystallography. The $Ag_{30}P_8W_{48}$ exhibits high and

Table 1 Structural characteristics and component building blocks of tungstophosphate-based compounds

Sl. no.	Formula	Abbreviation	Brief description	Ref.
1	$Li_{5.5}K_3H_{3.5}[P_2W_{12}(NbO_2)_6O_{56}]\cdot H_2O$	$\mathbf{P_2W_{12}(Nb\text{-}O_2)_6}$	Six {Nb–O_2} occupy six vacant positions of {P_2W_{12}}. The six Nb atoms are connected by four η^2-O atoms, one η^4-bridging O atom (cap sites or triply-bridging O atom on belt sites), and one terminal η^2-coordinated peroxo unit.	53
2	$K_7[Fe(OH_2)P_2W_{12}Mo_5O_{61}]$	$\mathbf{FeP_2W_{12}}$	All six-vacant positions of {P_2W_{12}} are filled up by five Mo^{VI} ions in the belt and one cap position and one cap position by a Fe^{3+} ion.	54
3	$K_7[\alpha_1\text{-}Fe(OH_2)P_2W_{13}Mo_4O_{61}]$ and $K_8[\alpha_2\text{-}Cu(OH_2)\text{-}P_2W_{13}Mo_4O_{61}]$	$\mathbf{\alpha_1\text{-}FeP_2W_{13}Mo_4, \alpha_2\text{-}CuP_2W_{13}Mo_4}$	Four Mo^{6+}, one Fe^{3+}/Cu^{2+} ion, and one extra tungsten atom fill the six vacancies of {P_2W_{12}}, generating a {P_2W_{13}} moiety.	54
4	$K_8[\alpha_2\text{-}Cu(OH_2)P_2W_{12}Mo_5O_{61}]$	$\mathbf{\alpha_2\text{-}CuP_2W_{12}Mo_5}$	The vacant positions of {P_2W_{12}} are occupied by five Mo^{VI} ions in the two belts and a cap and a Cu^{2+} ion in the other cap.	54
5	$Li_2K_4[H_4P_2W_{12}Fe_9O_{56}(OAc)_7]\cdot34H_2O$	$\mathbf{Fe_9(OAc)_7P_2W_{12}}$	The six vacancies of {P_2W_{12}} are occupied by Fe^{3+} ions, forming a {$P_2W_{12}Fe_6$} unit to which three additional Fe^{3+} atoms are coordinated.	58
6	$K_6Na_{10}[H_{12}P_4W_{28}Fe_8O_{120}]\cdot34H_2O$	$\mathbf{Fe_8P_4W_{28}}$	Dimeric clusters with four extra tungsten atoms in the cap position and eight iron atoms occupying the belt position.	59
7	$K_{12}[\{M(H_2O)_4\}_2\{H_{12}P_4W_{28}Fe_8O_{120}\}]\cdot30H_2O$ (M = Co^{2+}, Mn^{2+}, Ni^{2+})	$\mathbf{M_2Fe_8P_4W_{28}}$ (M = Co^{2+}, Mn^{2+}, Ni^{2+})	Two {P_2W_{12}} units with four extra tungsten atoms in the cap positions and eight Fe^{3+} atoms in the belt positions. Two such {$Fe_4P_2W_{14}$} units are bridged by Co^{2+}, Ni^{2+}, or Mn^{2+} ions.	59
8	$K_3Na_{17}[\{W_2Co_2O_8(H_2O)_2\}(P_2W_{12}O_{46})_2]\cdot30H_2O$	$\mathbf{W_2Co_2O_8(P_2W_{12})_2}$	The dimeric structure consists of two {P_2W_{12}} units fused *via* four W–O–W bonds and two W^{VI} and Co^{2+} atoms are bound in the vacant positions.	62
9	$K_4Na_4[H_6P_2W_{12}Nb_4O_{59}(NbO_2)_2]_2\cdot48H_2O$	$\mathbf{\{P_2W_{12}Nb_4(NbO_2)_2\}_2}$	Six Nb atoms occupy two cap and four belt sites of the lacunary {P_2W_{12}} precursor. Two such {$P_2W_{12}Nb_4(NbO_2)_2$} units are dimerized *via* Nb–O–Nb bonds.	63
10	$K_7[H_{13}\{Nb_6(O_2)_4P_2W_{12}O_{57}\}_2]\cdot31H_2O$	$\mathbf{\{P_2W_{12}Nb_6(O_2)_4\}_2}$	The Wells–Dawson dimer consists of two {P_2W_{12}} units linked by two Nb–O–Nb bridges and the six vacant sites of each {P_2W_{12}} unit are filled by a $Nb_6(O_2)_4$ group.	67
11	$(NH_4)_{16}[H_{14}\{P_2W_{12}Nb_7O_{63}(H_2O)_2\}_4\{Nb_4O_4(OH)_6\}]\cdot16H_2O$	$\mathbf{\{(P_2W_{12})Nb_7\}_4Nb_4}$	This polyanion comprises an adamantine-like {Nb_4O_6} core encapsulated by two $[Nb_6P_2W_{12}O_{61}]^{10-}$ units (without any Nb-peroxo groups).	67
12	$K_{3.5}Li_8[((CH_3)_2NH_2)_{4.5}[(PhXO)_2P_4W_{24}O_{92}]\cdot nH_2O$ (X = P, n = 35 and X = As, n = 40)	$\mathbf{PhXOP_4W_{24}}$, X = P, As	The structure consists of a {$P_4W_{24}O_{29}$} unit capped by two phenyl-phosphonate or -arsonate ligands.	68
13	$KLi_8[((CH_3)_2NH_2)_{10}[(o\text{-}H_2N\text{-}C_6H_4AsO_3)_4P_4W_{24}O_{85}]\cdot17H_2O\cdot LiCl$, $KHLi_2[((CH_3)_2NH_2)_6[Mn(H_2O)_4]_2\{Mn(H_2O)_4\}(o\text{-}H_2N\text{-}C_6H_4\text{-}AsO)_2P_4W_{24}O_{92}]\cdot25H_2O\cdot0.2KCl\cdot0.4LiCl$, $K_{1.5}Li_2[((CH_3)_2NH_2)_{6.5}\text{-}[Co(H_2O)_4]_2[\{Co(H_2O)_4\}(o\text{-}H_2N\text{-}C_6H_4\text{-}AsO)_2P_4W_{24}O_{92}]\cdot24H_2O\cdot0.5LiCl$, and $K_{1.5}Li_2[((CH_3)_2NH_2)_{6.5}[Ni(H_2O)_4]_2[\{Ni(H_2O)_4\}(o\text{-}H_2N\text{-}C_6H_4\text{-}AsO)_2P_4W_{24}O_{92}]\cdot24H_2O\cdot0.2LiCl$.	$\mathbf{(o\text{-}NH_2\text{-}C_6H_6\text{-}AsO)_4P_4W_{24}O_{92}M}$ $\mathbf{(o\text{-}NH_2\text{-}C_6H_6\text{-}AsO)_2P_4W_{24}}$ (M = Co^{2+}, Mn^{2+}, Ni^{2+})	The introduction of divalent transition metal ions (Mn^{2+}, Co^{2+}, Ni^{2+}) in the reaction mixture containing ($o\text{-}NH_2\text{-}C_6H_6\text{-}AsO$)$_4P_4W_{24}O_{92}$ resulted in 1D coordination polymers $[\{M(H_2O)_4\}P_4W_{24}O_{92}(C_6H_4AsNO)_2]^{14-}$ (M = Mn^{2+}, Co^{2+}, Ni^{2+}) ($\mathbf{M(o\text{-}NH_2\text{-}C_6H_6\text{-}AsO)_2P_4W_{24}}$).	69
14	$K_4Na_{15}[K_3C\{Mn(H_2O)_4\}_2\{WO_2(H_2O)_2\}_2\{WO(H_2O)\}_3(P_2W_{12}O_{48})_3]\cdot77H_2O$	$\mathbf{Mn_2(P_2W_{12})_3\{WO_2(H_2O)_2\}_2\{WO(H_2O)\}_3}$	Three {P_2W_{12}} units are connected by three WO(H_2O) hinges forming a cyclic P_6W_{39} assembly which accommodates two W^{VI} and two Mn^{2+} guest atoms.	71
15	$K_3Na_7Li_{5.5}Ni_{0.25}[Na_3C\{Ni_{3.5}(H_2O)_{13}\}\{WO_2(H_2O)_2\}_2\{WO(H_2O)\}_3(P_2W_{12}O_{48})_3]\cdot64H_2O$	$\mathbf{Ni_{3.5}(P_2W_{12})_3\{WO_2(H_2O)_2\}_2\{WO(H_2O)\}_3}$	Two W^{VI} and four Ni^{2+} ions are incorporated in the cyclic P_6W_{39} host. One of the Ni^{2+} ions is disordered with a Na ion.	71
16	$K_6Na_{11}[Na_3C\{Cu_3(H_2O)_9\}\{WO_2(H_2O)_2\}_2\{WO(H_2O)\}_3(P_2W_{12}O_{48})_3]\cdot47H_2O$	$\mathbf{Cu_3(P_2W_{12})_3\{WO_2(H_2O)_2\}_2\{WO(H_2O)\}_3}$	Two W^{VI} and three Cu^{2+} ions are incorporated in the cyclic P_6W_{39} host.	71
17	$Na_{15}[Na_3C\{Co(H_2O)_4\}_6\{WO(H_2O)\}_3(P_2W_{12}O_{48})_3]\cdot109H_2O$ and $Na_{15}[Na_3C\{Ni(H_2O)_4\}_6\{WO(H_2O)\}_3(P_2W_{12}O_{48})_3]\cdot110H_2O$	$\mathbf{Co_6(P_2W_{12})_3\{WO(H_2O)\}}$ and $\mathbf{Ni_6(P_2W_{12})_3\{WO(H_2O)\}_3}$	Six Co^{2+} or Ni^{2+} ions are incorporated in the cyclic P_6W_{39} assembly.	72
18	$K_3Na_8[K_3C\{GdMn(H_2O)_{10}\}\{HMnGd_2(tart)O_2(H_2O)_{15}\}\{P_6W_{42}O_{151}(H_2O)_7\}]_\infty\cdot44H_2O$	$\mathbf{\{(MnGd)(HMnGd_2P_6W_{42})\}_\infty}$	The trimeric crown-shaped P_6W_{39} encapsulates a Mn^{2+} and two Gd^{3+} ions in the cavity. In addition, a Mn^{2+} and Gd^{3+} ion are present outside the polyanion, resulting in a two-dimensional solid-state framework.	73
19	$K_3Na_{10}[K_3C\{GdCo(H_2O)_{11}\}_2\{P_6W_{41}O_{148}(H_2O)_7\}]\cdot43H_2O$	$\mathbf{(GdCoP_6W_{41})_\infty}$	The structure comprises a trimeric, crown-shaped P_6W_{39} ion encapsulating two Co^{2+} and a Gd^{3+} ion as well as two W^{VI} atoms. The second Gd^{3+} ion is outside P_6W_{39}, linking polyanions to a one-dimensional chain, where this Gd^{3+} ion shows a square-antiprismatic coordination geometry.	73
20	$K_4[H_{23}(Cr(H_2O)_2)_3(H_2P_2W_{12}O_{48})_3]\cdot34H_2O$	$\mathbf{Cr_3(P_2W_{12})_3}$	Trimeric, cyclic assembly of {P_2W_{12}} units joined by three Cr^{III} ions.	74
21	$Na_{16}K_{12}[H_{56}P_8W_{48}Fe_{28}O_{248}]\cdot20H_2O$	$\mathbf{Fe_{28}P_8W_{48}}$	The tetrameric polyanion comprises four {$P_2W_{12}Fe_6$} units, and each is bridged through Fe–O–Fe linkages to a {Fe_4O_6} cluster core. The linking is through pairs of three Fe–O–Fe bridges, which involve the three outer Fe atoms.	55–57
22	$Na_{16}K_{10}[H_{55}P_8W_{49}Fe_{27}O_{248}]\cdot yH_2O$	$\mathbf{Fe_{27}P_8W_{49}}$	Similar structure as $\mathbf{Fe_{28}P_8W_{48}}$ with one of the sites having an occupancy of 25% W and 75% Fe.	55–57
23	$K_4Na_{22}\{[Co(H_2O)_2Cl][Co(H_2O)_3]_2[Co(H_2O)_5]_{1.5}[Co(H_2O)_3H_4P_8W_{49}O_{187}(H_2O)]\}\cdot2NaCl\cdot41.5H_2O$, and, $Na_{30}\{[Ni(H_2O)_3]_2[\{Ni(H_2O)_3\}_{1.5}H_3P_8W_{49}O_{187}(H_2O)]\}\cdot41.5H_2O$	$\mathbf{Co_{5.5}P_8W_{49}}$, and $\mathbf{Ni_{3.5}P_8W_{49}}$	The transformation of four {P_2W_{12}} ions to the cyclic P_8W_{49} happens *in situ via* self-condensation, performed in aqueous acidic medium in the presence of Co^{2+}/Ni^{2+} ions. The extra W atom originates from partial decomposition of {P_2W_{12}}.	75
24	$(NH_4)_{36}[\{Nb_4O_6(OH)_4\}\{Nb_6P_2W_{12}O_{61}\}_4]\cdot16H_2O$	$\mathbf{(Nb_4O_6)(Nb_6P_2W_{12})_4}$	The polyanion comprises a {Nb_4O_6} core which is surrounded by four $Nb_6P_2W_{12}$ units.	78

Table 1 *(Contd.)*

Sl. no.	Formula	Abbreviation	Brief description	Ref.
25	$Na_{24}[Mn_8(H_2O)_{32}P_8W_{48}O_{184}]\cdot58H_2O$, $K_4Na_{16}H_4[Co_8(H_2O)_{32}P_8W_{48}O_{184}]\cdot76H_2O$, and $Na_{20}H_4[Ni_8(H_2O)_{32}P_8W_{48}O_{184}]\cdot72H_2O$	$(M_8P_8W_{48}, M = Mn, Co, Ni)$	Eight divalent 3d metal ions are incorporated in the cyclic P_8W_{48} host.	79
26	$K_{10}[H_{123}Nb_{36}P_{12}W_{72}Mn_{12}^{III}Mn_3^{II}NaO_{424}]\cdot26H_2O$	$Mn_{15}(Nb_6P_2W_{12})_6$	The structure consists of six $\{Nb_6P_2W_{12}\}$ units which are connected alternately by four Mn^{2+} ions and four trinuclear $\{Mn^{III}\}$ moieties.	80
27	$[(n\text{-}C_4H_9)_4N]_{20}\cdot5H_{21.5}[\{\gamma\text{-}P_2W_{12}O_{48}Mn_4(C_5H_7O_2)_2(CH_3CO_2)_6\}]\cdot35H_2O$	$\{P_2W_{12}O_{48}Mn_4\}_6$	The polyanion P_2W_{12} reacts with Mn(acac), forming a hexameric polyanion in an organic medium. Two types of manganese coordination sites are present in each unit of manganese-substituted $\{P_2W_{12}\}$, and each unit is connected to the other unit of manganese-substituted P_2W_{12} unit.	81
28	$[(n\text{-}C_4H_9)_4N]_{16.6}H_{7.4}[\{\gamma\text{-}P_2W_{12}O_{48}Mn_4(H_2O)_6\}_4(H_2O)_4]\cdot8H_2O$	$\{P_2W_{12}O_{48}Mn_4\}_4$	The tetrameric polyanion forms after removing the organic capping in the manganese cation from the hexameric complex.	81
29	$([(n\text{-}C_4H_9)_4N]_5[\gamma\text{-}P_2W_{12}O_{44}M_2(OAc)(CH_3CONH_2)_2]\cdot nH_2O\cdot mCH_3CN$; M = Mn^{2+}, Co^{2+}, Ni^{2+}, Cu^{2+}, or Zn^{2+}; OAc = acetate)	$(\gamma\text{-}P_2W_{12}O_{44}M_2(OAc))$	The polyanion comprises a central edge-shared bis(square-pyramidal) $\{O_2M(\mu_3\text{-}O)_2(\mu\text{-}OAc)MO_2\}$ group bound to the belt area of $\{\gamma\text{-}P_2W_{12}\}$ and two acetamide (CH_3CONH_2) groups are coordinated to the vacant cap positions.	82
30	$K_{12}H_2[Ce_4(OH_2)_9(OH)_2(\alpha_1,\alpha_1\text{-}P_2W_{16}O_{59})_2]\cdot48H_2O$	$Ce_4(\alpha_1\alpha_1\text{-}P_2W_{16})_2$	The polyanion has a dimeric structure composed of two $\{\alpha_1,\alpha_1\text{-}P_2W_{16}O_{59}\}$ units connected by four cerium(III) ions.	60
31	$K_{16}[\{La(CH_3COO)(H_2O)_2(\alpha_2\text{-}P_2W_{17}O_{61})\}_2]\cdot36H_2O$	$La(OAc)(\alpha_2\text{-}P_2W_{17})_2$	The polyanion consists of two $[\alpha_2\text{-}P_2W_{17}O_{61}]^{10-}$ units connected by two lanthanum acetate dimers $(La_2(CH_3COO)_2(H_2O)_4)^{4+}$, resulting in a head-on transoid dimer. In an acidic medium, P_2W_{12} quickly transforms into the monovacant $[\alpha_2\text{-}P_2W_{17}O_{61}]^{10-}$.	84
32	$K_4Na_{10}[\alpha_1\text{-}CuP_2W_{17}O_{60}(OH)]_2\cdot\sim58H_2O$	$Cu_2P_4W_{34}$	The dimeric polyanion cluster is formed from two units each of $\alpha_1\text{-}\{CuP_2W_{17}\}$, connected through the W-OH-Cu bonds resulting in the dimeric cluster.	86
33	$Na_2[H_2en][H_2hn]_{0.5}[Cu(en)_2]_{4.5}[\alpha_1\text{-}CuP_2W_{17}O_{60}(OH)]_2\cdot\sim43H_2O$	$\{Cu(en)_2CuP_2W_{17}\}_\infty$	The dimeric polyanion assembly $[\alpha_1\text{-}CuP_2W_{17}O_{60}(OH)]_2$ is linked to an extended network by $\{Cu(en)_2\}^{2+}$ units.	86
34	$Na_3[H_2hn]_{2.5}[P_2W_{17}O_{60}Cu(OH)_2]\cdot\sim14H_2O$	$\{(H_2hn)(CuP_2W_{17})_2\}_\infty$	The polyanion possesses a 3-D hybrid supramolecular framework with 1-D tunnels.	86
35	$Na_8H_2L(H_2enMe)_4[Mn(H_2O)_2(W_4Mn_4O_{12})(P_2W_{14}O_{54})]\cdot17H_2O$	$\{W_4Mn_4(MnP_2W_{14})_2\}_\infty$	The 1-D inorganic polymer building blocks comprise multi Mn^{2+}-substituted Wells–Dawson ions and Mn^{2+} linkers with the idealized C_2 symmetry, further connected into a 3-D supramolecular network via extensive hydrogen-bonding interactions.	87
36	$K_{56}Li_{74}H_{14}[Mn_{40}P_{32}W_{224}O_{888}]\cdot ca.$ 680 H_2O	(P_8W_{48}) $(Mn_4P_2W_{14})_4(Mn_3P_2W_{15})_8$	The polyanion consists of $\{P_2W_{14}\}$, $\{P_2W_{15}\}$ and $\{P_8W_{48}\}$ corner-sharing Wells–Dawson type units with no Mn^{2+} ions found inside the cavity of P_8W_{48}.	88
37	$[K(H_2O)_2]_4[K_4(\mu\text{-}H_2O)_4(H_2O)_4]_2\{[Ln_2(\mu\text{-}OH)_4(H_2O)x]_2(H_{24}P_8W_{48}O_{184})\}\cdot yH_2O$ (Ln = Nd, Sm, Tb)	$Ln_4P_8W_{48}$	Eight lanthanide ions occupy the cavities of P_8W_{48}, with each lanthanide ion being bridged through hydroxyl groups and having a 50% occupancy in each position.	89
38	$[K(H_2O)_2]_4[K_4(\mu\text{-}H_2O)_8]_2[K(H_2O)]_8\{[Mn_8(H_2O)_{16}](H_4P_8W_{48}O_{184})\}$	$K_8Mn_8P_8W_{48}$	Eight Mn^{2+} and eight K^+ ions are incorporated in the cavity of P_8W_{48}.	89
39	$[cis\text{-}(P_2W_{15}Nb_3O_{61})_2]^{14-}$ and two phases of $[trans\text{-}(P_2W_{14.7}Nb_{3.3}O_{61})_2]^{14.6-}$	$P_2W_{15}Nb_3$	Nb^V ions are taken up by P_2W_{12} in acidic media resulting in the dimer $[(P_2W_{15}Nb_3O_{61})_2]^{14-}$ and a mixture of derivatives with an average formula $[(P_2W_{14.7}Nb_{3.3}O_{61})_2]^{14.6-}$, indicating the coexistence of species with different composition, such as $\{(P_2W_{15}Nb_3)_2\}$ (70%) and $\{(P_2W_{14}Nb_4)_2\}$ (30%).	90
40	$[Fe_{48}(OH)_{76}(H_2O)_{16}(HP_2W_{12}O_{48})_8]^{36-}$	$Fe_{48}(P_2W_{12})_8$	This structure contains 48 Fe^{3+} ions surrounded by eight P_2W_{12} ions, comprising eight equivalent $\{Fe_6P_2W_{12}\}$ subunits, linked to each other via Fe–O–Fe/W bonds.	91
41	$K_{17}Li_{11}[\{Sn(CH_3)_2\}_4(H_2P_4W_{24}O_{92})_2]\cdot51H_2O$	$\{Sn(CH_3)_2\}_4(P_4W_{24})_2$	The structure consists of two P_4W_{24} units linked through four dimethyltin groups, resulting in a dimeric hybrid inorganic–organic polyanion cluster.	44
42	$K_6Li_{19}[Li(H_2O)K_4(H_2O)_3\{(UO_2)_4(O_2)_4(H_2O)_2\}_2(PO_3OH)_2P_6W_{36}O_{136}]\cdot74H_2O$	$Li(UO_2)_4(O_2)_4(PO_3OH)_2P_6W_{36}$	The structure consists of three P_2W_{12} units encapsulating two independent, neutral symmetrical uranium-peroxo $[(UO_2)(O_2)]_4$ units in the central cavity, resulting in a U-shaped $\{P_2W_{12}\}_3$ assembly for the first time.	92
43	$K_{12}Rb_3[Rb_3\subset\{V_3^VV_3^{IV}O_7(H_2O)_6\}_2\{H_6P_6W_{39}O_{147}(H_2O)_3\}]\cdot63H_2O$	$(V^VV_3^{IV}O_7)_2P_6W_{39}$	The polyanion cluster is composed of three $\alpha\text{-}\{P_2W_{12}\}$ subunits, which form a macrocyclic template of P_6W_{39}, capped by two mixed-valent $\{(V^V=O)(V^{IV}=O)_3(\mu_2\text{-}O)_3(H_2O)_6\}^{3+}$ ($\{V^VV_3^{IV}\}$) groups.	93
44	$Na_{12}K_8H_4[K_8\subset\{V_4^VV_2^{IV}O_{12}(H_2O)_2\}_2\{P_8W_{48}O_{184}\}]\cdot80H_2O$	$(V_4^VV_2^{IV}O_{12})_2P_8W_{48}$	In this polyanion, two $\{V_4^VV_2^{IV}O_{12}(H_2O)_2\}^{4+}$ units are observed to be trapped inside the cavity of P_8W_{48}. The $\{V_4^VV_2^{IV}O_{12}(H_2O)_2\}^{4+}$ unit consists of two octahedral V^{IV} and four tetrahedral V^V centers. The oxidation of V^{IV} to V^V occurs due to air.	94
45	$K_{12}Li_{13}[Cu_{20}Cl(OH)_{24}(H_2O)_{12}(P_8W_{48}O_{184})]\cdot22H_2O$	$Cu_{20}ClP_8W_{48}$	This structure was the first example demonstrating that d-metal ions can be incorporated in the cavity of P_8W_{48}. Here, twenty Cu^{2+} ions are grafted in P_8W_{48}, and the coordination geometry of Cu^{2+} ranges from octahedral to square-pyramidal and square-planar, with a chloride ion encapsulated in the center of the structure.	96

Table 1 (Contd.)

Sl. no.	Formula	Abbreviation	Brief description	Ref.
46	$K_{12}Li_{13}[Cu_{20}Br(OH)_{24}(H_2O)_{12}(P_8W_{48}O_{184})]\cdot60H_2O$ and $K_{12}Li_{13}[Cu_{20}I(OH)_{24}(H_2O)_{12}(P_8W_{48}O_{184})]\cdot50H_2O$	$\mathbf{Cu_{20}BrP_8W_{48}}$, and $\mathbf{Cu_{20}IP_8W_{48}}$	Identical structure to $\mathbf{Cu_{20}ClP_8W_{48}}$ but with bromide or iodide acting as the central template rather than instead of chloride.	97
47	$LiK_{14}Na_9[P_8W_{48}O_{184}Cu_{20}(N_3)_6(OH)_{18}]\cdot60H_2O$	$\mathbf{Cu_{20}(N_3)_6P_8W_{48}}$	The polyanion comprises two $\{Cu_5(OH)_4\}^{6+}$ and two $\{Cu_5(OH)_2(\mu_{1,1,3,3}\text{-}N_3)\}^{7+}$ units incorporated in the cavity of $\mathbf{P_8W_{48}}$.	116
48	$Li_4K_{16}[P_8W_{48}O_{184}Fe_{16}(OH)_{28}(H_2O)_4]\cdot66H_2O\cdot2KCl$	$\mathbf{Fe_{16}P_8W_{48}}$	The polyanion contains a cationic $\{Fe_{16}(OH)_{28}(H_2O)_4\}^{20+}$ cluster incorporated in the cavity of $\mathbf{P_8W_{48}}$. The 16-iron(III)-hydroxo core consists of eight pairs of structurally equivalent, edge-shared $\{Fe_2O_{12}\}$ units.	117
49	$K_9LiNa[Fe_{16}O_2(OH)_{23}(H_2O)_9P_8W_{49}O_{189}Gd_4(H_2O)_{19}]\cdot50H_2O$ and $K_{8.5}Na_{0.5}Li_{0.5}Eu_{0.5}[Fe_{16}O_2(OH)_{23}(H_2O)_9P_8W_{49}O_{189}Eu_4(H_2O)_{19}]\cdot70H_2O$	$\mathbf{Fe_{16}Ln_4P_8W_{49}}$ (Ln = Gd^{3+}, Eu^{3+})	The $\mathbf{Fe_{16}Ln_4P_8W_{49}}$ (Ln = Gd^{3+}, Eu^{3+}) polyanion can be described as a derivative of $\mathbf{Fe_{16}P_8W_{48}}$ with four Ln^{3+} ions grafted on the iron-oxo core and the $\mathbf{P_8W_{48}}$ wheel is cleaved with an extra tungsten atom being bound right there.	118
50	$K_{12}Li_{16}Co_2[Co_4(H_2O)_{16}P_8W_{48}O_{184}]\cdot60H_2O$	$\mathbf{Co_4P_8W_{48}}$	The structure has four Co^{2+} ions bound at two opposite hinge sites of $\mathbf{P_8W_{48}}$.	121
51	$K_{12}Li_{10}Mn_3[Mn_4(H_2O)_{16}(P_8W_{48}O_{184})(WO_2(H_2O)_2)_2]\cdot67H_2O$ and $K_{14}Li_8Ni_3[Ni_4(H_2O)_{16}(P_8W_{48}O_{184})(WO_2(H_2O)_{2)2}]\cdot44H_2O$	$\mathbf{Mn_4P_8W_{50}}$ and $\mathbf{Ni_4P_8W_{50}}$	This structure is identical to $\mathbf{Co_4P_8W_{48}}$, except that two additional W^{VI} ions in the form of $\{WO_2(H_2O)_2\}$ groups are grafted in the cavity, one each at the two hinges which are not occupied by M^{2+} (M = Mn, Ni) ions, resulting in a cyclic P_8W_{50} unit.	121
52	$K_{20}Li_{16}[(VO_2)_4(P_8W_{48}O_{184})]\cdot48H_2O$	$\mathbf{(VO_2)_4P_8W_{48}}$	Four V^VO groups are coordinated in the cavity of $\mathbf{P_8W_{48}}$.	121
53	$K_{15}Li_5[\{Co_{10}(H_2O)_{34}(P_8W_{48}O_{184})\}]\cdot54\,H_2O$	$\mathbf{\{Co_{10}(H_2O)_{34}P_8W_{48}\}_\infty}$	This polyanion structure is similar to that of $\mathbf{Co_4P_8W_{48}}$, except that an additional four external Co^{2+} ions link adjacent polyanions resulting in 1D chains.	122
54	$K_8Li_{12}[\{Co_{10}(H_2O)_{44}(P_8W_{48}O_{184})\}]\cdot60H_2O$	$\mathbf{\{Co_{10}(H_2O)_{44}P_8W_{48}\}_\infty}$	Similar to $\mathbf{Co_4P_8W_{48}}$, except an additional four external Co^{2+} ions link the adjacent polyanions, resulting in 3D networks.	122
55	$Na_8Li_8Co_5[Co_{5.5}(H_2O)_{19}P_8W_{48}O_{184}]\cdot60H_2O$	$\mathbf{Co_5\{Co_{5.5}P_8W_{48}\}_\infty}$	Five external Co^{2+} ions are observed to link adjacent polyanions of $Co_{5.5}P_8W_{48}$, resulting in two-dimensional chains.	123
56	$K_2Na_4Li_{11}Co_5[Co_7(H_2O)_{28}P_8W_{48}O_{184}]Cl\cdot59H_2O$	$\mathbf{Co_5\{Co_7P_8W_{48}\}_\infty}$	$\mathbf{Co_7P_8W_{48}}$ is linked via 5 external Co^{2+} ions are observed to link adjacent polyanions, resulting in two-dimensional chains.	123
57	$K_2Na_4LiCo_{11}[Co_8(H_2O)_{32}P_8W_{48}O_{184}](CH_3COO)_4Cl\cdot47H_2O$	$\mathbf{Co_{11}\{Co_8P_8W_{48}\}_\infty}$	$\mathbf{Co_8P_8W_{48}}$ is linked via 11 external Co^{2+} ions into a three-dimensional network.	123
58	$K_{18}Li_6[Mn_8(H_2O)_{48}P_8W_{48}O_{184}]\cdot108H_2O$	$\mathbf{\{Mn_8(H_2O)_{48}P_8W_{48}\}_\infty}$	The $\mathbf{Mn_8(H_2O)_{48}P_8W_{48}}$ polyanion forms an open framework nanocube structure with each $\mathbf{P_8W_{48}}$ fragment linked by Mn–O–W coordination bonds, which forms the higher order packing arrangement.	21 and 76
59	$K_{12}[Mn_{14}(H_2O)_{30}P_8W_{48}O_{184}]\cdot111H_2O$	$\mathbf{\{Mn_{14}P_8W_{48}\}_\infty}$	A solid-state framework formed by $\mathbf{P_8W_{48}}$ units linked by external Mn^{2+} ions.	21 and 76
60	$K_{13}Li_{11}[Mn_8(H_2O)_{26}(P_8W_{48}O_{184})]\cdot60H_2O$	$\mathbf{Mn_8(H_2O)_{26}P_8W_{48}}$	In this polyanion, six Mn^{2+} ions are observed to be located inside the $\mathbf{P_8W_{48}}$ cavity, while two other Mn^{2+} ions are co-ordinated to the outer rim of $\mathbf{P_8W_{48}}$.	77
61	$K_{12}Li_{13}[Mn_6(H_2O)_{22}(P_8W_{48}O_{184})\{WO_2(H_2O)_2\}_{1.5}]\cdot75H_2O$	$\mathbf{Mn_6\{WO_2(H_2O)_2\}_{1.5}P_8W_{48}}$	Four Mn^{2+} ions are located in the cavity of $\mathbf{P_8W_{48}}$, whereas two other Mn^{2+} centers are attached to the surface of the wheel. In addition, one or two $\{WO_2(H_2O)_2\}$ groups are grafted in the cavity, leading to a mixture of products.	77
62	$K_{10}Na_{14}[\{P_8W_{48}O_{184}\}\{Mo_4^{VI}O_2\}_4\{(H_2O)(O{=})Mo^V(\mu_2\text{-}O)_2(O{=})Mo^V(\mu_2\text{-}H_2O)(\mu_2\text{-}O)_2Mo^V({=}O)(\mu_2\text{-}O)_2Mo^V({=}O)(H_2O)\}_2]\cdot80H_2O$	$\mathbf{Mo_4^{VI}Mo_4^V P_8W_{48}}$	Observed to consist of two unprecedented neutral tetranuclear $\{Mo_4^VO_{10}(H_2O)_3\}$ and four $\{Mo^{VI}O_2\}^{2+}$ units connected to the $\mathbf{P_8W_{48}}$ ring via Mo–O–W bonds.	124
63	$K_{20}Li_6H_4[K_4\{Mo_4O_4S_4(H_2O)_3(OH)_2\}_2(WO_2)(P_8W_{48}O_{184})]\cdot95H_2O$	$\mathbf{(Mo_4O_4S_4)_2(WO_2)P_8W_{48}}$	Two cationic $[Mo_4O_4S_4(OH)_2(H_2O)_3]^{2+}$ groups are grafted on both sides of $\mathbf{P_8W_{48}}$. Different bonding modes of the oxothiomolybdenum groups result in two geometrical isomers.	126
64	$K_{26}Li_2H_8[\{Mo_4O_4S_4(H_2O)_3(OH)_2\}_2(P_8W_{48}O_{184})]\cdot90H_2O$	$\mathbf{(Mo_4O_4S_4)_2P_8W_{48}}$	This polyanion is composed of the same two disordered $\{Mo_4O_4S_4\}$ oxothiomolybdenum clusters observed in $\mathbf{(Mo_4O_4S_4)_2(WO_2)P_8W_{48}}$ but without the extra $\{WO_2\}^{2+}$ group.	126
65	$K_{16}Li_{11}[\{K(H_2O)\}_3\{Ru(p\text{-cymene})(H_2O)\}_4P_8W_{49}O_{186}(H_2O)_2]\cdot87H_2O$	$\mathbf{Ru_4P_8W_{49}}$	Four $\{Ru(p\text{-cymene})(H_2O)\}^{2+}$ groups are covalently grafted to the cavity of $\mathbf{P_8W_{48}}$ via two Ru–O(W) bonds.	127
66	$Ln_4(H_2O)_{28}K_6Li_2[K{\subset}P_8W_{48}O_{184}(H_4W_4O_{12})_2Ln_2(H_2O)_{10}]\cdot87H_2O$ (Ln = La^{3+}, Ce^{3+}, Pr^{3+}, Nd^{3+})	$\mathbf{Ln_2(W_4O_{12})_2P_8W_{48}}$	The cavity of $\mathbf{P_8W_{48}}$ contains four lanthanide ions and two $\{W_4O_{12}\}$ groups, along with two potassium ions.	128
67	$K_{10}Li_{17.5}[K_{4.5}{\subset}(ClSn)_8P_8W_{48}O_{184}]\cdot50H_2O$	$\mathbf{(ClSn)_8P_8W_{48}}$	Eight $Sn^{II}Cl$ groups are incorporated in the cavity of $\mathbf{P_8W_{48}}$.	129
68	$K_8Li_{17}[(CH_3)_2NH_2]_7[(C_6H_5AsO)_4P_8W_{48}O_{184}]\cdot130H_2O$, $K_{10.5}Li_{14}[(CH_3)_2NH_2]_{3.5}[(H_3NC_6H_4AsO)_4P_8W_{48}O_{184}]\cdot92H_2O$ [R = C_6H_5 or $p\text{-}(H_2N)C_6H_4$]	$\mathbf{(RAsO)_4P_8W_{48}}$, R = C_6H_5 or $p\text{-}(H_2N)C_6H_4$	Four $\{RAsO_3\}$ units are bound covalently to the cavity of $\mathbf{P_8W_{48}}$ through As–O(W) bonds.	131
69	$K_{7.2}Li_{23-x}[(H_3NC_6H_4AsO)_3P_8W_{48}O_{184}H_x\{WO_2(H_2O)_2\}_{0.4}]\cdot nH_2O$	$\mathbf{(H_3NC_6H_4AsO)_3P_8W_{48}(WO_2)_{0.4}}$	This compound has the $\mathbf{(RAsO)_4P_8W_{48}}$ structure, but in addition 0.4 equivalents of tungsten atoms are incorporated in the cavity, which indicates the presence of a compound mixture.	131
70	$K_8Na_3Li_5\{[Na(NO_3)(H_2O)]_4[Al_{16}(OH)_{24}(H_2O)_8(P_8W_{48}O_{184})]\}\cdot66H_2O$	$\mathbf{Al_{16}P_8W_{48}}$	The polyanion contains a cationic $\{Al_{16}(OH)_{24}(H_2O)_8\}^{24+}$ hydroxo-cluster inside the cavity of $\mathbf{P_8W_{48}}$. The 16-aluminium-hydroxo unit comprises eight pairs of edge-shared AlO_6 units connected via corners.	132

Table 1 *(Contd.)*

Sl. no.	Formula	Abbreviation	Brief description	Ref.
71	$K_{11}Li_9(NH_4)_4[Ga_{16}(OH)_{32}(P_8W_{48}O_{184})]\cdot112H_2O$	$\mathbf{Ge_{16}P_8W_{48}}$	The polyanion contains the cationic nanocluster $\{Ga_{16}(OH)_{32}\}^{16+}$ incorporated in the cavity of the crown-shaped $\mathbf{P_8W_{48}}$. The 16-gallium-hydroxo core $\{Ga_{16}(OH)_{32}\}^{16+}$ comprises eight pairs of structurally equivalent, edge-shared GaO_6 units interconnected *via* corners, and all bridging oxygens are monoprotonated.	132
72	$K_{26}Li_6[(SeO)_4P_8W_{48}O_{184}]\cdot98H_2O$	$\mathbf{Se_4P_8W_{48}}$	The crown-shaped $\mathbf{P_8W_{48}}$ polyanion has four $[SeO_3]^{2-}$ ions inside the cavity in such a way that each Se atom is located inside the cavity perpendicular to the main plan of $\mathbf{P_8W_{48}}$.	133
73	$K_{25.7}Li_5(NH_4)_5[(HP_8W_{48}O_{184})(NbO(C_2O_4)(H_2O))_{3.3}]\cdot73H_2O$	$\mathbf{[(NbO(C_2O_4)(H_2O))_{3.3}P_8W_{48}]}$	The $\{NbO(H_2O)\}^{3+}$ groups in the cavity of $\mathbf{P_8W_{48}}$ have two different types of coordination environments.	134
74	$K_{30.8}Li_{3.5}(NH_4)_3[(P_8W_{48}O_{184})(NbO(C_2O_4)(H_2O))_{1.7}]\cdot74.5H_2O$	$\mathbf{[(NbO(C_2O_4)(H_2O))_{1.7}P_8W_{48}]}$	The $\{NbO(H_2O)\}^{3+}$ groups in the cavity of $\mathbf{P_8W_{48}}$ have two different types of coordination environments.	134
75	$K_{21.6}Li_5(NH_4)_8[(P_8W_{48}O_{184})(NbO(C_2O_4)_{1.5}(H_2O))_{4.4}]\cdot66H_2O$	$\mathbf{[(NbO(C_2O_4)_{1.5}(H_2O))_{4.4}P_8W_{48}]}$	The $\{NbO(H_2O)\}^{3+}$ groups in the cavity of $\mathbf{P_8W_{48}}$ have two different types of coordination environments.	134
76	$K_{24.4}Li_5(NH_4)_{5.5}[(HP_8W_{48}O_{184})(NbO(C_2O_4)(H_2O))_{3.1}]\cdot59H_2O$	$\mathbf{[(NbO(C_2O_4)(H_2O))_{3.1}P_8W_{48}]}$	The $\{NbO(H_2O)\}^{3+}$ groups in the cavity of $\mathbf{P_8W_{48}}$ have two different types of coordination environments.	134
77	$K_{26.7}Li_4(NH_4)_{5.5}H_{2.6}[(P_8W_{48}O_{184})(NbO(C_2O_4)_{2.5}(H_2O))_{3.8}]\cdot55.5H_2O$	$\mathbf{[(NbO(C_2O_4)_{2.5}(H_2O))_{3.8}P_8W_{48}]}$	The $\{NbO(H_2O)\}^{3+}$ groups in the cavity of $\mathbf{P_8W_{48}}$ have two different types of coordination environments.	134
78	$K_{11.3}Li_{8.1}Na_{22}[(UO_2)_{7.2}(HCOOH)_{7.8}(P_8W_{48}O_{184})Cl_8]\cdot89H_2O$	$\mathbf{[(UO_2)_{7.2}(HCOO)_{7.2}P_8W_{48}]}$	The 7.2 uranyl groups are disordered over eight positions, suggesting a mixture of compounds.	135
79	$K_{18}Li_{22}[(UO_2)_8(O_2)_8(P_8W_{48}O_{184})]\cdot133H_2O$	$\mathbf{(UO_2)_4(O_2)_4P_8W_{48}}$	The polyanion contains four peroxo groups connected to two uranium ions. The connectivity of each peroxo-group is similar to the previously reported polyanion (**Li$(UO_2)_4(O_2)_4(PO_3OH)_2P_6W_{36}$**).	136
80	$K_3Li_8Mn_2[(P_8W_{48}O_{184})(W_4O_{16})K_{10}Li_4Mn_{10}Na(H_2O)_{50}Cl_2]\cdot62H_2O$	$\mathbf{Mn_{10}W_4P_8W_{48}}$	The cavity of $\mathbf{P_8W_{48}}$ contains six Mn^{2+} ions and a tetratungstate unit $\{W_4O_{16}\}^{8-}$, and four additional, external Mn^{2+} ions acting as linkers of the polyanions resulting in an extended network.	137
81	$K_7Li_2Na_{27}[\alpha\gamma\alpha\gamma\text{-}P_8W_{48}O_{184}\{Cu(H_2O)\}_2]\cdot78H_2O$	$\mathbf{(Cu_2\text{-}\alpha\gamma\alpha\gamma\text{-}P_8W_{48})}$	The molar ratio of Cu^{2+} and $\mathbf{P_8W_{48}}$, temperature, and reaction time were crucial for obtaining this compound.	141
82	$K_{7.5}Na_{17}Cu_{2.425}(WO_2)_{1.325}[\gamma\gamma\gamma\gamma\text{-}P_8W_{48}O_{184}\{Cu(H_2O)_{0.5}\}_4]\cdot102H_2O$	$\mathbf{(Cu_4\text{-}\gamma\gamma\gamma\gamma\text{-}P_8W_{48})}$	The molar ratio of Cu^{2+} and $\mathbf{P_8W_{48}}$, temperature, and reaction time were crucial for obtaining this compound.	141
83	$K_7Li_2Na_{19.5}Cu_{1.75}(WO_2)[\alpha\gamma\gamma\gamma\text{-}P_8W_{48}O_{184}\{Cu(H_2O)\}_3]\cdot72H_2O$	$\mathbf{(Cu_3\text{-}\alpha\gamma\gamma\gamma\text{-}P_8W_{48})}$	The molar ratio of Cu^{2+} and $\mathbf{P_8W_{48}}$, temperature, and reaction time were crucial for obtaining this compound.	141
84	$[(n\text{-}C_4H_9)_4N]_{14}H_2[\{M_2(OH_2)_2\}_2\{M(OH_2)_4\}_4P_8W_{48}O_{176}(OCH_3)_8]\cdot nH_2O\cdot mCH_3CN$	$\mathbf{M_8P_8W_{48}O_{176}}$ (M^{II} = Mn, Co, Ni, Cu, Zn)	Reaction of divalent 3d metal ions with $\alpha\text{-}P_2W_{12}$ resulted in a partial transformation to the $\gamma\text{-}P_2W_{12}$ isomer, yielding a new type of $\alpha,\gamma,\alpha,\gamma$-type $\mathbf{P_8W_{48}}$ ring, and the incorporation of eight metal ions M^{II}.	142
85	$Li_8K_{9.5}Ag_{21}[H_{16}P_{10}W_{66}O_{251}]_{0.5}[H_{14}P_9W_{63}O_{235}]_{0.5}Cl_2\cdot50H_2O$ and $Li_8K_{13}Ag_{13}[H_{12}P_8W_{51}O_{196}]\cdot50H_2O$ and $Li_{10}K_{12}Ag_4[H_{14}P_8W_{48}O_{184}]\cdot170H_2O$	$\mathbf{Ag_{21}P_9W_{63}O_{235}, Ag_{13}P_8W_{51}O_{196}, Ag_4P_8W_{48}O_{148}}$	Heating $\mathbf{P8W48}$ in the presence of Ag^+ ions at a high concentration (1:30). $\mathbf{Ag_{13}P_8W_{51}O_{196}}$ forms in a similar procedure with a lower concentration of silver ions (1:12) and at a lower temperature. The $\mathbf{Ag_4P_8W_{48}O_{148}}$ formed at even lower concentration of silver ions at room temperature.	147
86	$(C_{24}PH_{20})_{17}H_{37}[Mn_{18}P_8W_{48}O_{214}]\cdot16H_2O\cdot4CH_3CN$ and $(C_{16}H_{36}N)_{12}H_{16}[Mn_{20}P_8W_{48}O_{216}]\cdot4C_2H_3N\cdot C_2Cl_2H_4$	$\mathbf{Mn_{18}P_8W_{48}O_{214}, Mn_{20}P_8W_{48}O_{216}}$	The $\mathbf{Mn_{18}P_8W_{48}O_{214}}$ polyanion contains 18 Mn ions of oxidation state +2 or +3 in the cavity of $\mathbf{P_8W_{48}}$ and the four P_2W_{12} units were transformed from α- to γ-isomer in the course of the reaction. In the $\mathbf{Mn_{20}P_8W_{48}O_{216}}$ ion, the 20 Mn ions have an oxidation state either +3 or +4 and are aligned at the inner rim of $\mathbf{P_8W_{48}}$.	143
87	$[(n\text{-}C_4H_9)_4N]_{11}H_{13}[Cu_4(H_2O)_4P_8W_{48}O_{176}(OCH_3)_8]\cdot28H_2O\cdot3CH_3NO_2$, and $[(n\text{-}C_4H_9)_4N]_{14}H_2, [Cu_8(H_2O)_{12}P_8W_{48}O_{176}(OCH_3)_8]\cdot24H_2O\cdot CH_3CN$, and $[(n\text{-}C_4H_9)_4N]_{14}H_2[Cu_{12}(H_2O)_{16}P_8W_{48}O_{184}]\cdot4H_2O$, and $[(n\text{-}C_4H_9)_4N]_{16}H_8[Cu_{16}(OH)_{16}(H_2O)_4P_8W_{48}O_{184}]\cdot12H_2O\cdot C_3H_6O$	$\mathbf{Cu_4P_8W_{48}, Cu_8P_8W_{48}, Cu_{12}P_8W_{48}, Cu_{16}P_8W_{48}}$	In $\mathbf{Cu_4P_8W_{48}}$ and $\mathbf{Cu_8P_8W_{48}}$ the two middle P_2W_{12} units to which the copper(II) ions are connected, had transformed from from α- to γ-isomer with a 60° rotation of the PO_4 hetero groups. In $\mathbf{Cu_{12}P_8W_{48}}$ and $\mathbf{Cu_{16}P_8W_{48}}$ the same $\gamma,\gamma,\gamma,\gamma$-type $\mathbf{P_8W_{48}}$ framework is present, but the copper coordination geometry differs from each other.	144
88	$[(n\text{-}C_4H_9)_4N]_{17}H[Ag_{30}(P_8W_{48}O_{184})]\cdot10DMF\cdot30H_2O$	$\mathbf{Ag_{30}P_8W_{48}}$	This nanocluster material has exposed silver surfaces and interfaces with metal oxides, and it is highly stable despite the exposed silver surfaces, acting as a catalytically active sites for the selective reduction of organic substrates using H_2 under mild reaction conditions.	145
89	$(Bu_4N)_{16}H_8[Au_8Ag_{26}(P_8W_{48}O_{184})]$	$\mathbf{Au_8Ag_{26}P_8W_{48}}$	The polyanion comprises $\{Au_6\}$ as well as $\{Ag_6Au\}$ clusters embedded in the cavity of $\mathbf{P_8W_{48}}$.	148
90	$(Me_2NH_2)_{13}K_7Na_2Li_{10}[\{As_5^{III}O_4(OH)_3\}_2(P_8W_{48}O_{184})]\cdot32H_2O$, $K_{20}Li_{12}[(Sb^{III}OH)_4(P_8W_{48}O_{184})]\cdot52H_2O$, and $(Me_2NH_2)_8K_6Na_5Li_5[(Sb^{III}OH)_8(P_8W_{48}O_{184})]\cdot65H_2O$	$\mathbf{As_{10}P_8W_{48}, Sb_4P_8W_{48}, Sb_8P_8W_{48}}$	Ten As^{III} ions or four/eight Sb^{III} ions are grafted in the cavity of $\mathbf{P_8W_{48}}$.	149
91	$K_{22}Li_4[\{Fe_8^{III}Ce_4^{III}O_2(OH)_{12}(H_2O)_8(PO_4)_2\}(P_8W_{48}O_{184})]\cdot106H_2O$	$\mathbf{Fe_8Ce_4P_8W_{48}}$	The polyanion comprises an iron(III)–cerium(III)–phosphato moiety $\{Fe_8^{III}Ce_4^{III}O_2(OH)_{12}(H_2O)_8(PO_4)_2\}$ in the cavity of $\mathbf{P_8W_{48}}$.	150

selective catalytic activity towards reducing nitrobenzene and aromatic aldehydes under mild conditions. Very recently, Suzuki and coworkers have reported the mixed-metal silver–gold derivative of $\mathbf{P_8W_{48}}$, wherein a $[Au_8Ag_{26}]$ cluster is embedded within the $\mathbf{P_8W_{48}}$ core, $(Bu_4N)_{16}H_8$ $[Au_8Ag_{26}(P_8W_{48}O_{184})]$ ($\mathbf{Au_8Ag_{26}P_8W_{48}}$).[148] In the silver–gold cluster, six out of eight Au atoms form an octahedral $\{Au_6\}$ assembly, while in another one Au atom replaces the Ag site at

the center of a hexagonal $\{Ag_7\}$, forming the $\{Ag_6Au\}$ assembly. The 26 Ag atoms were thus observed to surround Au atoms to form the nano-cluster $Au_8Ag_{26}P_8W_{48}$.

Recently, Yang and coworkers were able to incorporate $As^{III}O_3$ and $Sb^{III}O_3$ in the cavity of P_8W_{48}, resulting in $[\{As_5^{III}O_4(OH)_3\}_2(P_8W_{48}O_{184})]^{32-}$ $(As_{10}P_8W_{48})$, $[(Sb^{III}OH)_4(P_8W_{48}O_{184})]^{32-}$ $(Sb_4P_8W_{48})$, and $[(Sb^{III}OH)_8(P_8W_{48}O_{184})]^{24-}$ $(Sb_8P_8W_{48})$.[149] Very recently, the same group has reported the 3d–4f iron(III)-cerium(III) derivative $[\{Fe_8^{III}Ce_4^{III}O_2(OH)_{12}(H_2O)_8(PO_4)_2\}(P_8W_{48}O_{184})]^{26-}$ $(Fe_8Ce_4P_8W_{48})$, comprising an iron(III)–cerium(III)–phosphato moiety $\{Fe_8^{III}Ce_4^{III}O_2(OH)_{12}(H_2O)_8(PO_4)_2\}$ encapsulated in the P_8W_{48} cavity, resulting in a polyanion with idealized D_{2h} symmetry and it exhibited high sensitivity and specificity to detect ascorbic acid (Table 1).[150] In Table 1, the structural characteristics and component building blocks of the compounds presented in this review are summarized.

6.   Summary and outlook

Over the years, many tungstophosphates have been synthesized and structurally characterized. This review focuses on the structural family P_2W_{12}, P_4W_{24}, and P_8W_{48} and their interaction with metal ions during the last 20 years emphasizing synthetic and structural aspects. We have discussed the formation and stability of these polyanions in different reaction conditions, including pH, temperature, solvent, concentration, counterions, and ionic strength. Although P_2W_{12}, P_4W_{24}, and P_8W_{48} all contain the P_2W_{12} unit as a key building block, their stability and reactivity with metal ions is vastly different, and hence, unique products are observed. While the monomeric P_2W_{12} is the least stable amongst the three in solution, the cyclic P_8W_{48} (comprising four P_8W_{48} units) is the most stable.

The reactivity, particularly the large, crown-shaped P_8W_{48} with transition metal ions, has been systematically developed only since 2005. All three derivatives, P_8W_{48}, P_4W_{24}, and P_2W_{12}, are multilacunary, containing six or more vacant sites, which in principle can accommodate multiple transition metal ions. The literature in this area has expanded dramatically in the last two decades, reflecting the synthesis and property studies of a wide variety of compounds.

Subsequently, we discussed the versatile nature of these three polyanions, and their chemistry with an emphasis on their reactivity towards d and f-block metal ions, including mixed d/f derivatives, leading to discrete monomeric, dimeric, trimeric, and tetrameric structures, or extended solid state frameworks. Furthermore, gaining extra tungsten atoms *in situ* (arising from trace decomposition of the parent polyanion) provides additional degrees of structural flexibility. Other interesting features of P_2W_{12}, P_4W_{24}, and P_8W_{48} are the multifunctional ways to accommodate high nuclearity transition metal oxo/hydroxo/aqua clusters according to their needs. Several novel and unexpected compounds have been isolated depending on the reaction conditions (*e.g.*, type of transition metal, reaction temperature, solution pH, solvent, ionic strength, ratio and concentration of reagents, and countercations), which are all important parameters in synthetic POM chemistry. Several compounds have shown attractive properties in homogeneous and heterogeneous catalysis, as well as in magnetic studies. Researchers are still searching for new materials based on P_2W_{12}, P_4W_{24}, and P_8W_{48}, which are yet to be explored and examined and can benefit their associated properties and potential applications.

Data availability

This is a review paper and hence no new data is presented.

Only scientific publications that can be accessed *via* the usual academic routes have been cited.

Conflicts of interest

The authors declare no competing conflicts of interest.

Acknowledgements

References

1 J. J. Berzelius, *Ann. Phys.*, 1826, **82**, 369.
2 M. T. Pope, *Heteropoly and Isopoly Oxometalates*, 1983.
3 D. A. Malikov, M. S. Milyuokova and B. F. Myasoedov, *Radiokhimiya*, 1993, **35**, 105.
4 M. T. Pope and A. Müller, *Angew. Chem., Int. Ed. Engl.*, 1991, **30**, 34.
5 A. Müller and S. Roy, in *The Chemistry of Nanomaterials*, Wiley-VCH Verlag GmbH & Co. KGaA, 2005, p. 452.
6 C. L. Hill, *Chem. Rev.*, 1998, **98**, 1.
7 D. L. Long, E. Burkholder and L. Cronin, *Chem. Soc. Rev.*, 2007, **36**, 105.
8 D. L. Long, R. Tsunashima and L. Cronin, *Angew. Chem., Int. Ed.*, 2010, **49**, 1736.
9 L. Cronin and A. Müller, *Chem. Soc. Rev.*, 2012, **41**, 7333.
10 M. I. Khan, *J. Solid State Chem.*, 2000, **152**, 105.
11 D. L. Long and L. Cronin, *Chem. – Eur. J.*, 2006, **12**, 3699.
12 B. Hasenknopf, *Front. Biosci.-Landmark*, 2005, **10**, 275.
13 T. Yamase, *J. Mater. Chem.*, 2005, **15**, 4773.
14 H. Y. Ma, J. Peng, Z. G. Han, X. Yu and B. X. Dong, *J. Solid State Chem.*, 2005, **178**, 3735.
15 K. Nomiya, H. Torii, T. Hasegawa, Y. Nemoto, K. Nomura, K. Hashino, M. Uchida, Y. Kato, K. Shimizu and M. Oda, *J. Inorg. Biochem.*, 2001, **86**, 657.

16 R. J. Errington, S. S. Petkar, B. R. Horrocks, A. Houlton, L. H. Lie and S. N. Patole, *Angew. Chem., Int. Ed.*, 2005, **44**, 1254.

17 J. T. Rhule, C. L. Hill and D. A. Judd, *Chem. Rev.*, 1998, **98**, 327.

18 M. V. Vasylyev and R. Neumann, *J. Am. Chem. Soc.*, 2004, **126**, 884.

19 I. M. Mbomekalle, B. Keita, L. Nadjo, P. Berthet, K. I. Hardcastle, C. L. Hill and T. M. Anderson, *Inorg. Chem.*, 2003, **42**, 1163.

20 D. Volkmer, B. Bredenkotter, J. Tellenbroker, P. Kögerler, D. G. Kurth, P. Lehmann, H. Schnablegger, D. Schwahn, M. Piepenbrink and B. Krebs, *J. Am. Chem. Soc.*, 2002, **124**, 10489.

21 S. G. Mitchell, C. Streb, H. N. Miras, T. Boyd, D. L. Long and L. Cronin, *Nat. Chem.*, 2010, **2**, 308.

22 T. B. Liu, E. Diemann, H. L. Li, A. W. M. Dress and A. Müller, *Nature*, 2003, **426**, 59.

23 G. Chaidogiannos, D. Velessiotis, P. Argitis, P. Koutsolelos, C. D. Diakoumakos, D. Tsamakis and N. Glezos, *Microelectron. Eng.*, 2004, **73–4**, 746.

24 S. Q. Liu, D. Volkmer and D. G. Kurth, *Anal. Chem.*, 2004, **76**, 4579.

25 S. Q. Liu, D. G. Kurth and D. Volkmer, *Chem. Commun.*, 2002, 976.

26 E. Coronado, C. Gimenez-Saiz and C. J. Gomez-Garcia, *Coord. Chem. Rev.*, 2005, **249**, 1776.

27 L. Xu, E. B. Wang, Z. Li, D. G. Kurth, X. G. Du, H. Y. Zhang and C. Qin, *New J. Chem.*, 2002, **26**, 782.

28 M. Luban, F. Borsa, S. Bud'ko, P. C. Canfield, S. Jun, J. K. Jung, P. Kögerler, D. Mentrup, A. Müller, R. Modler, D. Procissi, B. J. Suh and M. Torikachvili, *Phys. Rev. B: Condens. Matter Mater. Phys.*, 2002, **66**, 054407.

29 A. Müller, E. Krickemeyer, J. Meyer, H. Bögge, F. Peters, W. Plass, E. Diemann, S. Dillinger, F. Nonnenbruch, M. Randerath and C. Menke, *Angew. Chem., Int. Ed. Engl.*, 1995, **34**, 2122.

30 A. Müller, E. Beckmann, H. Bögge, M. Schmidtmann and A. Dress, *Angew. Chem., Int. Ed.*, 2002, **41**, 1162.

31 A. Mylonas, A. Hiskia and E. Papaconstantinou, *J. Mol. Catal. A: Chem.*, 1996, **114**, 191.

32 A. Hiskia, A. Troupis and E. Papaconstantinou, *Int. J. Photoenergy*, 2002, **4**, 35.

33 E. Gkika, P. Kormali, S. Antonaraki, D. Dimoticali, E. Papaconstantinou and A. Hiskia, *Int. J. Photoenergy*, 2004, **6**, 227.

34 A. Troupis, E. Gkika, A. Hiskia and E. Papaconstantinou, *C. R. Chim.*, 2006, **9**, 851.

35 P. Kormali, A. Troupis, T. Triantis, A. Hiskia and E. Papaconstantinou, *Catal. Today*, 2007, **124**, 149.

36 A. F. Wells, *Structural Inorganic Chemistry*, Oxford University Press, 2012.

37 B. Dawson, *Acta Crystallogr.*, 1953, **6**, 113.

38 R. Strandberg, *Acta Chem. Scand., Ser. A*, 1975, **29**, 350.

39 H. d'Amour, *Acta Crystallogr., Sect. B*, 1976, **32**, 729.

40 R. Acerete, C. F. Hammer and L. C. W. Baker, *J. Am. Chem. Soc.*, 1979, **101**, 267.

41 R. Acerete, S. Harmalker, C. F. Hammer, M. T. Pope and L. C. W. Baker, *J. Chem. Soc., Chem. Commun.*, 1979, 777.

42 R. Contant, W. G. Klemperer and O. M. Yaghi, in *Inorg Syn*, John Wiley & Sons, Inc., 2007, p. 104.

43 R. Contant and A. Tézé, *Inorg. Chem.*, 1985, **24**, 4610.

44 F. Hussain, U. Kortz, B. Keita, L. Nadjo and M. T. Pope, *Inorg. Chem.*, 2006, **45**, 761.

45 L. Vila-Nadal, S. G. Mitchell, D. L. Long, A. Rodriguez-Fortea, X. Lopez, J. M. Poblet and L. Cronin, *Dalton Trans.*, 2012, **41**, 2264.

46 R. Acerete, C. F. Hammer and L. C. W. Baker, *Inorg. Chem.*, 1984, **23**, 1478.

47 Sugiarto and M. Sadakane, *Chem. – Eur. J.*, 2023, **29**, e202301051.

48 S. Take, T. Minato and M. Sadakane, *Chem. Lett.*, 2024, **53**, upae118.

49 R. Acerete, C. F. Hammer and L. C. W. Baker, *J. Am. Chem. Soc.*, 1982, **104**, 5384.

50 P. Roussel, G. Mather, B. Domenges, D. Groult and P. Labbe, *Acta Crystallogr., Sect. B: Struct. Sci.*, 1998, **54**, 365.

51 T. Boyd, S. G. Mitchell, D. Gabb, D. L. Long and L. Cronin, *Chem. – Eur. J.*, 2011, **17**, 12010.

52 X. Xin and H. Lv, *Sci. Sin.: Chim.*, 2020, **50**, 1015.

53 D. A. Judd, Q. Chen, C. F. Campana and C. L. Hill, *J. Am. Chem. Soc.*, 1997, **119**, 5461.

54 R. Belghiche, R. Contant, Y. W. Lu, B. Keita, M. Abbessi, L. Nadjo and J. Mahuteau, *Eur. J. Inorg. Chem.*, 2002, 1410.

55 J. E. Toth and F. C. Anson, *J. Am. Chem. Soc.*, 1989, **111**, 2444.

56 B. Keita, A. Belhouari, L. Nadjo and R. Contant, *J. Electroanal. Chem.*, 1995, **381**, 243.

57 M. Sadakane and E. Steckhan, *Chem. Rev.*, 1998, **98**, 219.

58 B. Godin, Y.-G. Chen, J. Vaissermann, L. Ruhlmann, M. Verdaguer and P. Gouzerh, *Angew. Chem., Int. Ed.*, 2005, **44**, 3072.

59 B. Godin, J. Vaissermann, P. Herson, L. Ruhlmann, M. Verdaguer and P. Gouzerh, *Chem. Commun.*, 2005, 5624.

60 A. Ostuni and M. T. Pope, *C. R. Acad. Sci., Ser IIc*, 2000, **3**, 199.

61 U. Kortz, *J. Cluster Sci.*, 2003, **14**, 205.

62 Z. M. Zhang, S. Yao, Y. F. Qi, Y. G. Li, Y. H. Wang and E. Wang, *Dalton Trans.*, 2008, 3051.

63 Y. H. Ren, Y. C. Hu, Y. C. Shan, Z. P. Kong, M. Gu, B. Yue and H. Y. He, *Inorg. Chem. Commun.*, 2014, **40**, 108.

64 G. S. Kim, H. D. Zeng, D. VanDerveer and C. L. Hill, *Angew. Chem., Int. Ed.*, 1999, **38**, 3205.

65 C. C. Li, S. X. Liu, S. J. Li, Y. Yang, H. Y. Jin and F. J. Ma, *Eur. J. Inorg. Chem.*, 2012, 3229.

66 S. J. Li, S. X. Liu, N. N. Ma, Y. Q. Qiu, J. Miao, C. C. Li, Q. Tang and L. Xu, *CrystEngComm*, 2012, **14**, 1397.

67 D. D. Zhang, C. Zhang, P. T. Ma, B. S. Bassil, R. Al-Oweini, U. Kortz, J. P. Wang and J. Y. Niu, *Inorg. Chem. Front.*, 2015, **2**, 254.

68 X. F. Yi, N. V. Izarova and P. Kögerler, *Chem. Commun.*, 2018, **54**, 2216.

69 T. Iftikhar, N. V. Izarova and P. Kögerler, *Inorg. Chem.*, 2024, **63**, 99.

70 T. Iftikhar, N. V. Izarova, J. van Leusen and P. Kögerler, *Chem. – Eur. J.*, 2021, **27**, 13376.

71 Z. M. Zhang, S. Yao, Y. G. Li, Y. H. Wang, Y. F. Qi and E. B. Wang, *Chem. Commun.*, 2008, 1650.

72 S. Yao, Z. M. Zhang, Y. G. Li and E. B. Wang, *Dalton Trans.*, 2010, **39**, 3884.

73 S. Yao, Z. M. Zhang, Y. G. Li, Y. Lu, E. B. Wang and Z. M. Su, *Cryst. Growth Des.*, 2010, **10**, 135.

74 J. P. Guo, Y. Q. Zhao, C. Zhang, P. T. Ma, D. D. Zhang, J. Y. Niu and J. P. Wang, *Inorg. Chem. Commun.*, 2017, **75**, 5.

75 L. C. Zhang, H. Xue, Z. M. Zhu, Z. M. Zhang, Y. G. Li and E. B. Wang, *J. Cluster Sci.*, 2010, **21**, 679.

76 S. G. Mitchell, T. Boyd, H. N. Miras, D. L. Long and L. Cronin, *Inorg. Chem.*, 2011, **50**, 136.

77 S. W. Chen, K. Boubekeur, P. Gouzerh and A. Proust, *J. Mol. Struct.*, 2011, **994**, 104.

78 D. D. Zhang, Z. J. Liang, S. Q. Xie, P. T. Ma, C. Zhang, J. P. Wang and J. Y. Niu, *Inorg. Chem.*, 2014, **53**, 9917.

79 W.-D. Liu, H.-T. Zhu, X. Zhang, F. Su, X.-J. Sang, X.-L. Zhang and L.-C. Zhang, *Polyoxometalates*, 2025, **4**, 9140073.

80 D. D. Zhang, F. Cao, P. T. Ma, C. Zhang, Y. Song, Z. J. Liang, X. J. Hu, J. P. Wang and J. Y. Niu, *Chem. – Eur. J.*, 2015, **21**, 17683.

81 T. Minato, K. Suzuki, K. Yamaguchi and N. Mizuno, *Angew. Chem., Int. Ed.*, 2016, **55**, 9630.

82 K. Suzuki, T. Minato, N. Tominaga, L. Okumo, K. Yonesato, N. Mizuno and K. Yamaguchi, *Dalton Trans.*, 2019, **48**, 7281.

83 K. Wassermann, M. H. Dickman and M. T. Pope, *Angew. Chem., Int. Ed. Engl.*, 1997, **36**, 1445.

84 Q. H. Luo, R. C. Howell, J. Bartis, M. Dankova, W. D. Horrocks, A. L. Rheingold and L. C. Francesconi, *Inorg. Chem.*, 2002, **41**, 6112.

85 M. Sadakane, A. Ostuni and M. T. Pope, *J. Chem. Soc., Dalton Trans.*, 2002, 63.

86 Z. M. Zhang, Y. G. Li, Y. H. Wang, Y. F. Qi and E. B. Wang, *Inorg. Chem.*, 2008, **47**, 7615.

87 S. Yao, Z. M. Zhang, Y. G. Li and E. Wang, *Dalton Trans.*, 2009, 1786.

88 X. K. Fang, P. Kögerler, Y. Furukawa, M. Speldrich and M. Luban, *Angew. Chem., Int. Ed.*, 2011, **50**, 5212.

89 L. Huang, L. Cheng, W. H. Fang, S. S. Wang and G. Y. Yang, *Eur. J. Inorg. Chem.*, 2013, 1693.

90 A. A. Shmakova, T. S. Sukhikh, V. V. Volchek, V. Yanshole, D. V. Stass, E. Y. Filatov, E. M. Glebov, P. A. Abramov and M. N. Sokolov, *Inorg. Chim. Acta*, 2020, **502**, 119319.

91 J. Goura, B. S. Bassil, J. K. Bindra, I. A. Rutkowska, P. J. Kulesza, N. S. Dalal and U. Kortz, *Chem. – Eur. J.*, 2020, **26**, 15821.

92 S. S. Mal, M. H. Dickman and U. Kortz, *Chem. – Eur. J.*, 2008, **14**, 9851.

93 A. S. Assran, N. V. Izarova and U. Kortz, *CrystEngComm*, 2010, **12**, 2684.

94 A. Müller, M. T. Pope, A. M. Todea, H. Bögge, J. van Slageren, M. Dressel, P. Gouzerh, R. Thouvenot, B. Tsukerblat and A. Bell, *Angew. Chem., Int. Ed.*, 2007, **46**, 4477.

95 T. Boyd, S. G. Mitchell, D. Gabb, D.-L. Long, Y.-F. Song and L. Cronin, *J. Am. Chem. Soc.*, 2017, **139**, 5930.

96 S. S. Mal and U. Kortz, *Angew. Chem., Int. Ed.*, 2005, **44**, 3777.

97 S. S. Mal, B. S. Bassil, M. Ibrahim, S. Nellutla, J. van Tol, N. S. Dalal, J. A. Fernandez, X. Lopez, J. M. Poblet, R. Ngo Biboum, B. Keita and U. Kortz, *Inorg. Chem.*, 2009, **48**, 11636.

98 D. Jabbour, B. Keita, L. Nadjo, U. Kortz and S. S. Mal, *Electrochem. Commun.*, 2005, **7**, 841.

99 B. Keita, L. Nadjo, R. Contant, M. Fournier and G. Hervé, *France Pat*, 89/1, 728, 1989.

100 M. S. Alam, V. Dremov, P. Müller, A. V. Postnikov, S. S. Mal, F. Hussain and U. Kortz, *Inorg. Chem.*, 2006, **45**, 2866.

101 G. Liu, T. B. Liu, S. S. Mal and U. Kortz, *J. Am. Chem. Soc.*, 2006, **128**, 10103.

102 G. Liu, T. B. Liu, S. S. Mal and U. Kortz, *J. Am. Chem. Soc.*, 2007, **129**, 2408.

103 A. Müller, E. Krickemeyer, H. Bögge, M. Schmidtmann and F. Peters, *Angew. Chem., Int. Ed.*, 1998, **37**, 3360.

104 A. Müller, S. K. Das, V. P. Fedin, E. Krickemeyer, C. Beugholt, H. BöggeBögge, M. Schmidtmann and B. Hauptfleisch, *Z. Anorg. Allg. Chem.*, 1999, **625**, 1187.

105 R. Wang, Z. Zheng, F. W. Koknat, D. J. Marko, A. Müller, S. K. Das, E. Krickemeyer, C. Kuhlmann, B. Therrien, L. Plasseraud, G. Süss-Fink, A. D. Pasquale, X. Lei, T. P. Fehlner, E. L. Diz, S. Haak, E. Cariati, C. Dragonetti, E. Lucenti, D. Roberto, C. Y. Lee, H. Song, K. Lee, B. K. Park, J. T. Park, J. E. Hutchison, E. W. Foster, M. G. Warner, S. M. Reed and W. W. Weare, in *Inorg Syn*, John Wiley & Sons, Inc., 2004, p. 184.

106 B. L. Chen, H. J. Jiang, Y. Zhu, A. Cammers and J. P. Selegue, *J. Am. Chem. Soc.*, 2005, **127**, 4166.

107 A. Müller, H. Bögge, F. L. Sousa, M. Schmidtmann, D. G. Kurth, D. Volkmer, J. van Slageren, M. Dressel, M. L. Kistler and T. Liu, *Small*, 2007, **3**, 986.

108 M. L. Kistler, T. B. Liu, P. Gouzerh, A. M. Todea and A. Müller, *Dalton Trans.*, 2009, 5094.

109 C. Schaffer, A. Merca, H. Bögge, A. M. Todea, M. L. Kistler, T. B. Liu, R. Thouvenot, P. Gouzerh and A. Müller, *Angew. Chem., Int. Ed.*, 2009, **48**, 149.

110 T. B. Liu, M. L. K. Langston, D. Li, J. M. Pigga, C. Pichon, A. M. Todea and A. Müller, *Science*, 2011, **331**, 1590.

111 G. Liu and T. B. Liu, *Langmuir*, 2005, **21**, 2713.

112 Y. Y. Bao, L. H. Bi, L. X. Wu, S. S. Mal and U. Kortz, *Langmuir*, 2009, **25**, 13000.

113 J. M. Pigga, M. L. Kistler, C. Y. Shew, M. R. Antonio and T. B. Liu, *Angew. Chem., Int. Ed.*, 2009, **48**, 6538.

114 L. F. Chen, J. C. Hu, S. S. Mal, U. Kortz, H. Jaensch, G. Mathys and R. M. Richards, *Chem. – Eur. J.*, 2009, **15**, 7490.

115 P. Mialane, A. Dolbecq and F. SécheresseSécheresse, *Chem. Commun.*, 2006, 3477.

116 C. Pichon, P. Mialane, A. Dolbecq, J. Marrot, E. Riviere, B. Keita, L. Nadjo and F. Sécheresse, *Inorg. Chem.*, 2007, **46**, 5292.

117 S. S. Mal, M. H. Dickman, U. Kortz, A. M. Todea, A. Merca, H. Bögge, T. Glaser, A. Müller, S. Nellutla, N. Kaur, J. van Tol, N. S. Dalal, B. Keita and L. Nadjo, *Chem. – Eur. J.*, 2008, **14**, 1186.

118 A. H. Ismail, B. S. Bassil, G. H. Yassin, B. Keita and U. Kortz, *Chem. – Eur. J.*, 2012, **18**, 6163.

119 S. S. Mal, M. H. Dickman, U. Kortz, A. M. Todea, A. Merca, H. Bögge, T. Glaser, A. Müller, S. Nellutla, N. Kaur, J. van Tol, N. S. Dalal, B. Keita and L. Nadjo, *Chem. – Eur. J.*, 2008, **14**, 1186.

120 S. S. Mal, Ph.D. thesis, Jacobs University, Bremen, Germany, 2008, mentor U. Kortz.

121 B. S. Bassil, M. Ibrahim, S. S. Mal, A. Suchopar, R. Ngo Biboum, B. Keita, L. Nadjo, S. Nellutla, J. van Tol, N. S. Dalal and U. Kortz, *Inorg. Chem.*, 2010, **49**, 4949.

122 S. G. Mitchell, D. Gabb, C. Ritchie, N. Hazel, D. L. Long and L. Cronin, *CrystEngComm*, 2009, **11**, 36.

123 Y. Q. Jiao, C. Qin, X. L. Wang, C. G. Wang, C. Y. Sun, H. N. Wang, K. Z. Shao and Z. M. Su, *Chem. – Asian J.*, 2014, **9**, 470.

124 F. L. Sousa, H. Bögge, A. Merca, P. Gouzerh, R. Thouvenot and A. Müller, *Chem. Commun.*, 2009, 7491.

125 Y. Y. Bao, B. Wang, R. Q. Meng, L. H. Bi and L. X. Wu, *CrystEngComm*, 2012, **14**, 1550.

126 V. S. Korenev, S. Floquet, J. Marrot, M. Haouas, I. M. Mbomekalle, F. Taulelle, M. N. Sokolov, V. P. Fedin and E. Cadot, *Inorg. Chem.*, 2012, **51**, 2349.

127 S. S. Mal, N. H. Nsouli, M. H. Dickman and U. Kortz, *Dalton Trans.*, 2007, 2627.

128 M. Zimmermann, N. Belai, R. J. Butcher, M. T. Pope, E. V. Chubarova, M. H. Dickman and U. Kortz, *Inorg. Chem.*, 2007, **46**, 1737.

129 N. V. Izarova, L. Klass, P. de Oliveira, I. M. Mbomekalle, V. Peters, F. Haarmann and P. Kögerler, *Dalton Trans.*, 2015, **44**, 19200.

130 B. Kamenar and D. Grdenic, *J. Chem. Soc. (Resumed)*, 1961, 3954.

131 X. F. Yi, N. V. Izarova and P. Kögerler, *Inorg. Chem.*, 2017, **56**, 13822.

132 P. Yang, M. Alsufyani, A. H. Emwas, C. Q. Chen and N. M. Khashab, *Angew. Chem., Int. Ed.*, 2018, **57**, 13046.

133 K. Y. Wang, S. Zhang, D. Ding, T. Ma, U. Kortz and C. Wang, *Eur. J. Inorg. Chem.*, 2019, 512.

134 A. A. Shmakova, V. V. Volchek, V. Yanshole, N. B. Kompankov, N. P. Martin, M. Nyman, P. A. Abramov and M. N. Sokolov, *New J. Chem.*, 2019, **43**, 9943.

135 M. Dufaye, S. Duval, G. Stoclet, X. Trivelli, M. Huve, A. Moissette and T. Loiseau, *Inorg. Chem.*, 2019, **58**, 1091.

136 J. Goura, A. Sundar, B. S. Bassil, G. Ćirić-Marjanović, D. Bajuk-Bogdanović and U. Kortz, *Inorg. Chem.*, 2020, **59**, 16789.

137 M. Ibrahim, I. M. Mbomekalle, P. De Oliveira, G. E. Kostakis and C. Anson, *Dalton Trans.*, 2019, **48**, 15545.

138 I. D. Brown and D. Altermatt, *Acta Crystallogr., Sect. B: Struct. Sci.*, 1985, **41**, 244.

139 N. E. Brese and M. O'Keeffe, *Acta Crystallogr., Sect. B: Struct. Sci.*, 1991, **47**, 192.

140 W. Liu and H. H. Thorp, *Inorg. Chem.*, 1993, **32**, 4102.

141 X. Yi, N. V. Izarova, T. Iftikhar, J. van Leusen and P. Kögerler, *Inorg. Chem.*, 2019, **58**, 9378.

142 S. Sasaki, K. Yonesato, N. Mizuno, K. Yamaguchi and K. Suzuki, *Inorg. Chem.*, 2019, **58**, 7722.

143 K. Sato, K. Yonesato, T. Yatabe, K. Yamaguchi and K. Suzuki, *Chem. – Eur. J.*, 2022, **28**, e202104051.

144 Y. Koizumi, K. Yonesato, K. Yamaguchi and K. Suzuki, *Inorg. Chem.*, 2022, **61**, 9841.

145 K. Yonesato, D. Yanai, S. Yamazoe, D. Yokogawa, T. Kikuchi, K. Yamaguchi and K. Suzuki, *Nat. Chem.*, 2023, **15**, 940.

146 Y. Koizumi, K. Yonesato, S. Kikkawa, S. Yamazoe, K. Yamaguchi and K. Suzuki, *J. Am. Chem. Soc.*, 2024, **146**, 14610.

147 C.-H. Zhan, Q. Zheng, D.-L. Long, L. Vilà-Nadal and L. Cronin, *Angew. Chem., Int. Ed.*, 2019, **58**, 17282.

148 M. Kamachi, K. Yonesato, T. Okazaki, D. Yanai, S. Kikkawa, S. Yamazoe, R. Ishikawa, N. Shibata, Y. Ikuhara, K. Yamaguchi and K. Suzuki, *Angew. Chem., Int. Ed.*, 2024, **63**, e202408358.

149 Y. Niu, Y. Ding, H. Sheng, S. Sun, C. Chen, J. Du, H.-Y. Zang and P. Yang, *Inorg. Chem.*, 2022, **61**, 21024.

150 H.-X. Sheng, B.-Y. Lin, C.-Q. Chen, J. Du and P. Yang, *Polyoxometalates*, 2024, **3**, 9140060.